Improved *in vitro* bone-like tissue formation by human trabecular bone cells in a novel three dimensional cultivation system

Von der Naturwissenschaftlichen Fakultät
der Gottfried Wilhelm Leibniz Universität Hannover

zur Erlangung des Grades
DOKTORIN DER NATURWISSENSCHAFTEN
Dr. rer. nat.

genehmigte Dissertation
von

Apothekerin Nadia Zghoul
geboren am 21. August 1975, in Meppen

2007

Referent : Prof. Dr. Thomas Scheper
Institut für Technische Chemie
Universität Hannover

Korreferent : Prof. Dr. Martijn van Griensven
Ludwig Boltzmann Institut
für experimentelle und klinische Traumatologie
Wien

Tag der Promotion : 14. September 2007

Erklärung

Ich versichere, dass ich diese Dissertation selbstständig und nur unter Verwendung der angegebenen Hilfsmittel und Quellen durchgeführt habe.
Diese Arbeit wurde nicht als Diplomarbeit oder ähnliche Prüfungsarbeit verwendet.

Hannover, im Juni 2007

Zusammenfassung

Die *in vitro* Rekonstruktion von dreidimensionalem knochenartigen Gewebe erfordert die Verfügbarkeit einer ausreichenden Menge von Zellen, ein geeignetes Trägergerüst zur Zellbesiedlung, sowie eine geeignete Kultivierungsmethode, die eine homogene Zellverteilung und Gewebeneubildung in der gesamten Gerüststruktur ermöglicht. Zielsetzung dieser Dissertation war die Untersuchung von trabekulären Knochenzellen auf deren Eignung zur Geweberekonstruktion von Knochen, sowie die Entwicklung eines Herstellungsverfahrens zur Produktion von implantierfähigem menschlichen Knochengewebe *in vitro*. Hierzu wurde zunächst die Isolierung, Kultivierung und Expansion humaner trabekulärer Knochenzellen etabliert. Die Zellen wurden im größeren Maßstab in Wannenstapel erfolgreich expandiert und der mesenchymale Stammzellcharakter dieser Zellen durch ihr adipogenes, chondrogenes und osteogenes Potenzial verifiziert. Ein geeignetes Trägergerüst aus Poly-(lactid-glycolid)-Copolymer und Kalziumphosphat wurde mit den trabekulären Knochenzellen besiedelt. Die Kultivierungsverfahren unter statischen und dynamischen Bedingungen wurden miteinander verglichen. Die dynamische Kultivierung erfolgte in einem neuentwickelten Rotationskultivierungssystem, dass eine wipp- und rotationsartige Bewegung kombiniert und in einem Perfusionsbioreaktor. Unter Verwendung des Rotationskultivierungssystems, konnte im Vergleich zu den bislang bekannten Kultivierungstechniken, eine ausreichende Medium- und Sauerstoffversorgung, eine deutlich bessere Zellverteilung und eine deutlich bessere neu gebildete extrazelluläre Matrixverteilung im Inneren des Gerüsts erreicht werden. Histologische Untersuchungen, sowie unterstützende biochemische Analytik bestätigen eine *de novo* Knochenbildung. Die Qualität der Neubildung wurde durch die wipp- und rotationsartige Bewegung stark verbessert. Hinsichtlich einer klinischen Anwendung des kultivierten Zell-Gerüst-Konstrukts zur Regeneration von Knochendefekten *in vivo*, ist dieser Kultvierungsansatz sehr vielversprechend.

Schlagwörter : Mesenchymale Stammzellen, Osteogenese, Geweberekonstruktion.

Abstract

This dissertation set out to address the goal of optimizing and developing three dimensional cultivation conditions by exposing human mesenchymal-like stem cells in conjunction with a porous scaffold, to the correct mechanical and biochemical stimulus in an optimal microenvironment to improve current protocols and strategies in bone tissue engineering. Trabecular bone was demonstrated to be a good and readily available source of mesenchymal progenitor cells. A high yield isolation procedure was established from small bone tissue biopsies and the isolated cells were successfully expanded reproducibly on a large scale in cell factories. Their multilineage differentiation potential, displaying the ability to differentiate into the adipogenic, chondrogenic and osteoblastic lineage was also successfully demonstrated. For three dimensional bone-like tissue formation *in vitro*, these cells were cultivated in conjunction with a Poly-(lactic-co-glycolide)/calcium phosphate scaffold statically, as well as dynamically in a fixed bed perfusion bioreactor and in a novel tilted rotating system. Despite improved nutrient delivery in both dynamic systems, ubiquitous cell and newly deposited extracellular matrix distribution throughout the whole scaffold structure was observed to occur when cultivated in the tilted rotating bioreactor system. Improved osteogenesis through the tilted rotating movement was supported by in depth histological analysis and biochemical analysis of bone-specific markers. The viable reconstructed cell-scaffold construct generated *in vitro* in the tilted rotating system showed high resemblance to native bone tissue in terms of osteocytic cell shape held within the extracellular matrix, interacting with each other through specific bone gap junctional proteins with a very high chance of being integrated *in vivo* representing a promising tool for bone defect regeneration.

Keywords: Mesenchymal stem cells, osteogenesis, tissue engineering.

Table of Contents

1. General Introduction

1.1. Overview and State of Research

1.1.1. The Bone and Joint Decade: 2000-2010

In January 2000, the world health organization (WHO) declared 2000-2010 to be the "Bone and Joint Decade" with the goal of raising awareness regarding the growing burden of musculoskeletal diseases on society as well as healthcare systems worldwide and, further, to advance research in prevention, diagnosis and improving treatment of these disorders (Lidgren, 2000). In this context, more than 150 different musculoskeletal disorders exist, which can lead to limited mobility, complete disability and in some cases even death. Primarily, the focus of the initiative of the bone and joint decade lies on osteoarthritis, rheumatoid arthritis, osteoporosis, spinal disorders, low back pain and trauma cases to the extremities (Lidgren, 2003).

Musculoskeletal conditions have a major impact on society due to their frequency and the associated resulting chronic disability. As a result, in developed countries, they lead to high rates of sick leave from work and, further, constitute the second most common reason for consulting a doctor (Woolf and Pfleger, 2003). In Germany alone, up to 50% of all women and 15% of all men over 65 will eventually suffer from an osteoporotic fracture, more than half of the population over 60 is predicted to suffer from arthritis and more than 50% of all women and men over 30 will complain of back pain. In fact, in Germany, musculoskeletal conditions are responsible for 40% of all sick leave absences (Dreinhoefer, 2000; http://www.boneandjointdecade.de).

If the therapeutic approaches in treating these diseases fail, as for instance by the administration of estrogen replacement therapy, calcitonin or bisphosphonates (Rodan and Martin, 2000), then these conditions could eventually lead to extensive bone and to eventual fractures. Healing the resulting skeletal defects will mostly require bone tissue replacement to restore the function of the traumatized or lost bone, which remains an

important clinical challenge, especially in non-union cases when bone is not able to regenerate itself and the body needs outside help to overcome this limitation. Current clinical therapies for bone substitution include:

1. Autogenous bone grafts are well recognized as the gold standard with the best clinical results. Healthy bone is usually harvested from the iliac crest and implanted at the site of repair in the same patient, thus circumventing immunological incompatibilities as well as providing high viability and vascularization of the graft to be implanted. However, this method is associated with severe pain at the site of harvest for the patient as well as a significant risk of infection with a substantial morbidity rate (Goulet et al., 1997). Further limitations include the limited availability and size of the excised healthy bone tissue as well as difficulties in shaping the graft to fill the defect and the requirement for several procedures to complete the treatment (Kakar and Einhorn, 2005).
2. When autogenous graft material is not available, donated bone tissue from another individual can be transplanted into a patient, known as allograft or homograft. Allografts are often taken from cadaver and stored on ice. A major limitation associated with this procedure is the immunological rejection of the implant material, potential disease transmission and new bone is slower both in formation and in vascular penetration compared to autografts as it is devoid of viable osteogenic cells and therefore making it less effective, as well as limiting its application in orthopedic surgery (Brown and Cruess, 1982).
3. Acellular matrix based therapies: Structural implant like titanium fiber metals or ceramics (hydroxyapatite and/or tricalcium phosphate) are implanted to replace the missing bone tissue. Despite the mechanical support offered for instance by metals, their lack of biologic activity leads to poor integration into the host tissue. Ceramics, on the other hand, are very brittle and provide poor support. Moreover, despite their porous nature, they have a very slow resorption rate, therefore limiting their use (Bruder and Fox, 1999). To overcome these limitations, osteoinductive factors like bone morphogenetic proteins are provided at

the site of repair but the optimal dose of the protein as well as its mode of delivery has not been established yet (Gerhart et al., 1993).

The complications mentioned in the above methods associated with bone grafting procedures, point to the need of an alternative bone substitute solution that (i) minimizes dissection around the donor site, (ii) causes no immunologic reaction and (iii) is readily available off the shelf. The emerging field of bone tissue engineering with the goal to generate biological substitutes to replace damaged or lost bone tissue addresses this need. Tissue engineering has been defined as the application of the combined principles and methods of engineering and life sciences for the development of biological substitutes to restore, maintain or improve organ function (Langer and Vacanti, 1993; Vacanti, 2006).

1.1.2. Tissue Engineering of Bone

The aim of implanting tissue engineered bone is to activate bone regenerative abilities at a specific anatomic location in the body that has been damaged and needs to be restored or replaced. Ideally, in a way, that allows the newly formed bone to be completely integrated with the surrounding skeleton of the patient (Nerem, 2006). For an approach to reconstruct bone *in vitro*, which can best mimic an autogenous bone graft, the following essential fundamentals are required: **Firstly**, an osteogenic cellular component that is able to give rise to new bone tissue, needs to be provided at the site of treatment. Cells are either introduced from an external source or are recruited from within the body to the site of repair. **Secondly**, nutrients and stimulatory factors must be available for cellular proliferation and maturation, leading to matrix deposition and eventual mineralization of the newly laid down tissue. **Finally**, a scaffold* must be introduced to provide a substrate for the cellular attachment and serving as a temporary structural template supporting attachment, migration and proliferation of the cells (Bruder and Fox, 1999; Kakar and Einhorn, 2005). Successful protocols for bone regeneration will provide the scaffolds and associated cells to establish active contours and communication sites, which will enable complete functional integration of the

newly implanted tissue with the surrounding host tissue (Caplan, 2003). One scenario of a clinical relevant approach for bone tissue engineering would involve the use of autologous patient derived cells (to reduce graft versus host reaction) brought in close proximity in conjunction with a biodegradable scaffold in an environment leading to cell-cell interaction as well as cell-scaffold interaction. This is best achieved in a bioreactor**, which is designed to control the cellular environment via enhanced mass transfer leading to spatial and uniform cell distribution throughout the three dimensional scaffold, responding to signals for proliferation and differentiation (Vunjak-Novakovic, 2004).

*A scaffold is defined as a porous structure (made up of ceramic, polymer or natural compound), which either provides support at site of defect or within which cells are seeded, providing a geometrical structure for cells to reorganize and form three dimensional multicellular tissues.

**A bioreactor is defined as a device in which biological processes develop under regulated and controlled conditions (e.g. monitored temperature, pH, balanced nutrient supply and waste removal) (Martin et al., 2004).

1.1.3. Basic Bone Biology and Natural Formation of Bone

Bone is a composite material consisting of mineral, organic matrix (mainly composed of collagenous proteins), cells and water with its structure and composition varying with the tissue site as well as with age, diet and health status (Boskey, 2005). In general, there are two forms of bone: compact bone (cortical) and trabecular bone (cancellous). They share the same composition and mainly differ in their porosity, with compact bone being only 10% porous, thus rendering it stronger with a higher density than trabecular bone, which has a porosity ranging from 50-90% (Buckwalter et al., 1996b). Compact bone makes up ca. 80% of the mature skeleton and is mainly found in the diaphyses (the main mid section) of long bones, while cancellous bone is mainly found in short bones (e.g. tarsals, vertebral bodies) and flat bones (e.g. skull, pelvis) as well as in the metaphyses (the area between the diaphyses and the growth plates) of long bones (Buckwalter et al., 1996b). Histologically, bone can be

divided into woven and lamellar bone. Woven bone only appears in the embryonic skeleton as well as in fracture healing and repair processes with the later developed mature skeleton mainly composed of lamellar bone (Gratzl, 2002). Woven bone is characterized by an irregular pattern of collagen fibrils and random mineralization patterns while collagen fibrils in lamellar bone are tightly organized in parallel sheets, forming distinct lamellae with uniform distribution of minerals within the matrix (Cooper et al., 1966). There are three forms of lamellar bone (Figure 1): the trabecular lamellae of cancellous bone, the inner and outer circumferential lamellae of compact bone and the lamellae of osteons (also known as Haversian systems). Each lamella consists of collagen fibrils, the alignment direction of which alternates in adjacent lamellae. Osteons, longitudinally aligned cylindrical units, form the bulk of the diaphysal cortex and are formed by circular lamellae sheets surrounding central canals containing blood vessels and lymphatic vessels known as the Haversian canals (Kuehnel et al., 2002). Small canals termed canaliculi, branch from the central canal in a radial pattern delivering nutrients to the cells embedded in the matrix in spaces known as lacunae. The external surface of bone is covered by the periosteum, which consists of an outer fibrous layer containing bundles of strong collagenous fibers termed Sharpey's fibers and an inner cellular layer containing cells capable of forming bone. Oblique vascular channels known as Volkmann's canals connect the osteons to each other and to the periosteum. Both canal systems supplying bone tissue with a rich vasculature with no cell lying more than 300 μm away from a blood vessel (Buckwalter et al., 1996b). The bone marrow is contained in the central cavity of the diaphyses in compact bone as well as in the spaces in-between the bone trabeculae in cancellous bone.

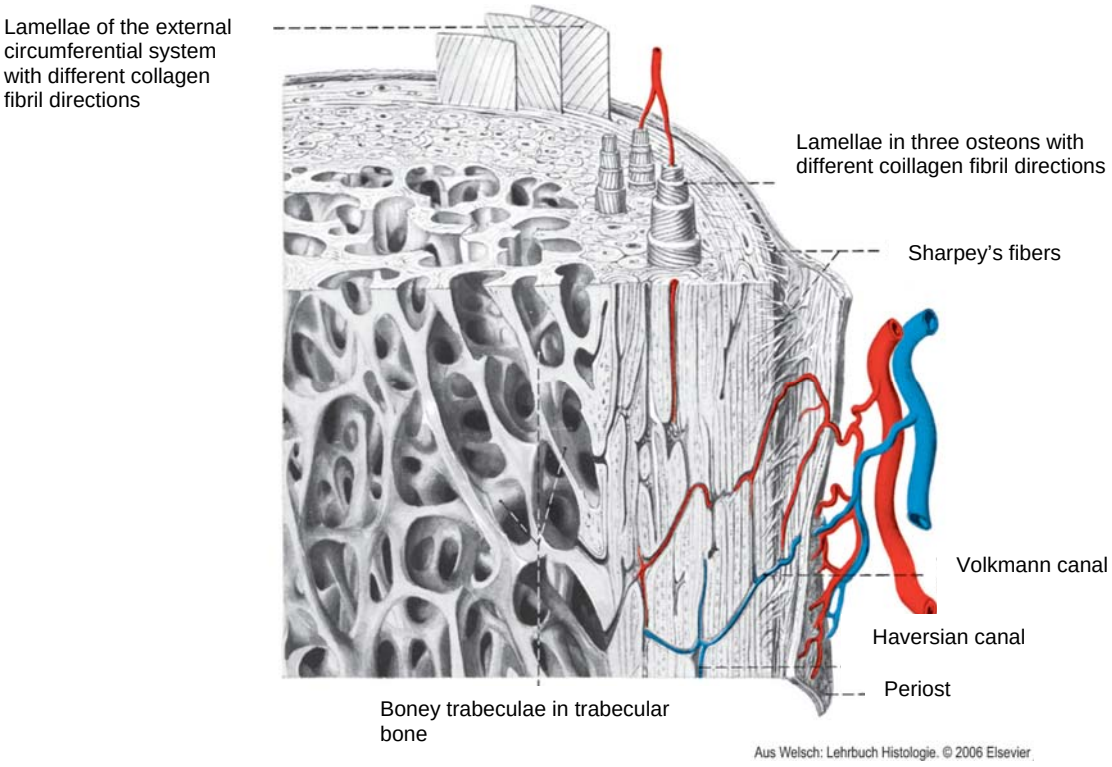

Figure 1 Diagram of the structure of lamellar bone. Showing the outer and internal circumferential lamellae of cortical bone, the osteonal lamellaes as well as the intraosseous vascular system with the Haversian and Volkmann canals and the periosteum covering the external surface of bone.

1.1.3.1. Bone Cells and Matrix Formation *in vivo*

The skeletal system is continuously remodeling with specialized bone cells keeping the balance between bone resorption and formation. Bone cells originate from a mesenchymal stem cell line including the undifferentiated cells, osteoblasts, bone lining cells and osteocytes and from a haematopoietic stem-cell line represented by the macrophages from which the osteoclasts arise (Doll, 2005; Gay, 2005).

Undifferentiated Bone Cells –Mesenchymal Stem Cells

Several studies have provided evidence for the presence of a pool of undifferentiated progenitor cells within bone tissue, residing in the bone canals, periosteum and the bone marrow (Friedenstein et al., 1976; Beresford, 1989; Diaz-Flores et al., 1990; Nakahara et al., 1990). Caplan called these cells

mesenchymal stem cells (Caplan, 1991). A stem cell is defined by textbooks as a cell that can divide asymmetrically to generate one daughter cell that is a stem cell and another daughter cell, which produces differentiated descendants (Weismann, 2000) including chondrogenic cells that form cartilage, osteogenic cells forming bone, adipogenic cells to form fat next to other cells fabricating connective tissue (summarized in Figure 2). Mesenchymal stem cells function to generate replacement for the differentiated cells, especially in cases of injury and disease repopulating the affected tissue with progenitor cells (also known as homing) to later become part and function in the tissue again (Verfaille, 2006). Their self- renewing activity decreases with progressing age after peaking in the late 20s in humans (Caplan, 2005).

Osteoblasts

Osteoblasts, are cells arising from the multipotent mesenchymal stem cells that form bone (Aubin, 2001). They line the surface of bone, tightly packing against neighboring osteoblasts with a round polyhedral morphology and extended cytoplasmic processes to communicate with other cells (Buckwalter et al., 1996b). Their function lies in matrix production by mostly secreting collagenous proteins (mainly collagen type I in addition to small amounts of type III, type V and type XII) next to other noncollagenous proteins (5% of the bone matrix) including osteopontin, osteocalcin and bone sialoprotein forming the organic matrix of bone known as osteoid (Heinegard and Oldberg, 1998). Matrix production is followed by mineralization, which is also facilitated by osteoblasts through a mechanism that is not completely understood so far. One hypothesis is that mineralization is initiated in association with extracellular matrix vesicles (Anderson, 1995). Matrix vesicles are defined as extracellular membranous particles released by budding from the surface of osteoblasts to be deposited into the newly formed matrix (Anderson, 1969).

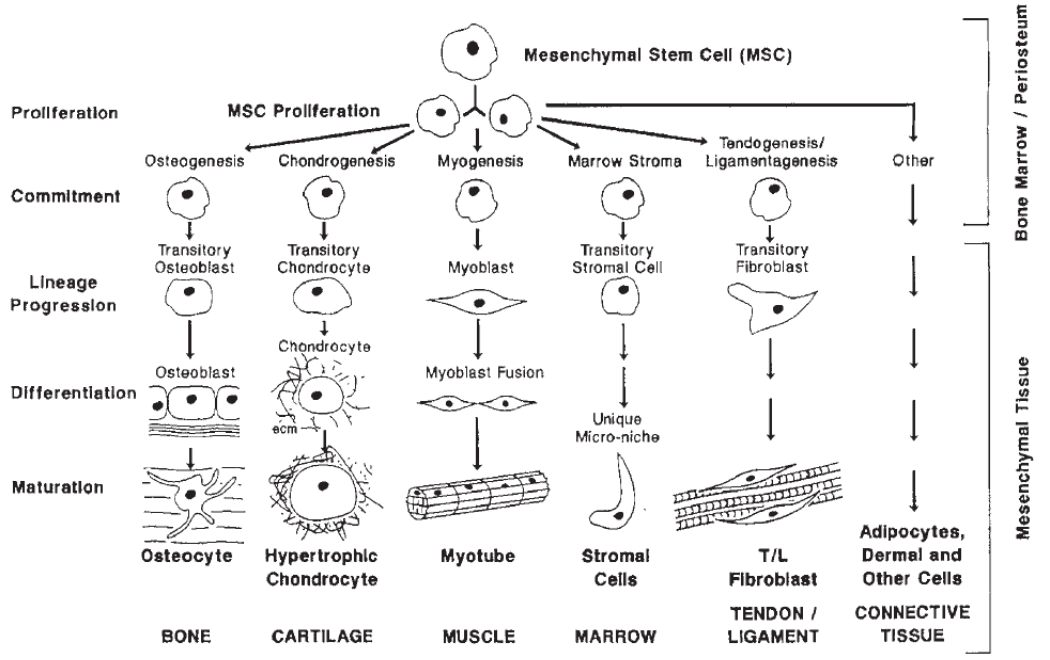

Figure 2 Schematic diagram showing the multipotential capacity of mesenchymal stem cell. Fibroblast like cells derived from bone marrow and periost have the ability to differentiate into bone, cartilage, muscle, marrow stroma, tendon and other connective tissue. The diagram is adapted from Caplan (2005).

Some time after the expulsion of the vesicles into the collagenous extracellular matrix, crystalline minerals first arising inside the vesicles, perforate the vesicle membranes and serve as templates for further mineralization. The rate of mineral crystal proliferation is governed by an interaction between the levels of ionic calcium and phosphate available in the extracellular fluid, the enzyme alkaline phosphatase that is enriched in the extracellular matrix vesicle membrane and the adjacent collagen fibrils (Anderson, 2003). Once the process has been initiated, mineral deposition occurs in and on the collagen fibrils in a spatially oriented axial and lateral manner (Arsenault et al., 1991). Mineralization gives bone its mechanical properties. Failure to mineralize the organic matrix by active osteoblasts, however, leads to weak bone and pathological fractures as in the case of rickets and osteomalacia. Osteoblasts in bone tissue either remain on the surface of bone, assuming a flat cell form and decreased synthetic activity or they surround themselves with matrix and become osteocytes, eventually disappearing from the site of bone formation.

Osteocytes

The most abundant cell in bone is the osteocyte, forming 90% of all cells (Donahue, 2005). They develop from osteoblasts that have become entrapped in their deposited mineralized matrix. Osteocytes have a stellate morphology with extensive dendritic-like processes found in the canaliculi of bone tissue (Kato, 1997; van der Plas and Nijweide, 2005). From their position deep inside the matrix of bone and through their long cytoplasmic processes, they communicate with neighboring osteocytes and surface osteoblasts and are able to detect mechanical loading signals, transducing them to an appropriate remodeling response (Palumbo et al., 1990; Yellowley et al., 2000).

Bone lining cells

Morphologically, they have an elongated flattened shape lying on the surface of the bone matrix with cytoplasmic extensions penetrating the matrix to communicate with the dendritic extensions of the osteocytes. They are also called resting osteoblasts or surface osteocytes and may have a role in attracting osteoclasts to specific sites for remodeling (Buckwalter et al., 1996b).

Osteoclasts

Osteoclasts are multinucleated cells identified as bone-resorbing cells and are generated from fusion of haematopoietic cells of the monocyte-macrophage lineage (Suda et al., 1992). In balanced states, bone remodeling usually involves equal participation of bone resorption activity by osteoclasts and bone formation by osteoblasts. Disturbing this balance like excessive bone resorption leads to osteopenic conditions (e.g. osteoporosis and arthritis), as opposed to osteopetrosis, which is a disorder characterized by extremely dense bone and calcified marrow which is caused by failure of resorption. Upon maturation of the osteoclasts, they cycle between active and inactive states of bone resorption. Morphologically, osteoclasts have a characteristic ruffled border (Scott and Pease, 1956) that consists of finger like cytoplasmic projections providing a high surface area. When actively resorbing, osteoclasts

flatten against and attach to the bone surface through the cytoplasmic protrusions, through which acidified solution is secreted and at which hydrolytic and photolytic enzymes are concentrated and released (e.g. carbonic anhydrase, acidic collagenase), dissolving the mineral deposits and breaking down the matrix (Hall and Kenny, 1985).

Bone Cell Interaction; Intercellular Communication

The interaction amongst osteogenic and osteolytic cells in between themselves as well as with the extracellular matrix is essential for skeletal development. The cells are in contact with each other through long cytoplasmic processes containing gap junctions. Gap junctions are membrane-spanning intercellular channels that allow for the passage and exchange of small molecules and ions between the cytoplasm of two communicating cells (Lecanda et al., 1998). Each gap junction pore requires the contribution of two adjacent cells and is formed by juxtaposition of two hexameric hemi-channels, known as connexons. Thus, two connexons of two cells interact in the extracellular space to form the complete intercellular channel, the gap junction. Each connexon in turn is composed of six similar proteins, which are termed connexins. Connexin 43, a gap junction channel protein, was found to be the most abundant one in osteoblasts and osteocytes (Civitelli et al., 1993; Mason et al., 1996; Kato et al., 1997; Thi et al., 2003). Figure 3 shows a schematic drawing adapted from Makowski et al. (Makowski, 1977), demonstrating the structure of a gap junction. This interconnection between osteoblasts, osteocytes and bone lining cells via gap junctions forms a 'social network' of cells that enables them to pass information between themselves in a coordinated manner, regulating the movement of ions in and out of the network as well as transmitting and amplifying signals from and to the extracellular matrix, whether it be mechanical signals or passage of ions, thus playing a pivotal role in bone formation (Yellowley et al., 2000; Cheng et al., 2001; Donahue et al., 2005). Figure 4 shows a scanning electron micrograph adapted from Doty (1981), displaying two adjacent bone cells communicating via a gap junction.

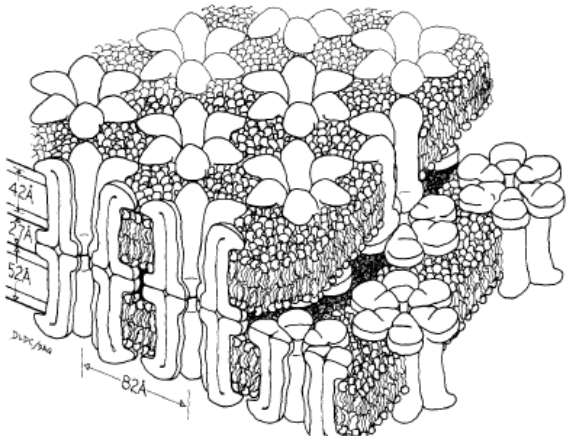

Figure 3 Drawing of a gap junction structure adapted from Makowski 1977. The illustration show two adjacent cell membranes of two cells in juxtaposition, with connexons spanning the membrane of each cell. Each connexon is made up of 6 units, the connexins. A gap junction is formed through the interaction of two hexons forming a channel like structure. Adapted from: Makowski, et al. (1977).

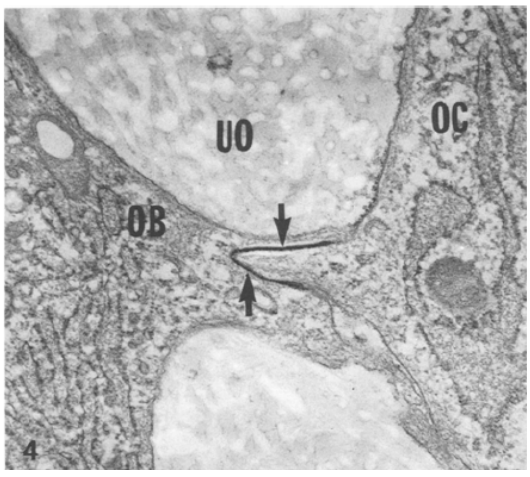

Figure 4 Scanning electron microscopy micrograph adapted from Doty 1981 showing a gap junction between two adjacent bone cells (indicated by arrows). An osteoblast (OB) communicating with an osteocyte (OC) through cytoplasmic processes surrounded by unmineralized osteoid (UO). X 24,000. Adapted from: Doty, S. B. (1981).

1.1.4. *In vivo* Bone Formation

Bone can be either formed via intramembranous ossification or endochondral ossification (Scott and Hightower, 1991). The basic mechanism for intramembranous skeletal bone formation begins with the accumulation of mesenchymal stem cells, followed by their direct differentiation into

osteoblasts, which actively secrete a specialized, densely fibrous extracellular matrix (osteoid) into which calcium phosphate crystals are deposited, culminating in a mineralized matrix (Doll, 2005). In endochondral ossification, the accumulated mesenchymal cells differentiate into chondrocytes first depositing a cartilage model (or anlage) of the future bone growing as a result of the proliferation of the chondrocytes and the secretion of matrix. The mesenchymal stem cells of the perichondrium, located at the mid-portion of the cartilaginous shaft, produce a layer of osteoblasts that deposit mineralized bone on the surface leading to gradual transformation of the perichondrium to the periost (Rosenberg and Roth, 2007). The cartilage is gradually resorbed by active osteoclasts while new bone tissue is being deposited by osteoblasts (Syftestad et al., 1985; Ferretti et al., 2006). Figure 5 shows the development of the osteoblasts into osteocytes embedded in the mineralized matrix as well into bone lining cells (osteoblasts aligned on the surface of the bone tissue).

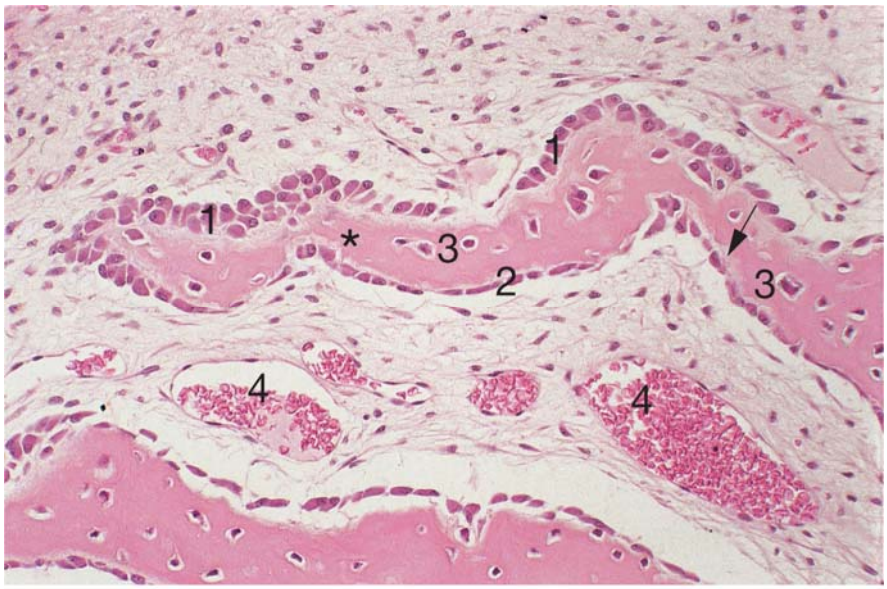

Figure 5 Micrograph showing bone cells in the process of bone formation (lower mandibular bone, human tissue). Haematoxylin&Eosin staining showing active osteoblasts **(1)** and bone lining cells **(2)** and osteocytes in lacunae embedded in the matrix **(3). (4)** Blood vessels. Magnification: x250.

Long bones such as the femur and humerus and bones of the vertebral column are formed this way. In intramembranous ossification, no cartilage is formed and the mesenchymal cells organize themselves into layers or membranes that contain blood vessels and osteogenic cells depositing matrix and mineralizing it. Flat bones of the skull, face and pelvis are formed this way as well as the

formation of new bone during healing of fractures (Buckwalter et al., 1996a; Thompson et al., 2002).

1.1.5. *In vitro* Bone Formation

Techniques for the isolation of bone derived mesenchymal cells and techniques for directing the cells into the osteogenic lineage have been established (Owen, 1988; Bruder and Caplan, 1990; Jaiswal et al., 1997; Pittenger et al., 1999; Buttery et al., 2001). To induce osteogenesis *in vitro*, the conditions necessary for *in vivo* bone formation provided by the active bone cells have to be mimicked by distinct additives to induce cells to produce an extracellular matrix and eventually mineralize it. Theses additives, which are classically added to osteoinductive medium for *in vitro* cell culture, include ascorbic acid, ß-glycerophosphate and dexamethasone. Ascorbic acid is known to induce matrix deposition, stimulating the cells to synthesize collagen (Blanck and Peterkofsky, 1975; Jeffrey and Martin, 1966). ß-glycerophosphate serves as a source for organic phosphate and encourages mineral deposition (Chung et al., 1992; Sottile et al., 2003). The effect of dexamethasone depends on the stage of differentiation of the osteoblasts (Cooper et al., 1999) and includes induction of alkaline phosphatase expression and an increase in the number and size of mineralized nodules (Cheng et al., 1994).

To better understand the process of *in vitro* bone formation, several studies have described the developmental sequence of the differentiation stages a cell undergoes *in vitro* to form bone (Owen et al., 1990; Stein and Lian, 1993; Siggelkow et al., 1999; Aubin, 2001). These can be summarized into the following three distinct stages:

1. **Cell proliferation and extracellular matrix formation:**

In this phase, the cells cultured in osteogenic medium gradually develop the osteoblast phenotype and start depositing the extracellular matrix with collagen type I as the major constituent, making up 30% of the dry non-mineralized matrix (Boskey, 2005). In general, type I collagen peaks during the proliferation phase and declines thereafter.

2. Cell differentiation and extracellular matrix maturation and organization:

The extracellular matrix is organized in this phase and prepared for the final mineralization. The proliferation of cells shuts down in this phase and proteins associated with the differentiated osteogenic cell phenotype like alkaline phosphatase are highly expressed in this phase declining thereafter.

3. Extracellular matrix mineralization:

The final phase in the osteoblast differentiation culminates in ordered mineral deposition along the collagen fibrils of the extracellular matrix.

Stein and Lian (1993) have elaborated two transition points osteogenic cells have to pass through before terminal mineralization occurs. The first is at the end of the proliferation period (phase 1), at which collagen type I production rate is down regulated after reaching a peak and expression of the proteins responsible for the maturation of the extracellular matrix (e.g. alkaline phosphatase) is initiated. The second transition point is from phase 2 into phase 3, at the onset of mineralization after alkaline phosphatase expression peaks and is down regulated thereafter. The developmental sequence of osteoblast differentiation is illustrated schematically in Figure 6, showing a reciprocal pattern between proliferation and differentiation (Stein and Lian, 1993).

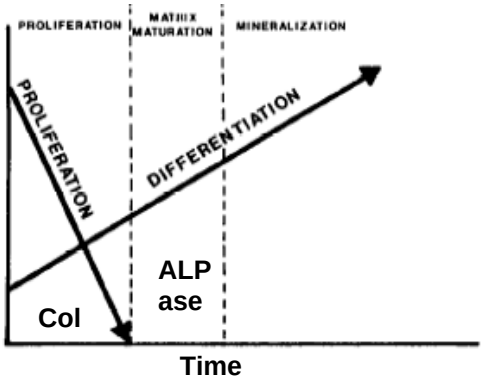

Figure 6 Schematic illustration of a proposed model for the three stage developmental sequence of osteogenic cells during *in vitro* bone formation. The relationship between proliferation and differentiation during development of the osteogenic phenotype showing the proliferation phase terminating with the down regulation of collagen type I (col), the matrix maturation phase marked by a peak in alkaline phosphatase expression (ALPase) which is down regulated upon transiting into the final mineralization phase. Illustration adapted from: Stein and Lian (1993).

1.1.6. Bone Tissue Engineering Strategy for the Generation of an *in vitro* Bone Construct

To successfully achieve bone tissue engineering (Section 1.1.2.), the three main requirements, namely, appropriate cells, a scaffold and a three dimensional cultivation environment (bioreactor) are elaborated in the following sections.

1.1.6.1. Stem Cells in Bone Tissue Engineering

One of the major limitations in engineering tissue constructs for clinical use is the availability of sufficient human derived cells. Stem cells, derived from either embryonic or adult tissue are considered to be an attractive cell source as they have the advantage of being able to undergo extensive *in vitro* replication on a sufficient scale for therapeutic applications without losing their ability to differentiate into various lineages, thus serving as ideal blocks for tissue regeneration (Gregory et al., 2005; Bianco and Robey, 2001). Which stem cells are most suited for tissue engineering purposes is still controversial.
Embryonic stem cells are cells derived directly from the inner cell mass of pre-implantation embryos after the formation of a blastocyst. They are characterized by their self-renewal and their capacity to differentiate into all cell phenotypes (pluripotent). Despite their pluripotency and extensive proliferative potential, there are major ethical limitations and legal controversies as well as the associated danger of them inducing a tumor, which has restricted their use so far.
Considering these controversies, researchers were prompted to study adult stem cells, cells residing in adult tissue as a possible source for tissue engineering purposes. In spite of their limited differentiation potential, compared to embryonic stem cells, their established and ease of isolation *in vitro* as well as their extensive expansion potential, has rendered them an attractive choice for tissue reconstruction *in vitro* (Fibbe, 2002; Tuan et al., 2003).

1.1.6.2. Scaffolds in Bone Tissue Engineering

A scaffold is designed to either just provide support at the site of repair or to deliver cells as well supporting their regenerative capability by providing temporary mechanical load at the site until it has been replaced by newly laid down tissue (Hollister et al., 2005).

To enhance bone regeneration, a scaffold should meet a number of requirements. Ideally, it should have the following properties (Bruder and Fox, 1999; Hutmacher et al., 2001; Vunjak-Novakovic, 2003; Caplan, 2005):

i. Scaffolds should be biocompatible (non-immunogenic), bioresorbable (totally eliminated in the body without residual by-products remaining) or biodegradable (when the material is broken down into by-products, which are moved away from the site but not necessarily totally eliminated from the body, ideally resulting in non toxic by-products).
ii. Possess a suitable surface chemistry allowing optimal cell attachment, proliferation and differentiation.
iii. Sufficient mechanical strength to initially maintain and support the defect site to be repaired.
iv. Be highly porous with an interconnected pore network for homogenous cell growth and flow transport of nutrients and metabolic waste, allowing bioactive molecules to have access to the cells as well as facilitating later neovascular invasion.
v. Ability of being reproducibly processed into a variety of shapes and sizes according to clinical needs.

Various suitable materials have been developed and investigated by tissue engineers and can be divided into the following:

1. Ceramics

Synthetic ceramics like ß-tricalcium phosphate and hydroxyapatite as well as natural ceramics like coralline hydroxyapatite have been used as their structure is very similar to the mineral phase of native bone. Despite their osteoconductivity and open porous structure, major drawbacks in their use

include their brittleness (low mechanical stability) and slow resorption rates (Yaszemski et al., 1996; Karageorgiou and Kaplan, 2005).

2. Natural Polymers

Polymers from natural sources include collagen, polysaccharides (e.g. agarose and chitosan) and hyaluronic acid. They have the advantage of low immunogenicity and biodegradability. Nevertheless, the low mechanical strength and high degradation rates results in them needing chemical modification, thereby reducing their biocompatibility (Salgado et al., 2004).

3. Synthetic Polymers

The versatility of chemically synthesized polymers enables fabrication of scaffolds with different porosities, rate of degradation and mechanical properties according to the needs of tissue engineers. Regulatory approved polymers include polycaprolactone (PCL), polyglycolide (PGA), polylactides (PLA) and the copolymer of PLA and PGA forming poly (lactic-co-glucolic acid), (PLGA). They are degraded *in vivo* into acidic by-products, which might result in inflammatory reactions. Therefore it is important that, at all times, the cell-scaffold construct is continuously exposed to sufficient quantities of neutral culture media so as to wash away the acidic by-products (Hutmacher et al., 2001).

4. Composites

By incorporating tricalciumphosphate or hydroxyapatite (ceramics) with synthetic polymers (e.g. PLGA), cell adhesion is improved and the mechanical strength can be tailored (Marra, 2005). Drawbacks of the individual components (brittleness and acidic metabolites) can be overcome with the basic ceramic nature buffering the acidic gradients of the synthetic polymers helping to avoid an unfavorable environment for the cells (Hutmacher, 2000).

1.1.6.3. Bioreactors in Bone Tissue Engineering

To provide the microenvironment necessary for osteogenic cells to regenerate functional bone in conjunction with a three dimensional scaffold structure, bioreactors are applied. They are designed to meet one or more of the following functions (Vunjak-Novakovic et al., 2003):

1. Lead to homogenous and uniform cell distribution within the three dimensional structure of the scaffold.
2. Control the cultivation conditions in terms of temperature, dissolved oxygen levels, pH, nutrients and metabolites.
3. Improve mass transport (soluble nutrients and oxygen) between the cells and the cultivation environment.
4. Provide mechanical stimulatory signals of physiological relevance leading to improved *in vitro* tissue formation simulating *in vivo* conditions.

Three bioreactors that are commonly used in bone tissue engineering are listed below: (illustrations are adapted from Martin, I., Wendt, D., Heberer, M., 2004.The role of bioreactors in tissue engineering. Trends Biotechnol 22, 80-86).

1. Spinner flasks, in which the cell-scaffold constructs are fixed in place, attached to needles hanging from the lid (Figure 7). The surrounding medium is mixed with a magnetic stirrer, creating a turbulent shear at the surface of the construct, enhancing mass transfer by induced distribution of the oxygen and nutrients throughout the medium and gas exchange takes place through surface aeration. The system has been used for bone and cartilage tissue engineering (Sikavitsas et al., 2002; Meinel et al., 2004a) with improved tissue formation compared to the static system.

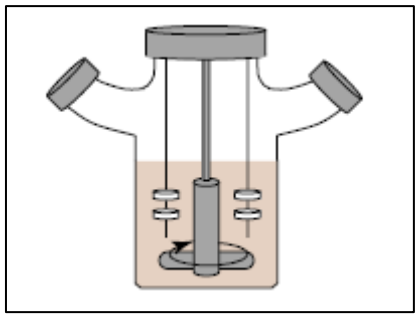

Figure 7 Spinner flask bioreactor.

2. Perfusion bioreactors, in which cell-scaffold constructs are directly perfused by pumping medium through the pores of the cells-scaffold construct, overcoming mass transport limitations by delivering nutrients and oxygen to all parts of the scaffold (Figure 8). The scaffold is usually placed in a perfusion chamber minimizing the non-perfusing flow that goes around the cultured scaffold (Bancroft et al., 2003). Direct perfusion is a valuable tool to overcome mass transport limitations and improve tissue cultivation *in vitro* compared to the static system but the effects of the perfusion are highly dependent on the medium flow rate and the maturation stage of the cell-scaffold construct. Therefore, a balance between the efficient mass transport and retention and maintenance of the newly synthesized extracellular matrix within the scaffold has to be met as increased shear stress could eventually lead to tissue components being flushed away from the scaffold structure (Martin et al., 2004).

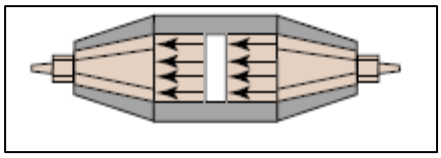

Figure 8 Perfusion bioreactor.

3. Rotating bioreactors, in which cell-scaffold constructs are freely suspended in a space between two cylinders or in which the cell-scaffold constructs are fixed and rotated during the cultivation. The bioreactor was first introduced by scientists at the National Aeronautics and Space Agency (NASA), as the rotating wall vessel bioreactor (Figure 9) which was originally designed to simulate microgravity conditions involving solid body rotation around a horizontal axis (Duray et al., 1997). Rotation of the medium around the constructs, whether free falling (Unsworth and Lelkes, 1998; Martin et al., 2004; Marolt et al., 2006) within the vessel or fixed in place (Kasper et al., 2007; Suck et al., 2007), enhances mass transport with low levels of shear stress and was shown to improve spatial cell distribution within the scaffold as compared to static cultivation conditions.

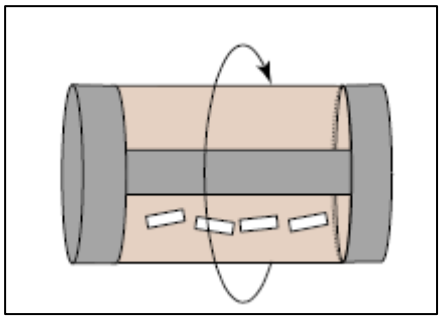

Figure 9 Rotating bioreactor.

1.2. Rationale of the Study

Successful tissue engineering of bone, essentially requires an available source of osteogenic cells brought into a cultivation environment, maintaining and promoting cell function in conjunction with a three dimensional matrix *in vitro*. A major limitation associated with three dimensional culture systems is the establishment of a technique that leads to the generation of tissue constructs showing homogenous cell distribution throughout the whole three dimensional structure of the scaffold, especially when scaffolds of relatively large parameters are used (Meinel et al., 2004b; Sikavitsas et al., 2002). Stationary culture is by now well known to only support cell growth at the periphery of a scaffold, leaving the central core free of cells due to the limited potential for soluble nutrients and oxygen to diffuse towards the interior. Maximum ingrowth has been reported between 200-400 µm from the outer scaffold surface (reviewed by Martin et al., 2004). To overcome this nutrient limitation, several dynamic cultivation systems have been investigated and are still being developed further to reach homogenous cell distribution and uniform tissue formation *in vitro*. Uniform cartilaginous and bone like constructs were successfully cultivated in rotating bioreactors using scaffolds 5-8 mm in diameter and 2 mm thick (Marolt et al., 2006; Vunjak-Novakovic et al., 2003). Furthermore, the hypothesis that perfusion increases cell ingrowth through the continuous exchange of medium and constant removal of metabolic waste, has also been supported by several groups, who have developed three dimensional perfusion systems for *in vitro* bone formation (Bancroft et al., 2002; Holtorf et al., 2005; Sikavitsas et al., 2003; Wendt et al., 2006). To meet this purpose as well and to provide a microenvironment for a high degree of differentiation and better tissue development, two different dynamic cultivation models were to be examined in this study. Namely, a fixed bed perfusion bioreactor developed by our group, which has been shown to improve the cultivation of rat bone marrow derived cells in conjunction with a porous matrix (Barthold, 2003) as well as rabbit bone marrow derived cells (Fargali, 2006). In addition to a novel tilted rotating bioreactor system producing a

tilted rotating motion, which so far has not been investigated for its applicability with regard to producing bone-like constructs *in vitro*.
The ultimate goal of bone tissue engineering is the translation of the outcome of basic research into suitable clinical protocols for improved human therapy potentials. Within this context, the present study wished to elucidate whether bone-like constructs can be cultivated using human derived mesenchymal-like cells in conjunction with a PLGA/CaP scaffold of 10 mm diameter and 10 mm thickness under perfusion or modified rotating conditions.

1.3. Goals of the Study

This study set out to address the goal of optimizing and developing three dimensional cultivation conditions by exposing human mesenchymal-like stem cells in conjunction with a porous scaffold, to the right mechanical and biochemical stimulus in an optimal microenvironment to improve current protocols and strategies in bone tissue engineering. Furthermore, this study examined the hypothesis that small trabecular bone specimens contain mesenchymal-like cells that can be isolated and expanded to an extent sufficient for autologous bone tissue engineering purposes.

To meet the above set goals, the current study was subdivided into two parts:

1. Human trabecular bone was investigated as a potential source for mesenchymal-like cells by comparing these cells to human bone marrow derived cells, especially in terms of their osteogenic capacity (Chapter 2).

2. Evaluation of growth and differentiation of human mesenchymal-like cells in conjunction with a poly (lactide-co-glycolide)-calcium phosphate composite scaffold in a three dimensional static and/or dynamic culture environment to produce spatially uniform bone like constructs *in vitro* and to provide us with a better understanding of how mechanical

signals and fluid dynamics affect bone tissue formation *in vitro* (Chapter 3).

To address the first part (Chapter 2), the following aims were set

- Establishing a technique for the isolation and expansion of human trabecular bone derived cells.
- Identification of a suitable expansion medium that ensures maximum proliferation, without loss of differentiation and that reproducibly supports a significant *in vitro* expansion of human mesenchymal-like cells.
- Large scale cell expansion (up to $10x10^6$ cells) sufficient for bone tissue engineering applications by using microcarriers and cell factories.
- Evaluation of the multilineage potential of human trabecular bone derived cells: namely the ability of these cells to differentiate into bone, fat and cartilage.
- Comparison of the osteogenic capacity of human trabecular bone derived cells to that of human bone marrow derived cells (i.e. developing a two dimensional model to study human osteogenesis *in vitro*).

And to address the second part (Chapter 3), the following aims were set:

- Determination of an optimal surface coating for the PLGA/CaP scaffold, promoting cell attachment, proliferation and differentiation of human trabecular bone derived cells.
- Comparison of proliferation and osteogenic differentiation of cells in static culture versus dynamic culture through biochemical and histological analysis to determine which regime of fluid flow (static, perfusion or tilted rotating cultivation mode) leads to the formation of spatially uniform bone-like constructs *in vitro*.

2. Isolation, Expansion and Characterization of Human Adult Tissue Derived Mesenchymal-like Cells for Bone Tissue Engineering Purposes

2.1. Introduction

Tissue engineering approaches for promoting the repair of skeletal tissues, such as bone cartilage and tendon, have focused on cell based therapies involving bone marrow derived mesenchymal stem cells (Bruder and Fox, 1999; Cancedda et al., 2000). These cells can be readily isolated and expanded in culture and have been selectively shown to form adipocytes, osteoblasts and chondrocytes *in vitro* (Pittenger et al., 1999). There is a growing body of evidence, demonstrating that multipotent progenitor cells can be obtained from a variety of other tissues including synovial membrane (De Bari et al., 2001), teeth (Miura et al., 2003), skin (Nakahara et al., 1990), periosteum (Hutmacher and Sittinger, 2003), adipose tissue (Zuk et al., 2001; Dragoo et al., 2003; Wickham et al., 2003; Ogawa et al., 2004), placenta (In 't Anker et al., 2004), in addition to evidence for circulating stem cells as in the human umbilical cord (Rosada et al., 2003). Since the availability of human bone marrow samples was limited when this study was initiated, an alternative source was sought, based on the studies by Noeth et al. (2002) and Nuttall et al. (1998), who have shown the multilineage potential of cells derived from human trabecular bone. This present thesis focused on the characterization and investigation of the potential of applying these cells to form three dimensional bone tissue *in vitro*. In the following sections, the isolation of mesenchymal-like cells from trabecular bone was established by comparing the properties of the isolated cells to the well characterized human bone marrow derived cells in terms of expansion and multilineage differentiation potential. A suitable expansion medium was developed and a method for large scale cell expansion was evaluated using cell factories™ and microcarrier culture. Finally, the osteogenic differentiation was assessed in time course studies by biochemical analysis determining bone specific markers supported by detailed histological analysis. A special focus was put on optimizing expansion and

differentiation media circumventing the use of fetal calf serum (FCS). Since mesenchymal-like stem cells are currently extensively investigated for possible clinical trials for future applied cytotherapy, this study focused on using FCS free conditions to avoid the mmunogenicity associated with applying a xenogenic protein (Spees et al., 2004) and to eliminate the risk of transmitting bovine spongiform encephalopathy (BSE) through infected serum (Bradley, 1999), so expansion and differentiation media were optimized using human serum.

2.2. Materials and Methods

- Chemicals, consumables and instruments are listed in Appendix I.
- Working solutions, buffer compositions, general cell culture methodology and staining methods are listed in Appendix II.
- Human samples were collected after patients signed informed consent and the study was performed according to the Declaration of Helsinki. The local IRB has approved the study.

2.2.1. Human Bone Marrow Derived Cells

Human bone marrow aspirate from an iliac aspiration (female, age: 80 years) was centrifuged over a Ficoll-Paque density gradient to separate the erythrocytes in a 50 ml tube (Rickard et al., 1996). The cell number was determined with the trypan blue exclusion method (see Appendix II) and initially cultured in ZKT-1 basal medium (see Appendix II) supplemented with 10% human serum and 1% penicillin-streptomycin solution in three T75 culture flasks. Following the initial plating, non-adherent cells were removed on day 7 at the first change of medium. The medium was replaced thereafter once a week. At 80-90% confluency, the primary culture was trypsinized and sub-cultured (see Appendix II), initially using a plating density of $2x10^4$ cells/cm² and gradually going down to $1.5x10^4$ cells/cm² and eventually to $1x10^4$ cells/cm². Cells were kept in culture and cryopreserved, depending on the harvested cell yield.

As an additional source, cryopreserved human bone marrow cells obtained at passage 1 were investigated as well. The cells were derived from human bone marrow of a male 19 year old patient isolated as described above and cryopreserved. The vial containing ~$3x10^6$ cells/vial was thawed and taken up into 5 ml ZKT-1 basal medium supplemented with 15% fetal bovine serum and seeded into a T25 culture flask. Cells were sub-cultured upon confluency at a plating density of $1x10^4$cells/cm² and further kept in culture and cryopreserved. Human bone marrow samples were obtained from the department of experimental trauma surgery of Hannover Medical School and from the department of biomaterials at Ulm University.

2.2.2. Human Trabecular Bone Derived Cells

Cells derived from human trabecular bone were isolated from explants of bone specimens with slight modifications to protocols from the literature (Beresford et al., 1984; Gronthos et al., 1997). Human bone fragments were aseptically collected during total knee or hip replacement, where the bones were otherwise discarded. Specimens were transported in NaCl directly after surgery to the laboratory for the cell isolation procedure. Trabecular fragments were washed extensively in sterile phosphate-buffered saline (1xPBS) to remove blood and marrow tissue. The bone was also freed of any surrounding tissue and dissected aseptically with a scalpel and knife into chips of 2-5 mm in diameter. Three to five bone chips were put into a T175 culture flask and covered with 40ml expansion medium (ZKT-1 supplemented with 15% human serum and 1% penicillin-streptomycin). The medium was exchanged once on a weekly basis. When migrating cells reached sub-confluency, cells were sub-cultivated at a plating density of $1x10^4$ cells/cm² as well as cryopreserved for later usage. Human bone specimens were regularly obtained from the experimental trauma surgery department, Hannover Medical School.

2.2.3. Cell Viability: WST-1

Cell viability was assessed using a WST-1 test, which is a colorimetric assay based on the cleavage of the tetrazolium salt (WST-1) by mitochondrial dehydrogenase in viable cells. WST-1 is cleaved to formazan by metabolically active cells as illustrated in Figure 10. An increase in mitochondrial dehydrogenase leads to an increase in the amount of formazan dye formed, correlating directly to the number of metabolically active cells in the sample. The formazan dye formed was detected using a spectrophotometer measuring absorbance at 450 nm with 620 nm as reference wavelength. The test was performed according to the instructions of the manufacturer. Briefly, 10 µl of the WST-1 reagent were added to 100 µl of supernatant per well (1:10), incubated for 2 hours at 37°C, 12% CO_2, shaken on a plate shaker for 1 minute and then absorbance was measured against a background control (WST-1 reagent in cell culture medium only, without cells). Samples were measured in at least doublets.

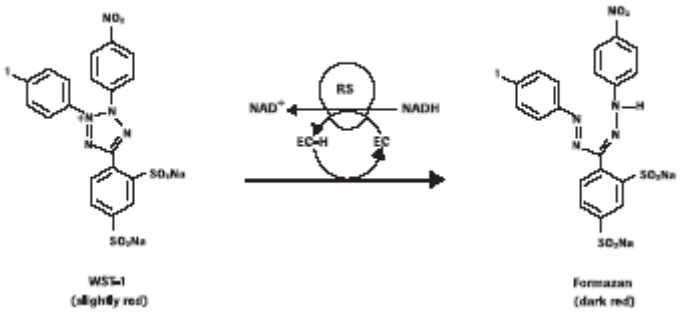

Figure 10 WST-1 test principle (illustration adapted from Roche Diagnostics GmbH). Cleavage of the tetrazolium salt WST-1 (4-[3-(4-Iodophenyl)-2-(4-nitrophenyl)-2H-5-tetrazolio]-1,3-benzene disulfonate) to formazan. (EC = electron coupling reagent, RS = mitochondrial succinate-tetrazoliumreductase system).

2.2.4. Total Protein Assay: Bicinchoninic Assay-Micro BCA™

Total protein content was determined according to the manufacturer's instructions. Briefly, the supernatant was removed and the cell layer washed with 1x PBS to be then lysed with 2% Triton-X 100 solution (for 48 well-plates: 200 µl/well) and incubated overnight at 37°C. The cell protein solution was scratched out of the well and frozen in 1.5 ml safe-lock tubes at -20°C. For the

assay, samples were thawed and centrifuged at 12000 rpm for 5 minutes. The supernatant was diluted 1:1 with distilled water and the samples were transferred to a 96-well plate and mixed with an equal amount of the kit working solution containing bicinchoninic acid (BCA). The plate was shaken shortly for 30 seconds at 300 rpm and incubated for two hours at 37°C. BCA detects Cu^{1+} that is formed when Cu^{2+} is reduced by protein in an alkaline environment forming a colored complex. This purple colored water-soluble complex is linear with increasing protein concentration. The absorbance was measured at 570 nm and samples were measured in doublets.

2.2.5. Cell Proliferation: DNA Determination with CyQUANT®

Adherent cells were grown in 48-well plates and, at predetermined time points, the medium was removed from the wells and the microplate containing samples were frozen until assayed at -70°C after the medium was removed. The CyQuant® kit is based on the use of a green fluorescent dye (CyQUANT GR dye), which exhibits strong fluorescence when bound to cellular nucleic acids (Jones et al., 2001). The frozen cells were thawed and lysed by covering the cell layer in the well with 200 µl of the lysis buffer, which contains the fluorescent dye (provided by the manufacturer) and diluted according to the manufacturer's instructions with nuclease free distilled water. Samples were incubated at room temperature for 5 minutes, mixing the plates gently and protected from light. Fluorescence was then measured directly in a fluorescence microplate reader with filters appropriate for ~480 nm excitation and an emission wavelength of ~520 nm. A reference standard curve for DNA content was created for converting sample fluorescence values into DNA nanograms (or cell numbers) using known concentrations of calf thymus DNA.

2.2.6. Human Serum

Human Serum Selection

The selection criteria for the most suitable preparation of human serum used in this study included cell morphology, cell proliferation and cell viability. Four

different preparations of human serum were selected from three different suppliers. Namely, two lots of serum from Pan Biotech (HS-1, HS-2), one lot of serum from PAA (HS-3) and one from the local blood bank of Hannover Medical School (HS-4).

Human trabecular bone derived cells were isolated as described above (2.2.2.), expanded and cryopreserved, to be then used at a seeding density of $5x10^3$ cells/cm². They were cultivated in T25 culture flasks for cell growth assessment and, further, regarding morphology and viability assessment, the cells were cultivated in 48-well plates. Cells were kept in ZKT-1 basal medium, supplemented with 1% penicillin-streptomycin and 15% of the appropriate human serum in a humidified atmosphere at 37°C and 12% CO_2. The medium was changed every 72 hours.

Cell growth was monitored by determining the number of population doublings, applying the formula (log *N* / log 2), where N is the cell count harvested of a confluent monolayer divided by the number of cells initially seeded (Stenderup et al., 2003). The number of viable cells was determined using the trypan blue exclusion method (see Appendix II).

Metabolic activity and viability was measured using the WST-1 test as previously described (2.2.3.). For morphological observation, the cells were examined under a phase contrast light microscope (Axiovert 120, Zeiss, Jena).

Human Serum Concentration

To determine the best human serum concentration for the proliferation and differentiation of human trabecular bone derived cell, four different serum concentrations were tested, including 1%, 5%, 10% and 15% human serum. Proliferation was assessed by the determination of total protein content throughout the cultivation period using the micro BCA™ assay (section 2.2.4.), as well as DNA content at the beginning (day 1) and at the end of the cultivation period (day 29) using the CyQUANT® assay (section 2.2.5.). Further, to examine the effect of supplemented serum concentrations on osteogenic differentiation, cells were expanded in the appropriate expansion medium and induced to differentiate in osteogenic medium for 14 days, to be then stained

for alkaline phosphatase. For the experiments, trabecular bone derived cells were seeded in 48-well plates at $5x10^3$ cells/cm^2.

Serum Rich *vs.* Serum Reduced Expansion and Differentiation Media

To compare serum rich expansion and differentiation media to serum reduced media, twenty different media formulations were tested. ZKT-1 basal medium supplemented with 1% penicillin-streptomycin served as the basic components in all twenty combinations (Table 1). To substitute for the growth factors available in serum, the following cytokines were added: recombinant platelet derived growth factor (PDGF) at 10 ng/ml, recombinant fibroblast growth factor (FGF) at 10 ng/ml, recombinant epidermal growth factor (EGF) at 5 ng/ml and recombinant insulin-like growth factor (IGF) at 15 ng/ml (Barthold, 2003). The cytokines were reconstituted according to the manufacturer's instructions and stored at -70°C. Serum reduced media were further supplemented with a mixture of insulin (10 µg/ml), transferrin (5 µg/ml), albumin (1 mg/ml) (ITA). This mixture is usually added to serum free formulations that substitute in a purified form for the factors normally supplied by serum. Cells were seeded at $5x10^3$ cells/cm^2 in 48-well plates and the medium was changed every 72 hours. Proliferation was monitored by the WST-1 proliferation assay.

Differentiation was induced by exchanging the expansion media (at day 9) with ZKT-1 basal medium, supplemented with 1% human serum and osteogenic factors (1x 10^{-8} M dexamethasone, 10mM beta-glycerophosphate and 200µM ascorbic acid). Membrane bound alkaline phosphatase activity was measured on both day 9 and 12 (as described in section 2.2.10.)

Table 1.	
Nr	**Expansion Media ZKT-1 supplemented with**
1	15% HS
2	10% HS
3	0% HS
4	1% HS
5	1% HS+ITA
6	1% HS+ITA+PDGF
7	1% HS+ITA+EGF
8	1% HS+ITA+IGF
9	1% HS+ITA+FGF
10	1% HS+ITA+PDGF +EGF+IGF+FGF
11	1% HS+ITA+PDGF+EGF
12	1% HS+ITA+PDGF+FGF
13	1% HS+ITA+PDGF+IGF
14	1% HS+ITA+EGF+FGF
15	1% HS+ITA+EGF+IGF
16	1% HS+ITA+FGF+IGF
17	1% HS+ITA+PDGF+EGF+FGF
18	1% HS+ITA+ PDGF+EGF+IGF
19	1% HS+ITA+PDGF+FGF+IGF
20	1% HS+ITA+EGF+FGF+IGF

Table 1 Twenty different combinations of tested media. For differentiation purposes the media were supplemented with the conventional osteogenic supplements: ß-glycerophosphate 10mM, ascorbic acid 200 µM and dexamethasone at 10nM. HS: Human serum. ITA: Insulin, transferrin and albumin mixture. All media were supplemented with 1% penicillin-streptomycin. PDGF: Platelet derived growth factor. EGF: Epidermal growth factor. FGF: Fibroblast growth factor. IGF: Insulin-like growth factor.

2.2.7. Large Scale Cell Expansion

Cell culture was usually performed on a small scale, in traditional T culture flasks ranging from T25 (25cm²) to T175 (175 cm²). Typical cell yields ranged from $250x10^3$ to $8x10^6$ cells per flask. To produce higher cell numbers in one batch, the following two methods were optimized that offered an increased surface area compared to conventional monolayer culture in T flasks.

2.2.7.1. *The Cell Factory™*

The protocol for culturing cells in the cell factory was adapted from the manufacturer of the cell factory (Nunc, Wiesbaden). A cell factory consists of polystyrene trays, treated for optimal cell attachment and spreading (Maroudas et al., 1977), assembled by sonic wedging on one another. They are available in 1, 2, 4, 10 and 40 tray versions for easy scale-up. One tray has a

culture area of 632 cm^2 (dimensions, 333 x 204 x 57 mm) and a suggested working volume of ca. 200ml per tray (Figure 11). In this study, four tray factories were used with an overall surface area of 2,528 cm^2. The cell suspension was prepared in an aspirator bottle with a sterile connector for the silicon tubing. Expansion medium, 1xPBS buffer, trypsin-EDTA solution or the cell suspension were all transferred into aspirator bottles and connected as needed to the cell factory, which is equipped with an identical connector for the silicone tubing (both supplied by the manufacturer). When cell suspension was to be poured into the cell factory, the bottle was gently agitated to evenly suspend the cells, allowing the fluid to flow into the trays. After the filling process, the autoclavable connector was removed and replaced by an adaptor cap (Nunc, Wiesbaden). The cell factory was placed in an incubator at 37°C with 12% CO_2. The trays were seeded at $10x10^3$ cells/cm^2 and cultured in 150 ml expansion medium per tray. Cells were harvested at confluence (see Appendix II) using 20 ml trypsin-EDTA and 40 ml 1xPBS per tray.

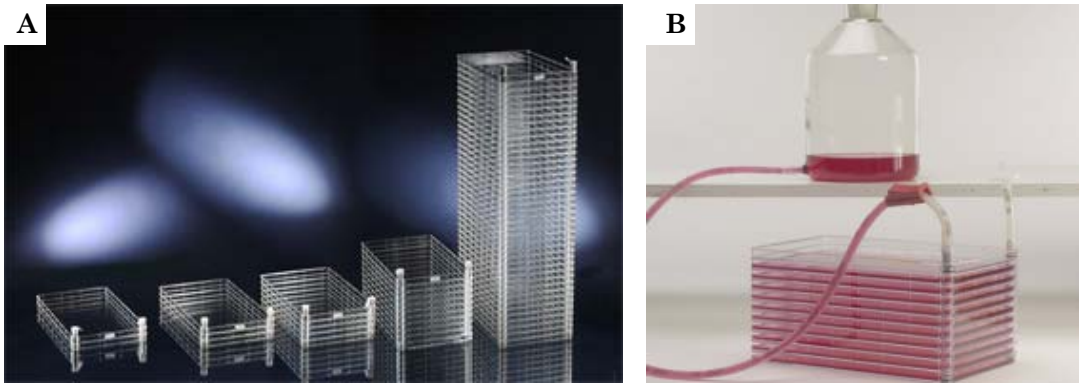

Figure 11 Cell factory™ illustrations adapted from Nunc (www.nuncbrand.com). (A) 1 tray, 2- 4-10 or 40 tray version of the cell factory. (B) The cell factory has two openings (ports): one to insert tubing into for liquid filling and the other for ventilation, connected to a filter.

2.2.7.2. *Spinner Flask-Microcarrier Culture*

Two different types of microcarrier were tested for adherent cell growth:

1. MicroHex™ (Nunc, Wiesbaden), microscopic non-porous polystyrene hexagons with a side length of 125 µm, a thickness of 25 µm and a surface culture area 760 cm^2/g.

2. Cytodex3® (Amersham Bioscience, Otelfingen, Switzerland) made up of a collagen coated dextran matrix with a diameter of 135-215 µm and a surface culture area 2700 cm²/g.

Microhex™ microcarriers were supplied sterile and ready to use, while Cytodex3® microcarriers were equilibrated in 1xPBS overnight (100 ml PBS/g of microcarrier) at 4°C, after which they were autoclaved at 115°C for 20 minutes. A total surface area of 380 cm² was chosen equivalent to 0.5 g Microhex™ and 0.14 g Cytodex3® in a final medium volume of 86.8 ml ZKT-1, supplemented with 15% human serum (typical expansion medium) in a 125 ml spinner flask (Bellco). The spinner flask is equipped with a central magnetic stirrer shaft to ensure cells being suspended in the medium and side rams for sampling, the cap of which was loosened in the incubator to ensure aeration with CO_2 enriched air and gas exchange. Inoculated spinner flasks were placed on a magnetic stirrer (with variable possible rpm settings) in a 37°C incubator with 12% CO_2. The medium volume, calculated according to the volume applied in the cell factories and T flask culture, was taken as ca. 0.24 ml/cm².

Human mesenchymal-like cells were used at passage 4 and an inoculum of $10x10^3$ cells/cm² ($3.8x10^6$ cells per spinner) was applied to ensure uniform coverage of all the microcarriers (same seeding density as previously applied in cell factories and T flasks). Cells in suspension without microcarriers were also cultivated as a control. Cells were inoculated into the spinner containing 50 ml medium (with or without the microcarriers) and stirring was started immediately. The stirring speed in the spinner was initially set to a low speed (20 rpm) to ensure cell attachment and coverage of all microcarriers increasing initial contact time of the cells with the microcarriers. After 24 hours, the rest of the medium was added and the speed increased to 30 rpm. The stirring speed was adjusted to prevent sedimentation and eventual clumping of the microcarriers by increasing the rpm's gradually so as not to reach too high shear forces, which might prevent cell attachment. The culture was continuously stirred throughout the cultivation. Cell attachment and growth on the microcarriers was assessed using a phase contrast microscope (Axiovert 120, Zeiss, Jena) by placing a few drops of the suspension onto a glass slide and medium samples were daily drawn for glucose and lactate analysis of the

cell suspension. To separate the cells from the microcarriers at confluence, according to microscopic observations, the stirring was stopped and the microcarriers settled relatively fast so the medium was easily aspirated and cells could be harvested. The cell covered microcarriers were first washed with 10 ml 1xPBS, decanted, replaced by 10 ml trypsin-EDTA and incubated for 15 min at 37°C with occasional agitation. Serum containing expansion medium was added and mixed vigorously to detach all cells and break up cell clumps before filtration of the cell suspension through a 70 μm filter to retain the microcarriers. The cell suspension was then centrifuged at 800 rpm for 3 minutes and the cell pellet re-suspended in fresh medium and cells counted with the trypan blue exclusion method (Appendix II).

The spinner flasks were siliconized in order to prevent microcarriers covered with cells sticking to the walls of the vessel. This was done by wetting the inside with a silicone solution (Sigmacote®) before sterilization (Malda et al., 2004). After drying in air, the spinner vessel was rinsed with deionized water several times to be then heat sterilized before culture initiation.

2.2.8. Glucose and Lactate Analysis

Glucose and lactate concentrations in the medium were analyzed by YSI 2700 Select Biochemistry Analyzer. The measurement is based on an immobilized biosensoring technique. The sample passes through a membrane, which contains three layers. An enzyme specific for both glucose (glucose oxidase) and for lactate (lactate oxidase) is immobilized between the two membrane layers, polycarbonate and cellulose acetate. The substrate is oxidized as it enters the enzyme layer, producing hydrogen peroxide, which passes through cellulose acetate to a platinum electrode, where the hydrogen peroxide is oxidized. The resulting current is proportional to the concentration of the substrate.

2.2.9. Multilineage Potential of Human Trabecular Bone Derived Cells

Human trabecular bone derived cells were analyzed for their capacity to differentiate towards the adipogenic, chondrogenic and osteogenic lineage. To induce differentiation into the corresponding lineages, trabecular bone derived cells were cultured with special induction media to lead to the specific differentiation. The phenotype was confirmed by histological analysis (section 2.2.13.). Cells were seeded at $1x10^4$ cells/cm^2 and cultivated in ZKT-1 basal medium, supplemented with 15% human serum and 1% penicillin-streptomycin until sub-confluence (80-90% confluence) was reached after 5-7 days of culture. The cell layers were then treated with the special differentiation media listed below. Control cultures were maintained in parallel without adipogenic, chondrogenic or osteogenic supplements, respectively.
All concentrations given below are final concentrations in cell culture medium.

2.2.9.1. *Adipogenesis*

For adipogenic differentiation, the expansion medium was exchanged with adipogenic medium as described by Erices et al. (2000) and Zuk et al. (2001). ZKT-1 basal medium was supplemented with 10% fetal bovine serum and 1% penicillin-streptomycin as well as with insulin (5 µg/ml), isobutylmethylxanthine (0.5 mM), indomethacin (200 µM) and hydrocortisone (0.5 mM). The medium was changed every 72 hours. After 21 days of induction, lipid vacuoles were visualized histologically with Nile Red staining (see section 2.2.13.5.).

2.2.9.2. *Chondrogenesis*

The *in vitro* chondrogenic assay was performed as described in the literature (Sottile et al., 2002). Upon sub-confluence, the medium was changed to chondrogenic induction medium made up of ZKT-1 basal medium

supplemented with 1% penicillin-streptomycin, ascorbic acid (50 µg/ml), bovine serum albumin (1.25 µg/ml), dexamethasone ($1x10^{-7}$ M) insulin (6.25 µg/ml), proline (40 µg/ml), sodium pyruvate (100 µg/ml), transferrin (6.25 µg/ml) as well as TGF-beta 1 (10 ng/ml), which was added fresh at each medium exchange every 72 hours.

The chondrogenic potential was demonstrated histologically by Alcian blue staining after a 21 day cultivation period in chondrogenic medium (see section 2.2.13.6.).

2.2.9.3. *Osteogenesis*

Osteogenic differentiation was induced by culturing the cells for a minimum of two weeks for up to 30-40 days in osteogenic medium. The osteogenic medium was prepared by adding 1x 10^{-8} M dexamethasone, 10 mM beta-glycerophosphate and 200 µM ascorbic acid to ZKT-1 basal medium, supplemented with 10% human serum and 1% penicillin-streptomycin. Medium was changed every 72 hours and samples of the supernatant were frozen in 1.5 ml safe-lock tubes at -20ºC. The osteogenic differentiation was assessed in time course studies over thirty days by measuring C Terminal Type I Collagen (CICP) levels, indicating collagen production and alkaline phosphatase at several time points. Histologically, alkaline phosphatase, calcein, von Kossa and alizarin red staining were routinely performed.

2.2.10. Alkaline Phosphatase Activity Assay

The alkaline phosphatase enzyme activity was determined by a biochemical colorimetric assay as described by the manufacturer (Sigma Fast ™ p-Nitrophenyl Phosphate tablet set, pNPP).

Briefly, a reaction mixture was made by dissolving the supplied tablet set in 20 ml deionized water, yielding a solution of 1.0 mg/ml p-nitrophenyl phosphate in 0.2 M Tris buffer and 5 mM Magnesium chloride. P-nitrophenol is formed through the enzymatic hydrolysis of p-nitrophenyl phosphate, used by the cellular enzyme alkaline phosphatase as the substrate, so its rate of

formation is proportional to the enzyme's activity. P-nitrophenol can be quantified by measuring its absorbance at 405 nm using a spectrophotometer. A standard curve was obtained from serial dilutions of a p-nitrophenol solution. The alkaline phosphatase enzyme activity was expressed in milli units (mU) per well. One unit is defined as the amount of the enzyme Alkaline phosphatase (ALP) that will produce 1 nmol of p-nitrophenol/min (milli units/well, mU per well). Values were normalized to total protein content of the cell layer in the well using the above mentioned protein assay (mU/mg). Unknown samples were measured in at least doublets. The activity of cellular alkaline phosphatase was determined either as cell-membrane bound alkaline phosphatase or as soluble alkaline phosphatase in the supernatant. Control wells without cells were also run with the assay.

2.2.10.1. *Membrane Bound Alkaline Phosphatase Activity Assay*

Briefly, the cell layer was washed with 1xPBS, incubated with 200 µl of the above described reaction solution for 30 minutes at 37°C. Aliquots of 50 µl of the reaction solution were then transferred to a 96-well plate to measure the absorbance of the formed p-nitrophenol at 405 nm in a spectrophotometer.

2.2.10.2. *Soluble Alkaline Phosphatase Activity Assay*

The activity of the alkaline phosphatase enzyme was also determined in the supernatant. Medium samples were taken every 72 hours throughout the cultivation period and frozen at -20ºC in 1.5 ml safe-lock tubes until analysis. Samples were thawed at room temperature and aliquots of 40 µl of the supernatant were transferred to a 96-well plate. 160 µl of the above described reaction solution were added and the plate was shaken at 700 rpm for 30 seconds, to be then incubated for 24 hours at 37ºC. Absorbance was measured at 405 nm.

2.2.11. Collagen Type I Assay

The amount of collagen type I COOH terminal propeptide was determined in the conditioned medium using the procollagen-C enzyme immunoassay kit (Metra™ CICP EIA kit, Quidel) (Reinholz et al., 2000). The test was performed according to the manufacturer's instructions. Briefly, the assay is a sandwich enzyme immunoassay in a microplate format, utilizing a monoclonal anti-CICP antibody coated on the plate, a rabbit anti CICP antibody and a goat anti-rabbit alkaline phosphatase conjugate and a p-nitrophenylphosphate substrate to quantify human CICP in the samples. Samples were diluted 1:2 with the supplied assay buffer and applied onto the coated plate and further handled according to the manufacturers instructions. Samples were measured in at least doublets.

2.2.12. Calcein for Mineralization

Calcium deposited in the extracellular matrix was quantified with the calcein assay. The calcein molecule is known to bind to the calcium ions during hydroxyapatite crystal formation (Uchimura et al., 2003; Hale et al., 2000) and is a widely accepted method for the quantification of calcium deposition.
Cells were seeded at $5x10^3$ cells/cm² or $10x10^3$ cells/cm² in 48-well plates and grown in osteogenic medium. At time of analysis, medium was discarded and the cell layers were washed with warm 1xPBS and then fixed with cold 100% ethanol for 30 minutes at room temperature. The ethanol was removed and the cell layers were rinsed twice with deionized water. The cell layers were stained with calcein solution (5 µg/ml), kept in the dark at 4°C overnight. The calcein solution was removed the next day followed by rinsing the cell layers three times with deionized water. The fluorescence of the cell incorporated calcein was quantified using a fluorescence microplate reader and the absorbance was measured at 485 nm excitation and 535 nm emission. Samples were measured in at least doublets.

2.2.13. Histochemical Analysis

For *osteogenic* identification, cells were stained for alkaline phosphatase as an early marker for osteogenesis and terminal mineralization was visualized by von Kossa, Alizarid Red and calcein. For *adipocyte* identification, Nile red staining was applied and for *chondrocyte* visualization, Alcian blue staining was undertaken. Cells were viewed under a phase contrast light and fluorescent microscope (Axiovert 120, Zeiss, Jena) and photomicrographs were taken with a digital camera (DXN 1200F, Nikon, Duesseldorf).

2.2.13.1. *Alkaline Phosphatase Staining*

Alkaline phosphatase was detected histochemically with a Sigma Alkaline phosphatase activity staining kit as described by the manufacturer. Briefly, the cell layer was fixed with 4% paraformaldehyde solution (PFA) for 30 minutes at room temperature, rinsed with deionized water, covered with the staining mixture and incubated at 37°C for 10 minutes. The staining-solution was prepared by dissolving an NBT/BCIP (NBT=Nitroblue tetrazolium salt, BCIP=5 –Brom-4-Chlor-3-Indolylphosphat) tablet in 10ml deionized water. The reaction was stopped by thoroughly rinsing three times with deionized water. Membrane bound alkaline phosphatase presence is indicated through a blue-black turbidity, which is formed due to a reaction between the two colorless NBT and BCIP substrates catalyzed by alkaline phosphatase.

2.2.13.2. *Alizarin Red Staining*

To detect mineralized nodules and determine mineralization extent of the extracellular matrix, culture medium was removed from the cell layer, rinsed with 1xPBS and fixed with 4% PFA for 30 minutes at room temperature. The cell layer was rinsed twice with deionized water and stained for 10 minutes with 1% alizarin red solution (Gregory et al., 2004; Romeis und Boeck, 1989). The cell layer was then rinsed with HPLC water (pH 7) and air dried. Alizarin red selectively binds to calcium, staining calcium depositions red.

2.2.13.3. *Von Kossa Staining*

Von Kossa staining was performed according to Puchtler and Meloan (1978) and Romeis and Boeck (1989) with slight modifications. The cell layer was fixed with 100% ethanol, rinsed with deionized water, covered with 5% $AgNO_3$ solution (see Appendix II) and incubated in the dark for 30 minutes. The solution was aspirated and the layer was rinsed with deionized water. To develop the brown-black colour of calcium phosphate deposits, the cell layer was incubated with 5% Na_2CO_3 solution (see Appendix II) for 20 seconds to 2 minutes. After color development, the solution was aspirated off and the cell layer rinsed with deionized water, mounted with glycerol gelatin and covered with a coverslip.

2.2.13.4. *Calcium Staining with Calcein*

The cell layer was fixed with 100% ethanol for 30 minutes at room temperature, rinsed three times with water and was then covered with calcein solution (5µg/ml) overnight at 4°C (Hale et al., 2000). After overnight staining, the cell layer was rinsed three times with deionized water. The fluorescence of the incorporated calcein was also visualized under a fluorescent microscope (Axiovert 120, Zeiss, Jena).

2.2.13.5. *Nile Red Staining for Adipocytes*

Cell layers were rinsed with 1xPBS and then fixed with 4% PFA for 30 minutes at room temperature, followed by rinsing with deionized water. The fixed cell layer was then incubated with the AdipoRed® solution (Cambrex), a Nile Red derivative staining solution, for 30 minutes at room temperature (Greenspan et al., 1985). The staining solution was then aspirated and the cell layer kept moist with 1xPBS and directly examined under the fluorescent microscope.

2.2.13.6. *Alcian Blue Staining for Chondrocytes*

Sulphated glycosaminoglycans and proteoglycans typically produced by chondrocytes were detected with Alcian blue. The staining solution was prepared by dissolving 0.2 g Alcian blue in 3% acetic acid solution (in deionized water) and filtrated through a 0.22μm filter. The cell layer was fixed with ice-cold methanol
(-20°C) for 30 minutes at room temperature, rinsed with deionized water and stained for 10 minutes with the Alcian blue staining solution, followed by rinsing again with deionized water (Miltenyi Biotec GmbH, MACS media, non-haematopoietic stem cell media package insert).

2.3. Results and Discussion

2.3.1. Cell Isolation and Culture of Human Mesenchymal-like Cells

2.3.1.1. Human Bone Marrow-Derived Cells

After preparation of the bone marrow aspirate (section 2.2.1.), a cell number of $4.7x10^7$ cells was initially cultured in three T75 culture flasks ($2x10^6$ cells/cm^2) with cell attachment noted on day 7. Non-adherent cells were removed with the first medium change at day 7 as well. After 34 days in culture, cells were still made up of a mixture of cells, and colonies were observed to spread over the culture surface area without completely reaching confluence. Thus, it was decided to increase the cell-cell contact by trypsinising and re-plating the cells at a plating density of $4x10^4$ cells/cm^2 (into two instead of three T75 culture flasks) and to increase the serum content to 15% human serum instead of 10%. After 40 days in culture, the first confluent cell layers were harvested. A total of 1.3 $x10^7$ cells were harvested and sub-cultured at $4x10^4$ cells/cm^2 to keep the high cell density, as the initial cell-cell contact seemed to be important for cell proliferation. Confluency was reached after only two days and a total $1.5x10^7$ cells was harvested. Due to the fast expansion rate noted, the seeding density was decreased gradually from $4x10^4$ cells/cm^2 to $1.5x10^4$ cells/cm^2 and $1x10^4$ cells/cm^2 so as not to risk growth inhibition through early cell-cell contact. A total of $6.8x10^7$ cells were harvested from initial $8.8x10^6$ cells (2.96 population doublings). Both cell densities reached confluency and $1x10^4$ cells/cm^2 was thereafter taken as the seeding density for cell expansion. Cells were further sub-cultured at $1x10^4$ cells/cm^2 and $1x10^8$ cells were harvested at day 50, after 4 days in culture. Table 2 summarizes initial cell numbers and the corresponding cell yield over the first four passages.

Cells were expanded for up to 14 passages with an average population doubling rate of 0.4 population doublings per day. The cells were continuously kept in culture for approximately 90 days after isolation, actively dividing up until the end of the 13th passage, where nuclei enlarged, cells broadened and cell growth slowed down immensely.

The morphology of the human bone marrow cells in their primary passage showed the typical star shape for the colony forming units and upon passaging acquired the fibroblast-like spindle shape (Figure 12).

Table2.			
Cell Preparation	**Time (days)**	**Cell number**	**Population doublings**
Initial Preparation		$4.7x\ 10^7$	
Primary Culture	34	$6x\ 10^6$	
1^{st} Passage	40	$1.3x10^7$ from initially $6x10^6$	2.31
2^{nd} Passage	42	$1.5x10^7$from initially $9.7x10^6$	0.61
3^{rd} Passage	46	$6.8x10^7$ from initially $8.8x10^6$	2.96
4^{th} Passage	50	$1.0x10^8$from initially $1.4x10^7$	2.88

Table2 Expansion of human bone marrow derived cells over 4 passages.

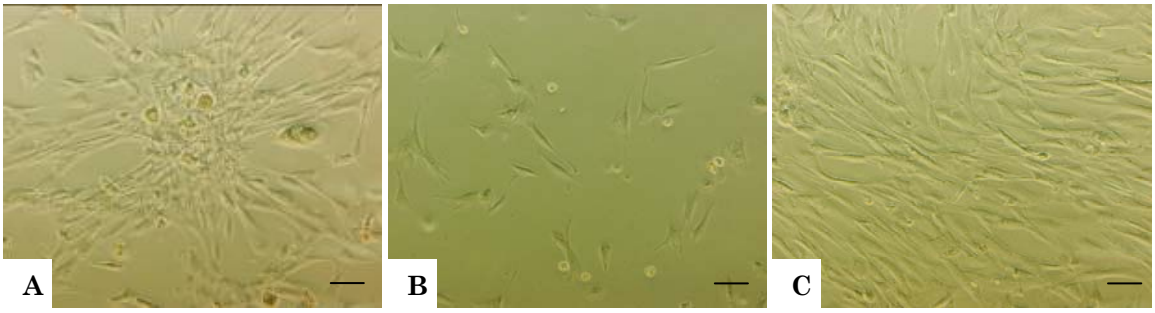

Figure 12 Photomicrographs showing the morphology of freshly isolated human bone marrow derived cells. (A) Typical star-shaped colonies of human bone marrow cells in their primary passage cultivated in ZKT-1 basal medium, supplemented with 15% human serum. **(B)** Human bone marrow derived cells after passaging into the third passage at $10x10^3$cells/cm^2 and **(C)** after reaching confluence in the third passage. Original magnification: x100; scale bar =100µm.

2.3.1.2. Cryopreserved Human Bone Marrow-derived Cells

The morphology (Figure 13) as well as the population doubling rate, an average of 0.42 population doublings per day, was found to be very similar to the freshly isolated bone marrow derived cells (0.4 population doublings per day).

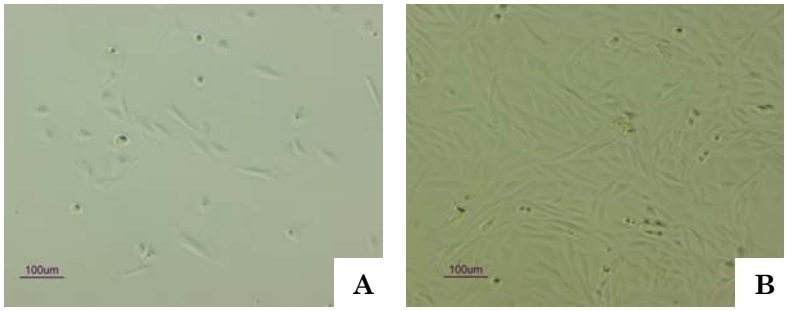

Figure 13 Photomicrographs showing the morphology of cryopreserved human bone marrow derived cells. (A) Cryopreserved human bone marrow cells upon seeding at $10x10^3$ cells/cm^2 and **(B)** at confluence. Original magnification: x100; scale bar=100µm.

2.3.1.3. Trabecular Bone-Derived Cells

Cells were observed to migrate from the bone explants after 7-14 days (Figure 14). With continued incubation, cells proliferated and formed a confluent monolayer after approximately 30 days. No differences in growth characteristics or cell morphology were noted among different patient samples. The initial adherent cells isolated grew as spindle shaped, remaining dormant for 7 to 14 days, after which they began to multiply and eventually reached confluency after 30-40 days in culture.

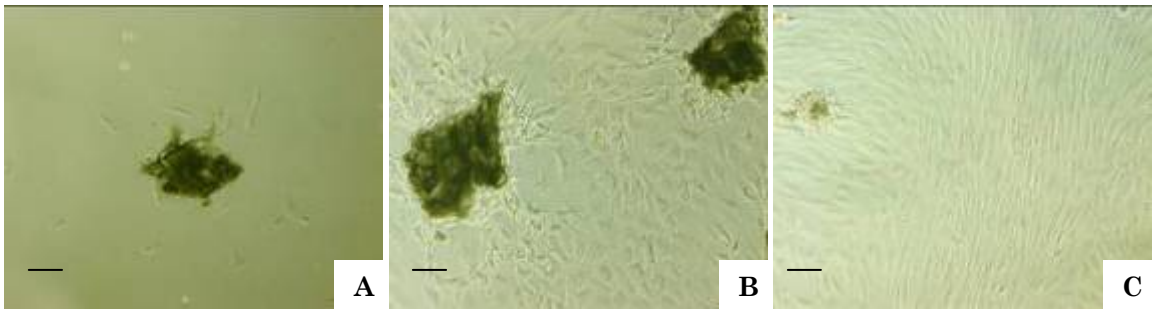

Figure 14 Micrographs representative of a trabecular bone explantation; cellular outgrowth from a human bone sample. (A) Appearance of bone fragments. **(B)** Cells migrating from the bone fragments after 14 days of culture in ZKT-1 basal medium, supplemented with 15% human serum. **(C)** Confluent monolayer of cells after 32 days of explant culture. Original magnification: x100.Scale bar =100µm.

Upon passaging, human trabecular bone derived cells showed a very similar morphology to passaged human bone marrow derived cells (Figure 15). Both cell types displayed a fibroblastic spindle-like shape with an average population doubling rate of 0.22 population doublings per day.

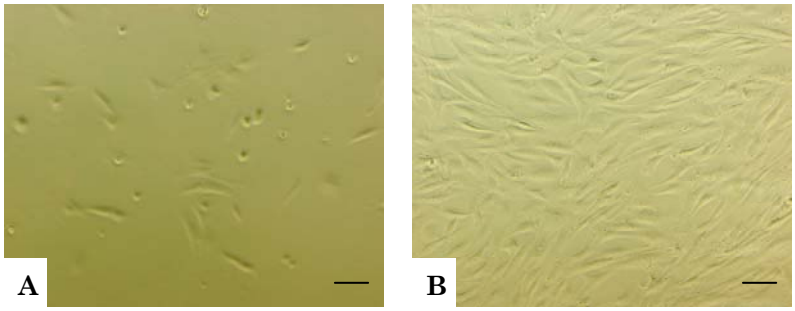

Figure 15 Photomicrographs showing the morphology of human trabecular bone derived cells upon passaging. (A) Human trabecular bone derived cells upon passaging in the third passage seeded at $10x10^3$cells/cm^2 and **(B)** at confluence. Original magnification: x100; scale bar=100µm

2.3.1.4. Discussion

Human bone marrow derived cells were successfully isolated and expanded, despite of the relatively long lag phase in their initial culture period. Cells were passaged up to 14 passages with an average population doubling rate of 0.4 population doublings per day. These results are in line with what was reported earlier by Bruder et al. (1997), who isolated human bone marrow derived cells and observed senescence to occur on average between passage 10 and 15. Furthermore, they have shown that daily fed cultures, exposed to consistently high serum derived factors had grown faster and generated more cells than cultures which were fed only twice weekly, where the concentration of available mitogenic factors in the medium might have become rate limiting with the cells actively metabolizing the nutrients. This might explain the improvement in growth that was noted in this study upon increasing the serum concentration from 10% to 15%, at which cells seemed to have been taken out of their prolonged lag phase (the time from first introducing the bone marrow derived cells into culture until first passage).

Sub-culturing the primary cells further, at relatively high cell densities up to 14 passages in this study, while maintaining the large expansion and differentiation potential of these cells is controversial to what was reported by Sekiya et al. (2002) and Stute et al. (2004). Both groups have demonstrated that low seeding density (20 cells/cm^2) was clearly better for prolonged expansion of bone marrow derived cells. On the other hand, Jaiswal et al. (1997) have used a density of $5x10^3$ cells/cm^2 and Bruder et al. (1997) have

passaged human bone marrow derived cells at $3x10^3$ cells/cm^2, which are close to the cell seeding densities that were applied in this study, starting initially with $4x10^4$ cells/cm^2 in the first passage of primary cells and then gradually going down to $1.5x10^4$ cells/cm^2 and $1x10^4$ cells/cm^2 for expansion purposes. Moreover, the freshly prepared bone marrow sample was seeded at $2x10^6$ nucleated cells/cm^2, which is very similar to Bruder et al. (1997), who used an initial seeding density of $1.7x10^6$ freshly isolated nucleated cells/cm^2, harvesting the first passage after fourteen days.

2.3.2. Medium Optimization

In establishing and optimizing the isolation of human bone marrow derived cells, it was noticed that when the serum content in the expansion medium was increased from 10% to 15%, better cell growth and faster proliferation could be observed. To verify this observation and to determine the most suitable human serum and its concentration for optimal expansion and differentiation, the following experiments were undertaken.

2.3.2.1. Human Serum Selection and its Effect on Cell Proliferation and Morphology

Of the four human serum preparations, the preparation from the local blood bank of Hannover Medical School (HS-4) consistently yielded the highest cell counts. A comparison of cell counts of human trabecular bone derived cells expanded in the different human serum preparations is shown in Table 3.

Table 3

Human Serum Type		Cell # Day 6
Pan Biotech Lot No P50208	HS-1	$150x10^3$
Pan Biotech Lot No P520221	HS-2	$150x10^3$
PAA Lot No CO 2104-0167	HS-3	$100x10^3$
Hannover Medical School	HS-4	$300\ x10^3$

The faster cell growth in the HS-4 preparation (obtained from the local blood bank of Hannover Medical School) was also noted in the microscopical analysis. Cells cultivated in parallel in the four different human serum preparations were initially morphologically similar, showing the typical spindle shaped fibroblast-like appearance. Upon further cultivation, however, the cells cultivated in the serum (HS-4) displayed an accelerated growth rate (faster confluence) and a more elongated spindle shape (Figure 16).

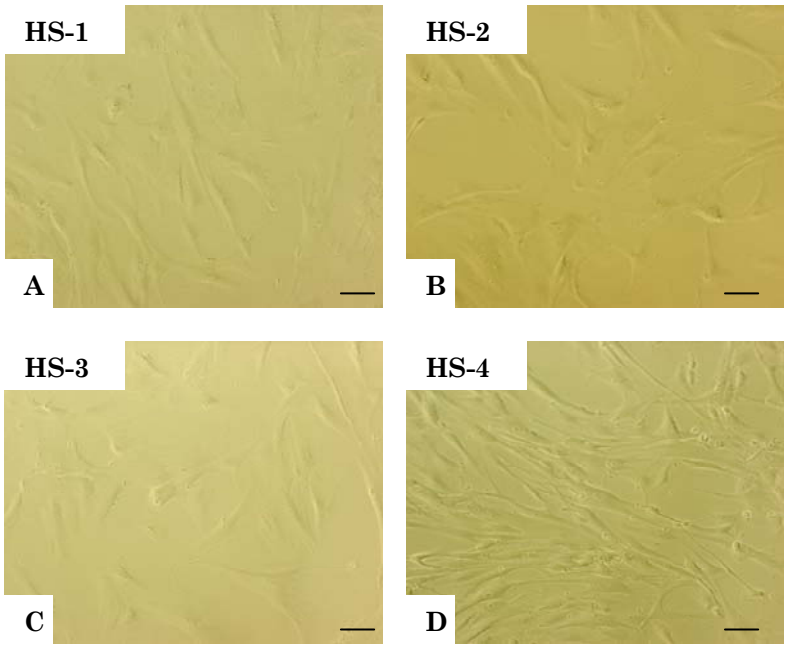

Figure 16 Micrographs showing the effect of human serum preparation on cell morphology and growth of human trabecular bone derived cells. Cells were cultivated in parallel culture flaks in ZKT-1 basal medium supplemented with 15 % of the corresponding human serum preparation. Differences in cellular growth and morphology were noted according to the type of human serum used. **(A)** Cells cultivated in HS-1: Pan Biotech human serum lot 1. **(B)** HS-2: Pan Biotech human serum lot 2. **(C)** HS-3: PAA human serum. **(D)** HS-4: Human serum from Hannover Medical School. Original magnification: x100; scale bar= 100µm.

Furthermore, viability of the cells was measured at the end of the cultivation period and it was found that the highest metabolic activity was demonstrated by the cells treated with the human serum (HS-4) supplied by the local blood bank of Hannover Medical School (Figure 17). Thus, HS-4 was selected for all further analyses in this study.

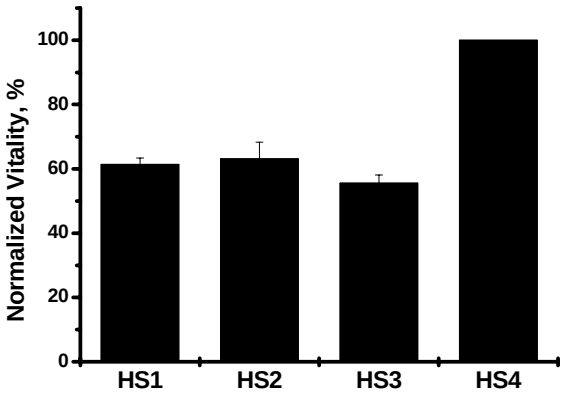

Figure 17 Effect of human serum type (or lot) on human trabecular bone derived cell proliferation measured by WST-1. Human trabecular bone derived cells were seeded at 5x10³cells/cm² in 48-well plates and cultivated in 4 different human serum preparations at 15% in ZKT-1 basal medium. WST-1 was determined on day 6. The bars represent the absorbance as a percentage of the maximum absorbance measured at 450 nm. HS-1= PanBiotech Lot1. HS-2 =PanBiotech Lot 2. HS-3=PAA. HS-4= Medical school Hanover. Error bars, means ± standard deviation. n≥3.

2.3.2.2. Human Serum Concentration and its Effect on Cell Morphology, Proliferation and Differentiation

After choosing the serum preparation for the cultivation of human trabecular bone derived cells, the most suitable human serum concentration was determined for expansion and differentiation purposes. Four different serum concentrations were tested, including 1%, 5%, 10% and 15% human serum.

2.3.2.2.1. Effect of Serum Concentration on Cell Morphology

Initially the morphology of the cells was very similar, all showing a long spindle fibroblast-like shape (Figure 18). Cells treated with 15% human serum were observed to grow faster and denser after only 5 days of culture compared to the lower concentrations.

Later in cultivation, after 11 days, cells which were grown in the lowest serum concentration (1%) barely proliferated and were shorter and broader in shape compared to cells grown at the higher serum concentrations (Figure 19). Cell confluency was reached in the following order: 15%>10%>5%>1%.

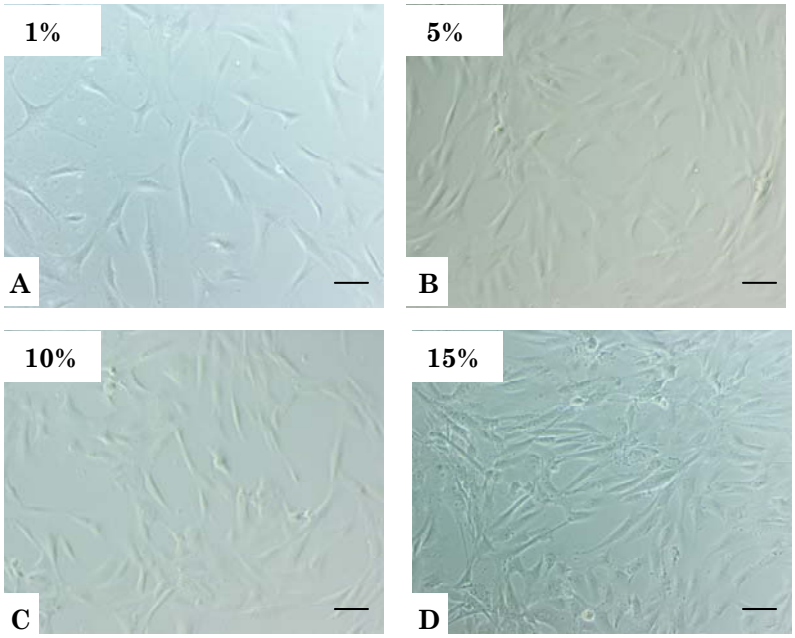

Figure 18 Micrographs showing the effect of human serum concentration on human trabecular bone derived cell morphology after 5 day cultivation. Human trabecular bone derived cells were seeded at 5x10³ cells/cm² in 48-well plates and cultured with ZKT-1 basal medium supplemented with (A) 1% human serum, (B) 5% human serum, (C) 10% human serum and (D) 15% human serum. Cells were viewed under a phase contrast light microscope after 5 days of cultivation. Original magnification: x100; scale bar=100µm.

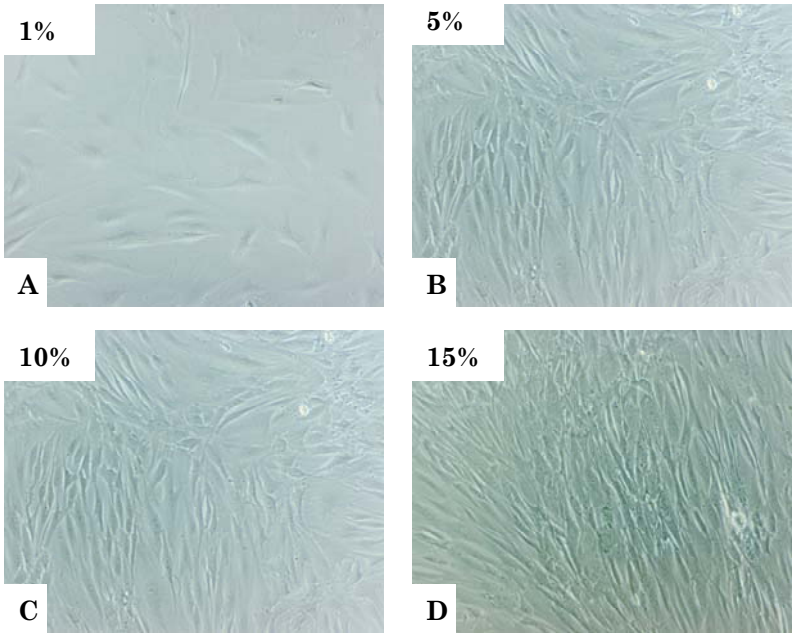

Figure 19 Micrographs showing the effect of human serum concentration on human trabecular bone derived cell morphology after an 11 day cultivation period. Human trabecular bone derived cells were seeded at 5x10³ cells/cm² in 48-well plates and cultured with ZKT-1 basal medium, supplemented with **(A)** 1% human serum, **(B)** 5% human serum, **(C)** 10% human serum and **(D)** 15% human serum. Cells were viewed under a phase contrast light microscope after 11 days of cultivation. Original magnification: x100; scale bar=100µm.

2.3.2.2.2. Effect of Serum Concentration on Cell Proliferation

To quantify the effect of serum concentration on cell proliferation, total DNA content (Figure 20), total protein content (Figure 21) and total DNA content were assessed, which verified the microscopical data.

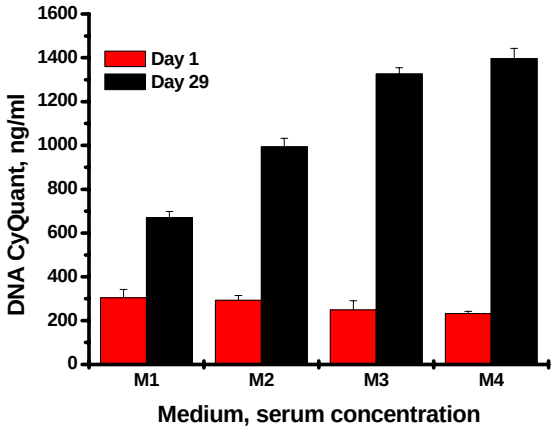

Figure 20 Effect of human serum concentration on DNA content of trabecular bone derived cells. Cells were seeded at 5x10³ cells/cm² in 48-well plates and cultured with ZKT-1 basal medium, supplemented with 1%, 5%, 10% or 15% human serum. The red bars represent the total DNA amount in ng/ml after 1 day of cultivation and the black bars after 29 days. M1=1% human serum. M2=5% human serum. M3=10% human serum. M4=15% human serum. Error bars, means ± standard deviation n≥3.

The DNA amount on day 29 of cells treated with 10% human serum was very close to that of cells cultivated with 15% human serum. This could be explained by the fact that confluency was actually reached at a time point earlier than day 29, as was observed microscopically. With the cells in both media eventually filling the culture area they are provided with, they stopped proliferating at confluence and therefore stopped increasing in number with the DNA amount reaching a maximum most probably at different points but before day 29.

The total protein content data show (Figure 21) that throughout the cultivation time, the amount of protein production for cells treated with 15% human serum is higher compared to the 10%. Taking this into consideration, 15% serum supplementation was found to be most suitable for expansion purposes, as confluency was reached faster (higher growth rate).

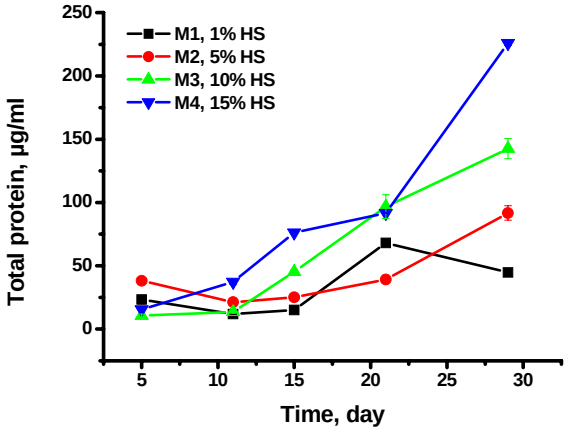

Figure 21 Effect of human serum concentration on total cellular protein content of human trabecular bone derived cells. Human trabecular bone derived cells were seeded at 5x10³cells/cm² in 48-well plates and cultured with ZKT-1 basal medium, supplemented with either 1%, 5%, 10% or 15% human serum. Total protein was determined over the whole cultivation period of 29 days. M1=1% human serum, black line. M2=5% human serum, red line. M3=10% human serum, green line. M4= 15% human serum, blue line. Error bars, means ± standard deviation n≥3.

2.3.2.2.3. Effect of Serum Concentration on Cell Differentiation

To ensure, that optimal cell proliferation was also followed by optimal differentiation, the ability of the cells treated with different expansion media to undergo differentiation into the osteoblastic lineage was investigated by treating the cells with osteogenic induction medium followed by staining the cell layer for alkaline phosphatase (section 2.2.13.1.). All cells treated with osteogenic medium displayed an osteoblastic flattened phenotype and stained positive for alkaline phosphatase, the strongest staining was observed for cells expanded in 15% human serum (Figure 22). It was thus shown, that a better expansion rate (a higher cell number in shorter time) was accompanied by optimal differentiation.

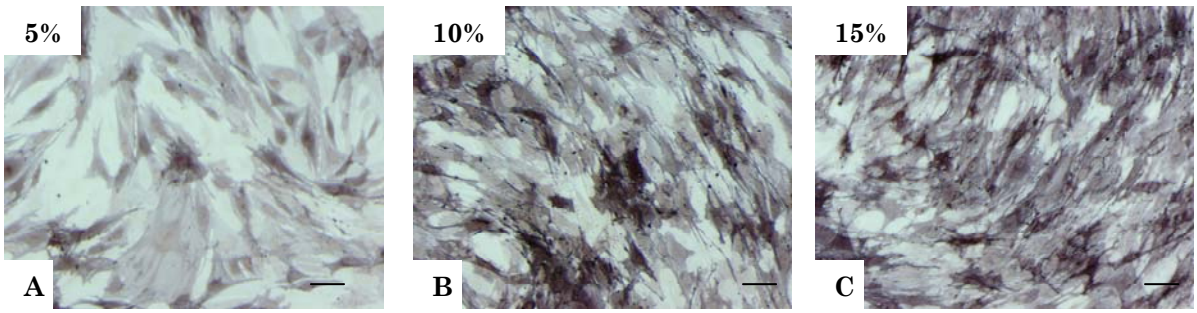

Figure 22 Osteogenic differentiation capacity of cells treated with different serum concentrations. Human trabecular bone derived cells were seeded at 5x10³cells/cm² in 48-well plates and cultured with ZKT-1 basal medium supplemented with 5%, 10% or 15% human serum. Cells were treated with osteogenic medium for 14 days and differentiation was assessed with alkaline phosphatase staining for cells expanded in **(A)** 5% human serum, **(B)** 10% human serum and **(C)** 15% human serum. Original magnification: x100; scale bar = 100µm.

2.3.2.3. Discussion

It was demonstrated that with increasing human serum concentrations in the medium, better (faster) proliferation was obtained (15%>10%>5%>1%). These results are in line with another study published by Stute et al. (2004). They compared the effects of 1%, 3% and 10% autologous human serum on the expansion of human bone marrow derived cells and demonstrated that 10% human serum was at least as good as 10% FCS. Furthermore, they showed that cells grown with 10% human serum had more osteogenic potential than those expanded in 3% and 1%.

In this study, the use of FCS was avoided and protocols were established using human serum. However, a potential limitation of using 15% human serum for clinical purposes is the availability of human serum in these relatively large amounts, especially if autologous serum is to be applied*****. Considering that 15% showed the highest rate of expansion and especially because of the key effect noted in the isolation of human bone marrow derived cells upon using 15% in the initial isolation phase, this concentration was considered to be optimal for expansion and was used in the study thereafter. This can be explained by a higher availability of mitogenic factors essential for the cells in the initial growth phase. Confluency will eventually be reached upon longer cultivation with media supplemented with lower amounts of serum. Having observed that cells cultivated with 10% human serum approached those

cultivated with 15% closely in protein content and DNA amounts as well as in alkaline phosphatase staining intensity, the concentration of 10% to induce osteogenic differentiation was considered to be sufficient for osteogenic medium supplementation.

*** Note**

The fact that 15% human serum was applied is not only a limitation for the later clinical application but the availability of human serum is not always provided for basic research as well. Therefore, osteogenic differentiation for this study was also partly verified using fetal bovine serum (see Appendix II, section 7.5.).

2.3.3. Cell Expansion and Differentiation Media

Although very satisfactory results were obtained using human serum concerning both proliferation and differentiation, and the fact that serum is usually included in most media as a readily available supplement to promote cell proliferation (Gregory et al., 2004), serum free formulations are an attractive substitute and have been developed for various applications. Advantages of serum free media include: (i) growth improvement by excluding inhibitors found in sera, (ii) precise analysis of the effects of known factors, therefore facilitating the identification of new factors, (iii) enables the production of customized media, and finally, (iv) provides consistent lot to lot activity, thus eliminating the tedious task of serum screening before purchase, as described earlier.

The possibility to increase the *in vitro* proliferation rate and osteogenic potential of trabecular bone derived cells was studied by investigating the effects of different growth factors in an attempt to develop a serum free medium compared to human serum supplemented medium. In the literature, several growth factors have been described as having a proliferative and/or osteoinductive effect. PDGF and EGF were reported to have an inductive effect on proliferation and differentiation of osteoblasts (Zheng et al., 1992), as well as FGF (Hankemeier et al., 2005; Martin et al., 1997; Pri-Chen et al., 1998;

Walsh, 2000). IGF showed an osteoinductive effect (Kveiborg et al., 2000), while EGF was proliferative only, inhibiting osteogenesis (Zheng et al., 1992). Based on these studies the cytokines were chosen in this experiment at different combinations and compared to the effect of serum supplemented medium.

Cell Expansion Media

Twenty different combinations of expansion media (see section 2.2.6., Table1) were compared in terms of proliferation, monitored by determining cell viability using the WST-1 proliferation assay (Figure 23). The highest proliferation was observed in cells expanded in 15% human serum. The serum reduced formulation containing PDGF as a supplement also showed very good proliferation.

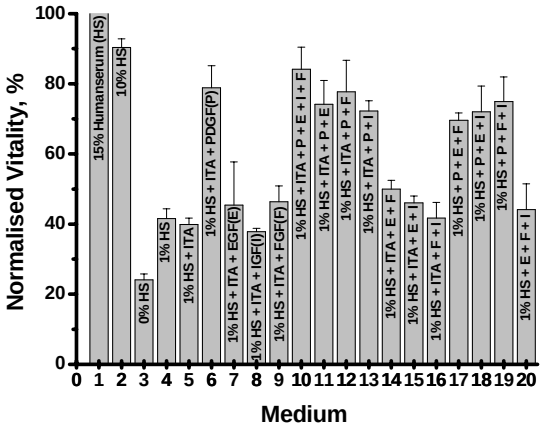

Figure 23 Proliferation of human trabecular bone derived cells in twenty different media combinations. Comparing serum rich medium to cytokine supplemented serum reduced media. Cells were seeded at $5x10^3$ cells/cm^2 in ZKT-1 basal medium, supplemented with either human serum (15%, 10%, 1%, 0%) or different cytokines (PDGF, FGF, IGF, EGF), individually or in combinations. Serum reduced media were supplemented with ITA: a mixture of insulin, transferrin and albumin. WST-1 was measured after 9 days in culture. Values of the absorbance are shown as percentages from the mean value of absorbance of cells cultivated in 15% serum supplemented medium. Error bars, means ± standard deviation n≥3.

Cell Differentiation Media

The potential of the serum reduced media to induce osteogenic differentiation was assessed via measurement of alkaline phosphatase activity and compared

to differentiation in serum rich media. The highest increase in ALP activity was found to be for the cells previously expanded in ZKT-1 medium, supplemented with 15% human serum followed by the medium supplemented with 10 % human serum (Figure 24).

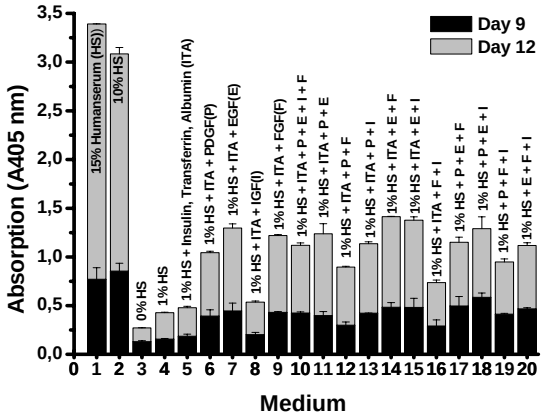

Figure 24 Osteogenic differentiation of human trabecular bone derived cells in twenty different media combinations. Comparing serum rich medium to cytokine supplemented serum reduced media. Cells were seeded at $5x10^3$ cells/cm^2 in ZKT-1 basal medium supplemented with either human serum (15%, 10%, 0%, 1%) or different cytokines (PDGF, FGF, IGF, EGF) individually or in combinations. Serum reduced media were supplemented with ITA: a mixture of insulin, transferrin and albumin. Osteogenic supplements were added at day 9 to all media. The black bars represent ALPase activity at day 9 and the grey bars represent ALPase activity at day 12. Error bars, means ± standard deviation n≥3.

Although, some growth factors individually or in combination showed a promising effect in terms of proliferation, differentiation was affected rather negatively by substituting human serum with growth factors. Data suggest that PDGF was the most active in increasing growth rate, whereas EGF and FGF-2 were the most active in promoting bone formation (indicated by higher ALP activity).

For the final three dimensional tissue reconstruction *in vitro*, in the experiments to follow (Chapter 3), the medium delivering the fastest expansion as well as the best osteogenic differentiation was chosen to be the most suitable. Therefore, ZKT-1 basal medium supplemented with 15% human serum was thereafter used for expansion of human trabecular bone derived cells as well as for human bone marrow derived cells.

In this study human serum supplementation was chosen, as it was a readily available source from the local blood bank of Hannover Medical School (HS-4) and very satisfactory levels of proliferation and differentiation were reached. As the eventual goal of bone tissue engineering is to implant a patients own isolated cells grafted on a suitable biomaterial back into the same patient, it is more appropriate to establish the protocols for *in vitro* tissue engineering purposes using human serum, ideally autologous human serum.
Moreover, an array of serum free media for growing mesenchymal like stem cell have already been developed by companies like Miltenyi Biotec GmbH, Cambrex and Stem Cell Technologies for various cell types. The development for a serum free medium is by far a more complicated task than what was attempted in the experiments above. However, the price of these media excluded them for further use within this study.

2.3.4. Large Scale Cell Expansion

Having identified the most suitable expansion medium for human mesenchymal like stem cells, a suitable expansion method next to the conventional adherent cell culture in T culture flasks for the production of up to$10x10^8$ cells to meet the needs for *in vitro* tissue engineering experiments (Chapter 3) was to be developed. For this purpose, the following two methods were investigated.

2.3.4.1. Spinner Flask-Microcarrier Culture

Two different types of microcarrier were tested, namely Microhex™ (Figure 25A) and Cytodex® (Figure 25B). Cells were observed to attach on the bead surface after 24 hours and spread out on the surface of the microcarrier with a fibroblast like appearance. Cell proliferation was monitored throughout the period of cultivation by measuring glucose (Figure 26A) and lactate concentration (Figure 26B) in the medium. Higher glucose utilization, the main energy source, by cells cultivated on Microhex™ indicated better cell growth as was later confirmed by a higher cell harvest as well. Cells cultivated

as a control, in suspension without the adherence on a microcarrier, utilized almost no glucose.

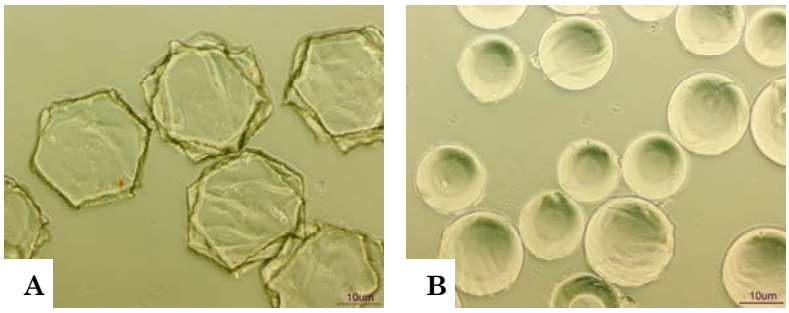

Figure 25 Phase contrast micrographs of microcarriers for adherent cell culture. A monolayer of well spread and attached cells was observed on the surface of **(A)** Microhex™ and **(B)** Cytodex®. The microcarriers were inoculated with 10x10^{3}cells/cm^2 human mesenchymal-like stem cells and cultivated in a spinner flask in ZKT-1 basal medium supplemented with 15% human serum. Original magnification: x100, scale bar=10*10µm=100 µm.

At harvest, cells were separated from the microcarrier beads by trypsin-EDTA digestion and filtration. Only 3.95x10^6 cells were retrieved from the spinner in the case of Microhex™ and only 1.73x10^6 with respect to Cytodex®. To ensure that this low cell number was not due to growth inhibition through the microcarrier beads, the harvest was replated in a T175 flask at 1x10^4 cells/cm^2 and growth was monitored by calculating the population doubling rate, which was found to be very similar compared to cells of the same passage cultivated in parallel in T flasks.

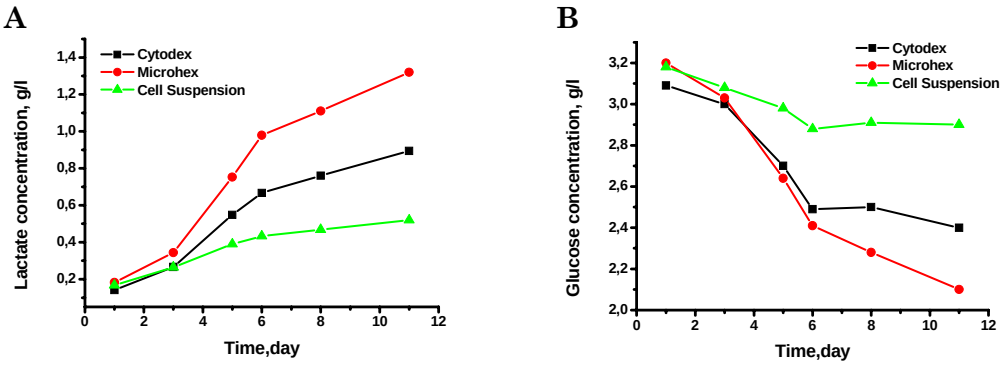

Figure 26 Glucose utilization and lactate production in microcarrier cell culture. Cells were cultivated either in conjunction with a microcarrier; Microhex™ (red line) and Cytodex® (black line) or without a microcarrier as a control (green line) in suspension spinner culture in ZKT-1 medium supplemented with 15% human serum. **(A)** Glucose and **(B)** lactate concentration (g/l) were measured in the supernatant throughout the cultivation period by the YSI 2700 Select biochemistry analyzer.

The population doubling rate was calculated to be 0.43 population doublings per day for the cells replated in a T flask after being separated from the microcarrier beads and 0.46 from the continuous T flask culture. It was demonstrated that cells were successfully cultivated and expanded on both microcarrier types with slightly better proliferation on Microhex™. These results are consistent with the findings of other investigators as well (Granet et al., 1998; Sautier et al., 1992), who have postulated that it was the charge of the surface (negative) rather than the affinity for collagen that is responsible for cell attachment on the microcarrier. However, final conclusions could not be drawn due to problems encountered in the final harvesting of the cells at the end of the cultivation period. As an alternative to the trypsin method, collagenase in addition to the use of various sieves was applied (data not shown) but complete separation of the cultivated expanded cells from the microcarriers was not achieved. In general, the use of the microcarriers as an alternative to cultivate adherent cells in large amounts did not meet the expectations and a novel method for expanding mesenchymal-like stem cells *in vitro* was sought, so the use of cell factories as an alternative for large scale cell expansion was investigated in the following section.

2.3.4.2. Cell Factories™

The growth kinetics of cells cultivated in the cell factories were very similar to T flask cell culture and the optimized growing conditions of the lab scale culture could be transferred without any further developmental work concerning seeding density and expansion medium. In Table 4, the culture of human trabecular bone derived cells in conventional T flask culture is compared to culture in a four-tray cell factory in terms of population doubling rate. Similar population doubling rates and morphology (data not shown) could be noted between the two cultivation systems. However, with the use of the cell factory, the amount of time required for repeated passaging of the cells and the demand in incubator space and cost could be drastically reduced, considering that the surface culture area of one four tray cell factory (2528 cm^2) is equivalent to approximately fifteen T175 culture flasks. A further

advantage of the cell factory is the minimized risk of microbial contamination with the cells kept in one closed system. An inoculation density of $10x10^3$ cells/cm² in a four-tray cell factory yielded a harvest of up to approximately $115x10^6$ cells per cell factory (and an average of 85 $x10^6$ cells).

Table 4			
	Initial cell number	**Confluent cell number**	**PD Rate**
T175 flasks (7x)	$12x10^6$	$32\ x10^6$	0.28
Cell Factory (1x)	$25.28\ x\ 10^6$	$112.5\ x\ 10^6$	0.31
PD Rate = Number of population doublings per day			

Table 4 Population doubling rate of human trabecular bone derived cells cultivated in T175 flasks versus a four tray cell factory. Cells were seeded at $10x10^3$cells/cm² in seven T175 flasks parallel to a four-tray cell factory and cell number was determined after expansion in ZKT-1 basal medium supplemented with 15% human serum.

2.3.5. Cell Characterization

Since the cells derived from human trabecular bone displayed a large expansion potential, similar to cells derived from human bone marrow, in addition to being morphologically very similar, the isolated cell population was further examined concerning the ability to undergo differentiation into fat (adipogenesis), cartilage (chondrogenesis) and bone (osteogenesis).

2.3.5.1. Multipotentiality of Human Trabecular Bone Derived Cells

The cells were shown to differentiate into cartilage, fat and bone like tissue. ***Chondrogenic differentiation*** was demonstrated by Alcian blue, staining the proteoglycans produced by the chondrocytes light blue. ***Adipogenic differentiation*** was first evident after 14 days in culture, when first intra-cytoplasmic lipid droplets started to appear, visualized by Nile red staining. ***Osteogenic differentiation*** was evident in cells treated with osteogenic medium, which underwent a change in their shape, namely, from spindle shaped to the typical cuboidal shape, which could be demonstrated clearly with alkaline phosphatase staining. Figure 27 shows the multipotentiality of

trabecular bone derived cells of a representative patient sample (male, age: 60 years). As expected, control cultures maintained without supplements did not stain positive.Adipogenesis and osteogenesis were induced and observed in all tested patient samples. Chondrogenesis, on the other hand, was not routinely performed because of the complexities involved. No correlation could be drawn between with donor age, gender, passage number and the ability to undergo differentiation into the different lineages. Multipotentiality was always successfully performed on cryopreserved cultures. Therefore, cryopreservation did not alter the ability of these cells to differentiate into various tissue lineages.

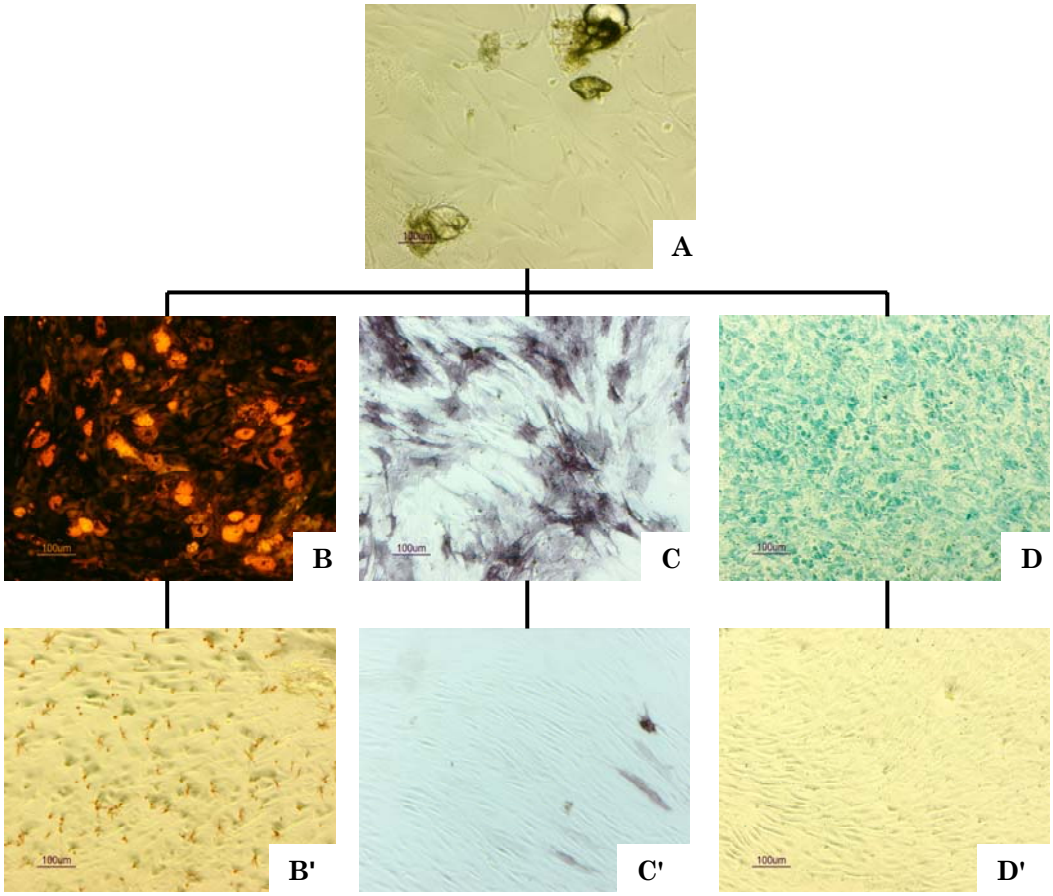

Figure 27 Multipotentiality of human trabecular bone derived cells. (A) Cells obtained from human trabecular bone explantation were seeded at 10x10^{3}cells/cm^2 until sub-confluence in expansion medium (ZKT-1+15%HS) and then changed to chondrogenic, adipogenic and osteogenic medium. Control cultures were cultivated in expansion medium in parallel. **(B)** Adipogenesis was verified with Nile red staining, visualising the intra-cytoplasmically accumulated lipid vacuoles in the typical round adipocytic cell shape at day 21 of cultivation in adipogenic medium. **(C)** Osteogenic potential is shown by alkaline phosphatase staining. **(D)** Chondrogenic potential was visualised by Alcian blue staining after 21 days in chondrocyte induction medium. Parallel control cultures maintained without the respective inductive supplements did not stain positive for all three lineages **(B'), (C')** and **(D')**. Original magnification: x100; scale bar=100µm.

2.3.6. Osteogenic Differentiation of Trabecular Bone Derived Cells *vs.* Human Bone Marrow Derived Cell

The osteogenic differentiation potential of human trabecular bone derived cells was compared to that of human bone marrow derived cells. Osteogenesis was biochemically assessed over a 40-day time course study in parallel cell cultures. Cells were seeded at $5x10^3$ cells/cm^2 in 48-well-plates, cultivated in expansion medium for 5 days until confluence after which the medium was exchanged with osteogenic medium (Appendix II).

2.3.6.1. Collagen I Production: Matrix Formation

Expression of collagen I was determined by collagen type I COOH terminal propeptide (CICP) secretion in the supernatant (section 2.2.11.). In Figure 28, CICP levels in both cell types showed that the synthesis of new collagen type I protein was initially high, distinctive for osteoblasts in their proliferative phase (Owen et al., 1990) reaching a maximum level followed by a down regulation in collagen production between day 15 and day 20 indicating the transition of the cells into the matrix maturation phase. Both cell types displayed a similar pattern, decreasing the production rate in collagen I, however, human bone marrow derived cells appeared to have laid down a higher total amount of collagen I than trabecular bone derived cells.

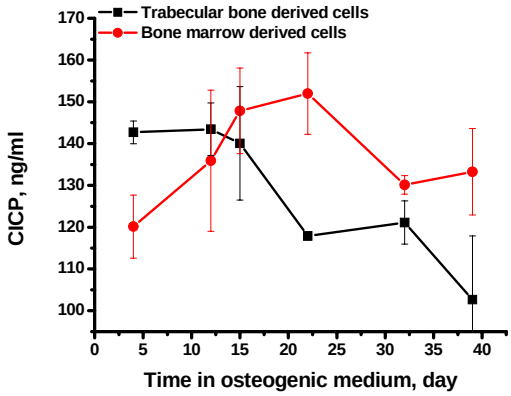

Figure 28 Collagen I production in trabecular bone derived cells versus human bone marrow derived cells. Both cell types were cultivated in parallel at $5x10^3$ cells/cm^2 in 48-well pates in expansion medium (ZKT-1+15%HS) followed by osteoinductive medium (ZKT-1+10%HS+osteogenic supplements) at confluence. CICP was determined in the supernatant throughout the cultivation period and expressed in ng/ml. The black line shows collagen I production in trabecular bone derived cells and the red line in bone marrow derived cells. Error bars, means ± standard deviation n=2.

2.3.6.2. Alkaline Phosphatase Activity: Matrix Maturation Phase

Alkaline phosphatase activity was determined in human trabecular bone derived cells cultivated in parallel to cells derived from human bone marrow under identical osteogenic conditions. Both cell types displayed a very similar pattern, the classical rise and fall pattern in ALP activity (Figure 29). These data are in agreement with what has been reported in the literature about osteogenic cells, showing maximum alkaline phosphatase activity following the down regulation of collagen I production. The higher peak value in ALP activity in human trabecular bone derived cells, indicative for the matrix maturation phase (Owen et al., 1990; Stein and Lian, 1993) might be explained by the higher activity of the individual cells. Considering the CICP levels in Figure 28, the proliferation phase of trabecular bone derived cells reached an earlier endpoint and the cells have transited into the matrix maturation phase before human bone marrow derived cells, which continued to lie down matrix.

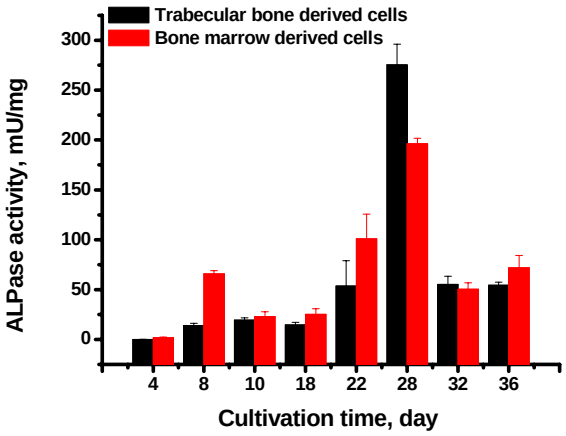

Figure 29 Comparison of alkaline phosphatase activity in human trabecular bone derived cells to human bone marrow derived cells. Cells were seeded at $5x10^3$cells/cm^2 in 48-well plates and cultivated in parallel in osteoinductive medium. Alkaline phosphatase activity was determined as milli units/min per well and normalized to the total protein content of the cell layer. The black bars represent ALPase in trabecular bone derived cells and the red bars the ALPase in human bone marrow derived cells. Error bars, means ± standard deviation n=3.

Histochemically, both cell types stained negative for alkaline phosphatase after 4 days in osteoinductive medium, indicating still ongoing proliferation and more intense staining was noted after 15 days of osteoinduction, a sign for cell maturation and the development of the osteoblastic phenotype (Figure 30).

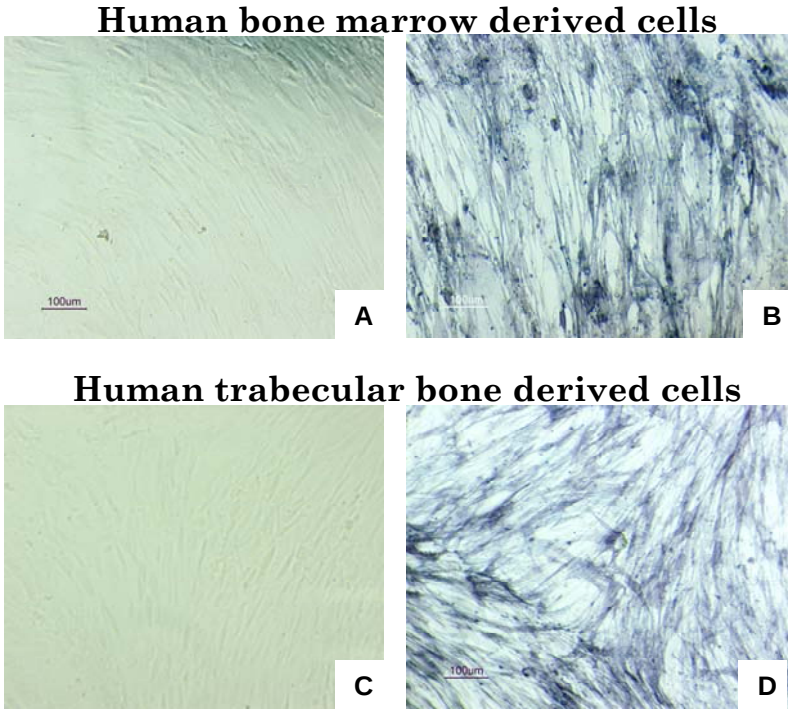

Figure 30 Alkaline phosphatase staining of human trabecular bone derived cells *vs.* human bone marrow derived cells. Alkaline phosphatase staining was performed in human bone marrow derived cells **(A)** after 4 days and **(B)** after 15days of culture in osteogenic medium and in human trabecular bone derived cells at the same time points **(C)** after 4 days and **(D)** after 15 days in osteogenic medium. Original magnification: x100; scale bar=100µm.

2.3.6.3. Extracellular Matrix Mineralization Phase

Mineralization, the terminal marker for osteoblastic differentiation, was quantified by measuring the amount of calcium deposited in the extracellular matrix (section 2.2.12.) throughout the cultivation period (Figure 31). Human bone marrow derived cells were observed to lie down greater amounts of calcium deposits compared to trabecular bone derived cells, which seemed to "catch up" in matrix mineralization with detectable amounts becoming apparent at a later time point (a delay of ca. 5 days), when compared to the human bone marrow derived cells.

The steep increase in calcein levels (calcium deposition) coincided well with the fall in collagen I production levels (Figure 28), indicating that cells start the mineralization process once enough collagen has been laid own.

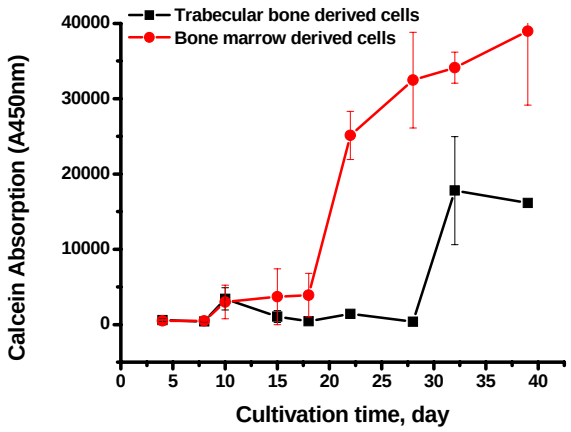

Figure 31 Calcium accumulation in the extracellular matrix of trabecular bone derived cells versus human bone marrow derived cells. Cells were seeded at 5x10³cells/cm² in 48-well plates and cultivated in parallel in osteoinductive medium. Calcein binding to calcium deposits was detected through recording absorbance of the fluorescent calcein (at 450nm), which is proportional to the amount of calcium laid down throughout the cultivation period. The red line represents the calcium amounts in human bone marrow derived cells and the black line of trabecular bone derived cells. Error bars, means ± standard deviation n=3.

2.3.6.4. Mineralization in Histology

To further unveil the process of mineralization of human bone marrow derived- and trabecular bone derived cells, cells were fixed at day 8, 15, 18, 23, 28 and 32 for histological staining (section 2.2.13.) to visualize the mineral deposition pattern in the cell cultures.

First signs of mineralization in the form of nodules or vesicles were evident after approximately 8 days of cultivation in osteogenic induction medium in both cell types (Figure 32). Light microscopy revealed vesicular structures along the collagen fibrils in both cell types and light positive von Kossa staining. After 15 days, mineralized spots scattered across the cell layer were detected with alizarin red staining in both cell types (Figure 32).

The onset of mineralization observed histologically coincided with the steep decrease in collagen I production noted in Figure 28. Genge et al. (1988) have found that a loss in alkaline phosphatase activity correlated with the initiation of mineralization of the matrix vesicles. Both cell types were observed to uncover a similar pattern in mineral deposition and staining, indicating *de novo in vitro* bone formation.

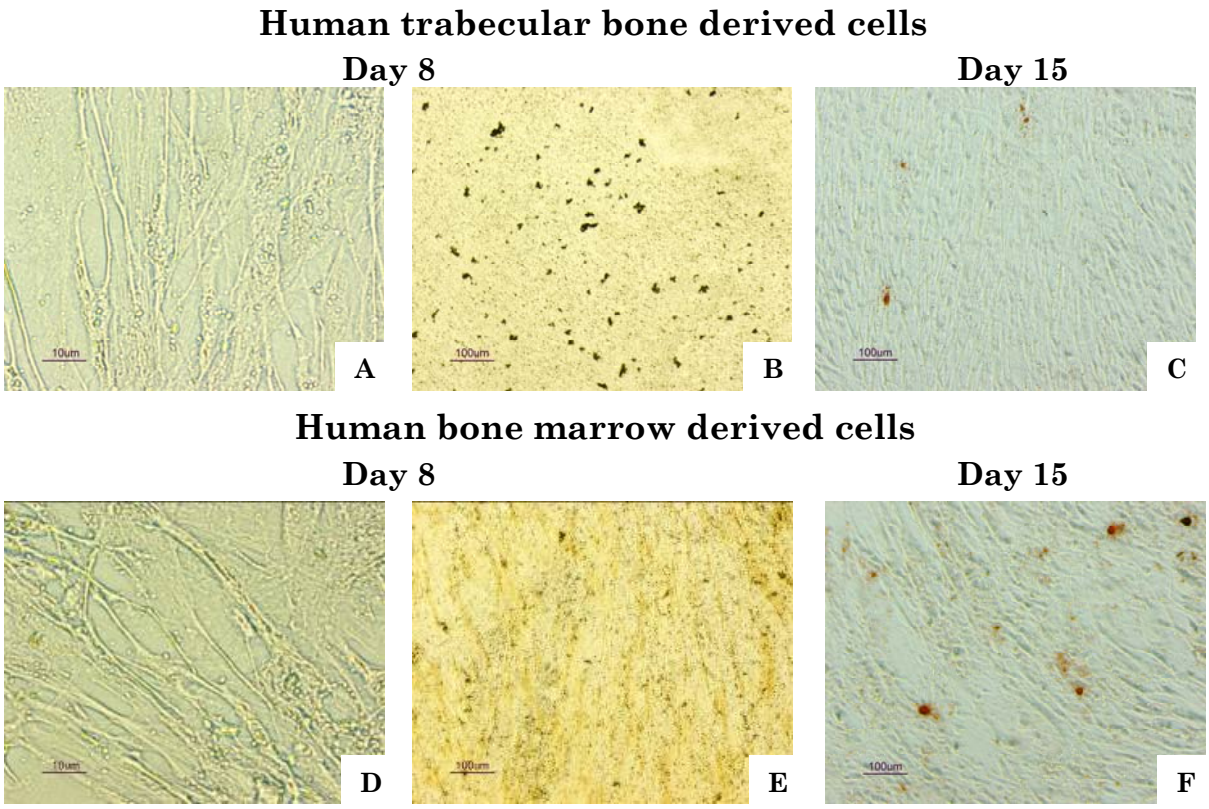

Figure 32 Phase contrast micrographs showing first signs of mineralisation in human trabecular bone derived cells and bone marrow derived cells. Cells were seeded at $5x10^3$cells/cm^2 and induced with osteogenic medium at confluence. Cell layers were fixed at day 8 and 15. Light microscopy revealed structures vesicular in shape along the collagen fibrils in both trabecular bone derived cells **(A)** and human bone marrow derived cells **(D)** (Original magnification: x 1000; scale bar=10µm). Von kossa staining after 10 days in osteoinduction medium showed a few mineral depositions along the collagen fibres in both trabecular bone derived **(B)** and human bone marrow derived cells **(E)**. (Original magnification: x100; scale bar=100 µm). Alizarin red staining at day 15 revealed a few scattered mineralised spots stained in red in trabecular bone derived **(C)** and bone marrow derived cells. Original magnification: x100; scale bar =100 µm).

The vesicular structures and the stained nodules were continuously examined under the light microscope throughout the cultivation period. They were observed to increase in number with time correlating with the intensity of mineral staining demonstrated by von Kossa staining in Figure 33.

Both cell types were observed to form these typical vesicles along the collagen fibrils of the extracellular matrix, however, more frequently observed in the case of human bone marrow derived cells.

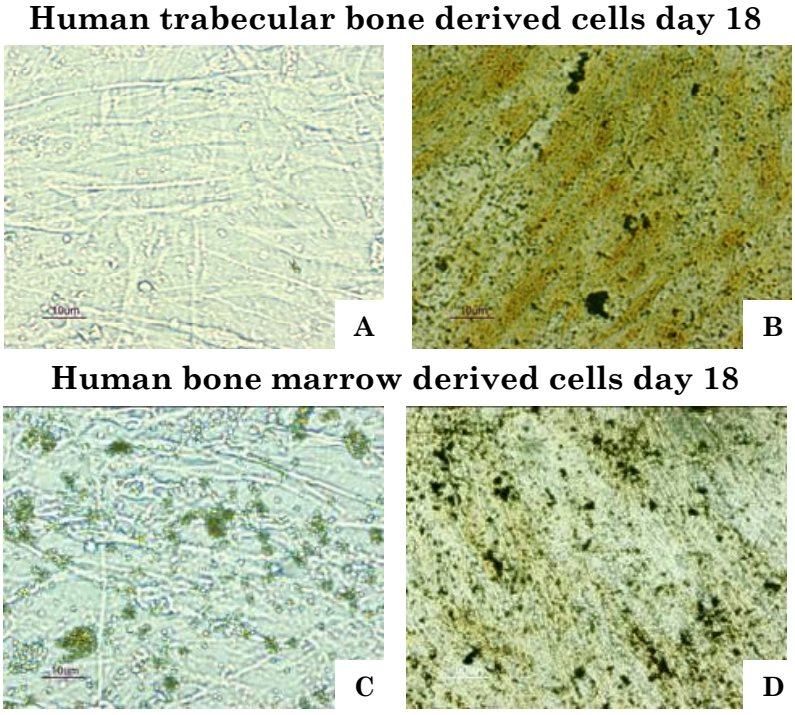

Figure 33 Phase contrast micrographs showing human trabecular bone derived cells and human bone marrow derived cells in the process of bone formation. Cells were seeded at $5x10^3$ cells/cm^2 and induced with osteogenic medium at confluence. Cell layers were fixed at day 18. The vesicular structures along the collagen fibrils were noted to increase in number for both trabecular bone derived cells **(A)** and human bone marrow derived cells **(C)** revealed with light microscopy. (Original magnification: x1000; scale bar=10μm). Von Kossa staining after 18 days in osteoinduction medium showed more intense staining with black nodules increasing in number along the collagen fibrils in both trabecular bone derived **(B)** and human bone marrow derived cells **(D)**. (Original magnification: x100; scale bar=100 μm).

The vesicular structures were found to increase further in size and number accompanied by more extensive extracellular matrix mineralization upon longer exposure of the cells to osteogenic medium in both cell types. Mineral deposition was observed to occur along the collagen fibrils in and/or around theses vesicular structures, which apparently formed the initial loci for mineralization. Those areas in the cell layer, which underwent mineralization could be observed as red vesicles by alizarin red staining, black-brown clusters visualized by von Kossa and green emitted fluorescence by bound calcein after 32 days cultivation in osteogenic medium (Figure 34). More intense staining was noted in human bone marrow derived cells, which is in agreement with the greater amounts of calcium deposited by these cells as shown in Figure 31.

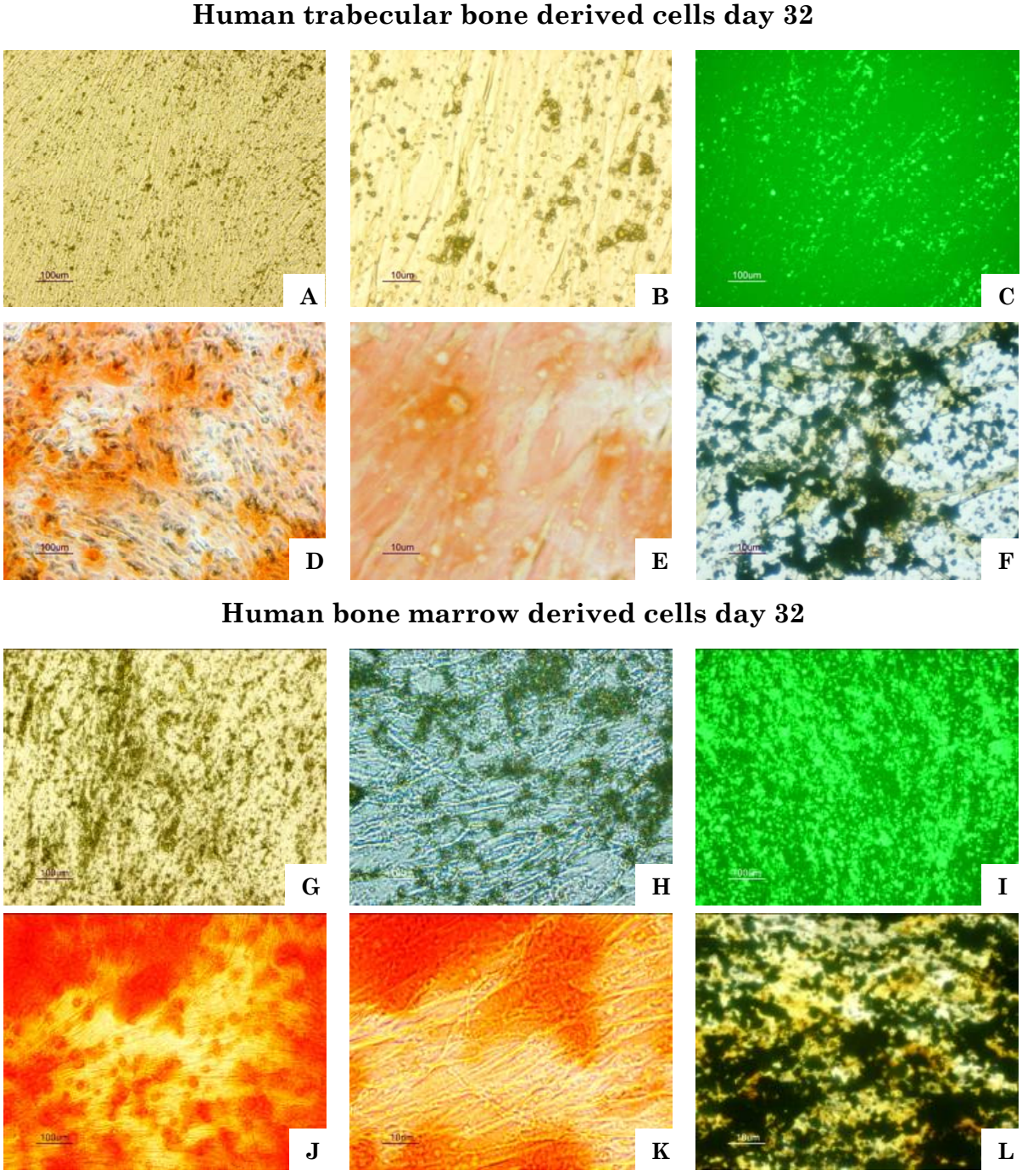

Figure 34 Terminal and complete mineralisation of the extracellular matrix in human trabecular bone derived and bone marrow derived cells. Light microscopy of the mineralised extracellular matrix revealed the vesicular structures decorating the collagen fibrils in both trabecular bone derived cells **(A)** and in bone marrow derived cells **(G)** Original magnification: x100; scale bar=100 µm. **(B)** and **(H)** showing these vesicular structures at a larger magnification:x1000; scale bar =10µm. Calcein binding pattern revealed more intense calcification (green fluorescence) of the bone marrow derived cells **(I)** compared to cells from trabecular bone **(C)**. Classical alizarin red staining patterns were noted to occur around these vesicular structures in trabecular bone derived cells **(D)** and bone marrow derived **(J)**. **(E)** and **(K)** show these at a larger magnification x1000; scale bar =10µm .Von Kossa stain in both trabecular bone derived cells **(F)** and bone marrow derived cells **(L)** verified the extensive mineralisation across the vesicular structures. Original magnification: x1000; scale bar=10 µm

2.3.6.5. Interpatient Variation

Like other authors, interpatient variability was observed in the ability of the cells to undergo osteogenesis. The mineralization patterns of cells isolated from three patients were compared in terms of alizarin red staining after 25 days of osteoinduction. The cell layers displayed various degrees of staining (Figure 35). To exclude the effect of the age factor (Martinez et al., 1999a; Martinez et al., 1999b) on osteogenic differentiation, cells were isolated form patient samples with an average age of 63±7 years.

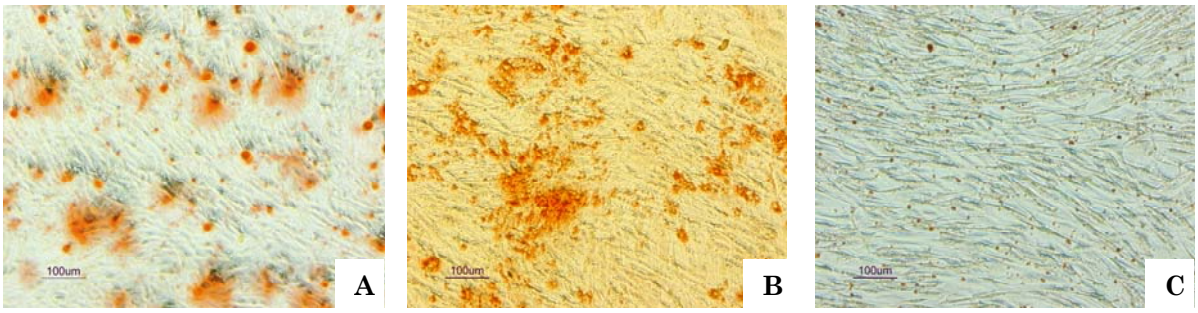

Figure 35 Alizarin red staining in trabecular bone derived cells from three patients. Cells isolated from three patients were osteoinduced for 23-28 days, fixed and stained for alizarin red. Patients **(A)** and **(B)** showed red stained calcium accumulations, indicating terminal mineralisation, whereas cells from patient **(C)** showed almost no mineralisation, staining negative. Original magnification: x100; scale bar=100µm.

These differences in patients are in line with data reported in the literature (Siggelkow et al., 1999; Kassem et al., 2003; Stenderup et al., 2003). Based on the developmental sequence described earlier in the introduction (chapter 1, section 1.1.5.), terminal differentiation of an osteoblast culminating in mineralization is preceded by a peak in alkaline phosphatase activity (typical rise and fall pattern). Civitelli et al. (1993) and Jaiswal et al. (1997) have also demonstrated that the decrease in ALP activity correlated with advanced matrix mineralization. So the peak in alkaline phosphatase is a prerequisite for osteogenic cells to transit into the final mineralization phase. Cells isolated from the above three patients were cultivated in osteoinductive medium and analyzed for ALP activity throughout the cultivation period (Figure 36). Cells from patients (A) and (B) both peaked in ALP, while the activity in cells from patient C increased linearly with ongoing cultivation.

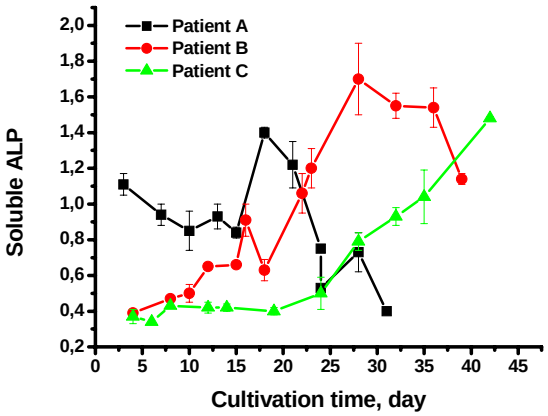

Figure 36 Alkaline phosphatase activity in three different patients. Cells were cultivated in osteogenic medium and soluble ALP activity was measured using a biochemical assay (Sigma) based on conversion of p-nitrophenyl phosphate to p-nitrophenol, which was measured spectrophotometrically at 405 nm. Patients A (black line), B (red line) showed the typical rise and fall pattern while the absorption in cultures of cells form patient (C) kept rising. Error bars, means ± standard deviation n=3.

These results need to be confirmed by further biochemical analysis. As the implementation of a thorough biochemical analysis for osteogenic differentiation for each patient sample in this study was not feasible. An easy to perform and fast screening test for ALP activity was performed in an attempt to explain the differences in mineralization. This variability reflects the well known heterogeneity within cells isolated from different donors.

However, these results could be applied in establishing a screening method to ensure that cells will eventually mineralize. As for cells to undergo terminal osteogenic differentiation, reaching a peak in ALP activity appears to be an inevitable transition point the cells must go through.

Note:

Detailed investigation for basic research purposes usually requires the availability of a consistent batch of serum throughout the experiments. As human serum might not be available in sufficient amounts for a series of experiments, mineralization of human bone marrow derived cells was also investigated using fetal bovine serum instead. A similar mineralization pattern was successfully obtained as demonstrated by alizarin red, calcein and von Kossa staining (data shown in Appendix II, section 7.5.).

2.3.6.6. Discussion: Osteogenesis in Trabecular Bone Derived Cells *vs.* Bone Marrow Derived Cells

Human trabecular bone derived cells as well as human bone marrow derived cells, showed an expression pattern of bone related proteins during the proliferation phase and matrix maturation phase very similar to the classical developmental sequence (Genge et al., 1988; Jaiswal et al., 1997; Lian et al., 1998; Owen et al., 1990; Stein and Lian, 1993). Initially, there was a period of active proliferation, in which collagen I levels increased following a down regulation of this phase, when alkaline phosphatase activity reached maximum levels and the extracellular matrix was rendered competent for the third and final stage of the developmental sequence, terminal mineralization.
Although both cell types displayed similar patterns in osteoblast maturation, the onset of mineralization, the final stage for bone formation *in vitro*, was slightly delayed in the case of trabecular bone derived cells and the intensity of mineralization was observed to be higher for human bone marrow derived cells. A possible explanation for this could be the higher levels in collagen type I production (Figure 28) in the human bone marrow derived cell cultures. This could be attributed to the fact that prior to osteoinduction, both cell types were seeded at $5x10^3$ cells/cm^2 in 48-well plates and cultivated for 5 days in expansion medium (ZKT-1 basal medium supplemented with 15% human serum). Considering that the average population doubling rate for human bone marrow derived cells was calculated as 0.4 compared to 0.22 population doublings per day for human trabecular bone derived cells, it can be inferred that the amount of cells available after expansion in the case of the human bone marrow derived cells are higher in number than the trabecular bone derived ones. Bearing in mind that proliferation is down regulated gradually upon the addition of the osteogenic supplements, directing the cells towards differentiation. Thus, human trabecular bone derived cells might have started out with a lower cell density, which led to the higher ALP activity per cell observed in Figure 29 and to less collagen production, which is an essential requirement for mineralization to occur. Still, trabecular bone derived cells did manifest a fully differentiated phenotype, culminating in a mineralized matrix.

The data suggest that a prolonged initial expansion period prior to osteoinduction might render the mineralization intensity more similar to that observed in human bone marrow derived cells.

Altogether, the data suggest that the mineralization process in both cell types follows the well accepted pattern of osteogenic differentiation in the literature and that similarities do exist between both cell types. These similarities include:

Firstly, the down regulation of collagen I levels. Secondly, the alkaline phosphatase peak, and lastly the positive histological staining revealing a similar mineralization pattern by the formation of vesicular like structures (matrix vesicles). The differences observed, between the intensity and onset of mineralization in trabecular bone versus human bone marrow cells can be explained by the higher initial proliferation by human bone marrow derived cells, which is in line with what has been reported by Jaiswal et al. (1997). The group has shown that, while initial higher seeding densities did not result in significant different cell numbers beyond a certain time point, there was significantly more mineral deposited in cultures seeded at higher densities.

2.4. Conclusions

- Trabecular bone was demonstrated to be a good and readily available source of mesenchymal progenitor cells. A simple and high yield isolation procedure was established from small bone tissue biopsies. It was shown to be of comparable efficiency to bone marrow aspirates with the characteristics of self-renewal with a high expansion potential, demonstrating a stable phenotype over the passages. Their multilineage differentiation potential, displaying the ability to differentiate into the adipogenic, chondrogenic and osteoblastic lineage is very similar to that of bone marrow derived cells. Further, this study supports the hypothesis that multipotential mesenchymal-like cells are present in many connective tissues in the adult human and that the isolation and manipulation of these adult stem cell-reserves represent a promising tool of candidate cells for engineering, repair and regeneration of tissues and organ systems.

- A suitable expansion medium for expanding human mesenchymal like cells ensuring maximum proliferation without the loss of differentiation capacity was successfully developed. 15% human serum supplementing the basal medium was found to be optimal for isolation and expansion purposes.

- Human mesenchymal-like stem cells were successfully expanded in cell factories, a disposable single batch closed system to generate a large amount of cells in a reproducible way. It was shown that using the cell factory, up to 115 million human mesenchymal-like cells in a single batch were harvested from one four tray cell factory. The cellular morphology and growth kinetics were unaltered from the T-flask laboratory scale culture and the multipotential of the isolated cells was unaffected. Therefore, it was found to be a good way to reproducibly expand primitive cells *in vitro*. Being a closed system, it has a very low contamination risk as well as providing a large growth surface in

limited space areas. Further, it is easy to handle as well as cost efficient and can be predictably up-scaled. For large scale expansion purposes, T culture flasks were entirely replaced by the cell factory expansion method. Theoretically, the cultivation can be up-scaled to a commercially available forty-tray cell factory™ (Nunc, Wiesbaden), for instance, whereby a total surface area of 10 m^2 can be obtained which is operated as one single unit. The equipment and surface quality of the cell factory and the necessary handling equipment are suitable for work in aseptic conditions or clean rooms so that the production of human mesenchymal-like stem cells could eventually be cultivated under GMP conform conditions using this method. Cultivation of human mesenchymal like cells at this scale is a novel application as cell factories are mainly used for industrial scale production of vaccines, monoclonal antibodies or pharmaceuticals. For cell expansion purposes, it has so far only been applied for the generation of dendritic cells (Berger et al., 2002; Tuyaerts et al., 2002).

- In this study, a model for osteogenic differentiation from human patient samples was established, demonstrating the three classical phases of osteogenic differentiation *in vitro*, providing a useful model for evaluating multiple factors affecting the progression of cells from undifferentiated precursors to mature osteoblasts and eventually terminated osteocytes. This model could be useful in studying cellular response to a variety of drugs, hormones and cytokines known to affect bone tissue formation *in vivo* or metabolic or genetic diseases leading to bone dysfunction as an alternative to animal models for instance. Moreover, studying and visualizing the mineralization of matrix vesicles *in vitro*, might help us understand the reasons behind decreased mineralization in diseases like hereditary skeletal dysplasias (e.g. hypophosphatasia), where the basic clinical manifestation is defective bone and cartilage mineralization and its mechanism of occurrence still being unclear.

3. Improved *in vitro* Bone-like Tissue Formation by Trabecular Bone Derived Cells in Three Dimensional Culture

3.1. Introduction

In the previous chapter, it was demonstrated that human trabecular bone cells have mesenchymal-like characters, including a high expansion potential and multilineage capacity. The osteogenic differentiation in particular, was examined in detail to ensure the ability of these cells to form bone tissue *in vitro*, in a two dimensional culture environment. Having successfully isolated and expanded a large amount of osteogenic cells from a small bone biopsy, the approach of using autologous cells for clinically applicable bone tissue engineering was to be examined next.

The objective of this chapter is to develop a bone tissue engineering strategy for bone tissue repair by the creation of an appropriate osteoinductive microenvironment to later facilitate the capacity of an *in vitro* reconstructed tissue transplant to be integrated *in vivo*. The major drawback associated with three dimensional cultures of cell seeded constructs so far, pertains to the limited diffusion of nutrients throughout the whole scaffold structure, especially when cultivated statically. To overcome this limitation, two different dynamic cultivation modes were investigated besides stationary culture: a fixed bed perfusion bioreactor (Jaeger and Barthold, 2004) and a novel tilted rotating bioreactor system for the three dimensional cultivation of human trabecular bone derived cells in conjunction with a poly (lactide-co-glycolide)-calcium phosphate composite scaffold.

Currently available bioreactors include spinner flask, rotating and perfusion bioreactors. All improve mass transfer of nutrients and oxygen, yet, inadequacies and disadvantages remain in each system: whether it be the decreased internal medium transport in the spinner flasks leading to growth on the peripheries and leaving the interior empty or the potential limitation of insufficient medium mixing at the surface of the scaffold in the rotating bioreactor also leading to decreased medium transfer to the interior of the

scaffold or the relative complexity and difficulty in assembling and operating a perfusion bioreactor (Glodstein et al., 2001; Sikavitsas et al., 2002; Bancroft et al., 2003; Meinel et al., 2004a). With the rotating bioreactor, showing the most promising results in generating bone-like constructs *in vitro* (Vunjak--Novakovic, 2003; Marolt et al. 2006; Martin et al., 2004; Kasper et al., 2007), it was to be investigated whether introducing a further dimension to the rotating movement, namely, a tilted rotating motion would improve medium mixing and nutrient transport to the interior of the scaffold. To generate this type of motion, a commercially available tube rotator (Miltenyi Biotec GmbH) designed for sample mixing was used.

Briefly, regarding the experimental set up, after expanding the cells as previously described, they were seeded onto a poly (lactide-co-glycolide)-calcium phosphate composite scaffold (PLGA/CaP) and cultivated under either static or dynamic conditions for up to 35 days *in vitro* and subsequently assayed for cell attachment and proliferation using phase contrast light, confocal laser and scanning electron microscopy. Osteogenic differentiation was analyzed further biochemically by determining the expression of alkaline phosphatase and collagen type I production.

3.2. Materials and Methods

3.2.1. Poly (lactide-co-glycolide)-Calcium Phosphate Composite Scaffold

A commercially available scaffold (OsteoScaf™) was obtained from BoneTec (Toronto, Canada). Briefly, the composite scaffold was made by combining biodegradable poly (lactide-co-glycolide) (PLGA, 11.5%) with bioresorbable calcium phosphate (CaP) cement particles (2 parts CaP with 1 part PLGA by weight) as described by Guan and Davies (2004). The PLGA/CaP scaffold dimensions are approximately 10x10 mm (Figure 37) with ~90% porosity. The interconnective pores form a network of macropores (100-approx.2000 µm) as well as micropores (< 100 µm), which mimics trabecular bone in structure. Further, the PLGA/CaP scaffold degrades into nontoxic components that can be eliminated from the body.

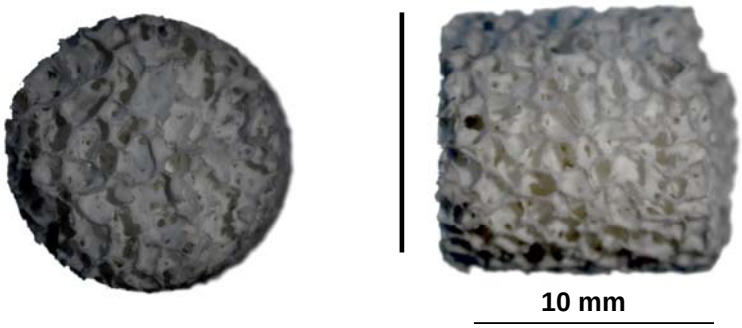

Figure 37 Poly (lactide-co-glycolide)/calcium phosphate composite scaffold. Dimensions are 10x10 mm with a pore range of <100 µm-2000 µm.

3.2.2. Scaffold Sterilization

The PLGA/CaP scaffolds were sterilized by dipping in 100% ethanol for 1 minute and then consecutively three times in 70% ethanol, each time for 10 minutes. Scaffolds were then washed in 1x PBS, followed by immersion in an appropriate coating solution as described below for 24 hours prior to seeding.

3.2.3. Scaffold Surface Coating

Scaffolds were pre-coated overnight with various purified extracellular matrix proteins including human serum, collagen type I, fibronectin and gelatin to assess the optimal surface coating for the individual cell type.

3.2.3.1. *Serum Coating*

For serum coating, the sterilized scaffolds were immersed in human serum or fetal bovine serum and incubated overnight. Prior to cell seeding, the excess serum was removed and the cell suspension was applied.

3.2.3.2. *Collagen I*

Scaffolds were covered with sterile 0.1% collagen type I solution (in 0.1% N acetic acid) from calf skin, overnight at 4ºC. Excess collagen solution was removed and the coated scaffolds were washed with ZKT-1 basal medium before cell seeding.

3.2.3.3. *Fibronectin*

Scaffolds were coated with fibronectin according to the manufacturer's instructions. The lyophilized fibronectin was re-suspended with 1 ml sterile deionized water. The solution was diluted to 2.5 µg/ml, washed with ZKT-1 basal medium and immediately used for cell seeding.

3.2.3.4. *Gelatin*

Scaffolds were immersed in 0.1% gelatin solution and incubated overnight at 4ºC. The solution was aspirated off and the scaffolds washed with ZKT-1 basal medium and immediately used for cell seeding.

3.2.4. Scaffold Seeding or Cell Culture on Scaffolds

A seeding density of $5x10^6$ cells per PLGA/CaP scaffold was applied for osteogenic cells. Cells were harvested from cell factories (as described earlier in chapter 2) and the cell pellet was re-suspended in a volume, predetermined as the amount of medium needed to completely fill the pores of the foam-like PLGA/CaP scaffold. For cell seeding, the scaffolds were placed in individual wells of a 24-well plate and each inoculated drop wise with 0.4 ml cell

suspension. For cell adhesion, the freshly seeded scaffolds were then incubated for 90 minutes at 37°C and 12% CO_2 and then each carefully transferred to a 50 ml tube containing 15 ml expansion medium (ZKT-1, 15% human serum, 1% penicillin-streptomycin). The medium was filled up to 30ml after 24 hours.

3.2.5. Three Dimensional Cultivation Systems for *in vitro* Tissue Reconstruction

After cell seeding, the cell-scaffold construct was further cultivated in one of the following three dimensional cultivation systems for up to 35 days. Two dynamic systems were compared to the classic static culture with the cell-scaffold constructs being assayed for alkaline phosphatase activity, total protein content and viability via the WST-1 test. Detailed histological analysis including light -, confocal laser- and scanning electron-microscopy was also performed.

3.2.5.1. Static Culture

For static culture, the seeded scaffolds were carefully placed in aerated 50 ml tubes (Figure 38) containing 30 ml osteogenic medium (see Appendix II) and placed upright in the incubator (37°C, 12% CO_2) with medium being sampled and exchanged every 72 hours. Medium samples were frozen at -20°C and cell-scaffold constructs were fixed and analyzed at day 7, 15, 27 and 35.

Figure 38 Picture and drawing of the aerated tube used for three dimensional cultures. A 50 ml tube supplied with a filter cap allowing exchange of oxygen, carbon dioxide (and humidity) through the openings. Sterility is maintained at all times by means of the additional filter membrane (0.22 µm). The picture is adapted from TPP product website: http://www.tpp.ch/tissue_culture/filter_and%20pcv_tubes/filter_pcv_tubes.html

3.2.5.2. The Tilted Rotating Bioreactor System

To tilt the medium from one side to the other in addition to continuously rotate it, the commercially available tube rotor (MACSmix™ Miltenyi Biotec GmbH) was applied. It is equipped with a rack to hold 15 ml or 50 ml tubes and can be placed in the incubator at 37°C for cultivation. A schematic illustration of the generated motion is shown in Figure 39. The freshly seeded cell-scaffold construct was placed in an aerated 50 ml tube (section 3.2.5.1.) and immersed in 30 ml osteogenic medium. Following a 24 hour static cultivation period, the tube was built into the tube rotor in a tilted position and rotated continuously at 12 rpm for 35 days with medium being sampled and exchanged every 72 hours. Gas exchange is supported by the aerated filter cap of the tube. The motion generated in the aerated tube is illustrated in Figure 40. The cell-scaffold construct is continuously gently swirled in the medium in a rotating manner when tilting upwards and downwards with the whole bulk of the medium volume flushing through the cell-scaffold construct ensuring nutrient and oxygen delivery to cells deep within the interior of the scaffold.

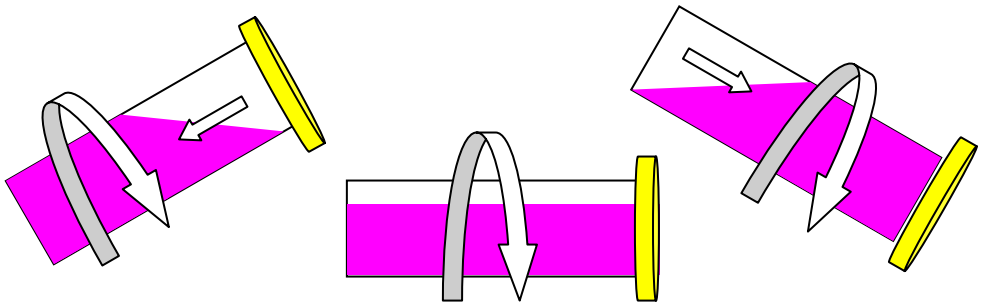

Figure 39 Schematic illustration of the generated movement in the tilted rotating bioreactor system. The medium is swirled in a rotating manner in addition to being gently tilted from one side of the tube to the other.

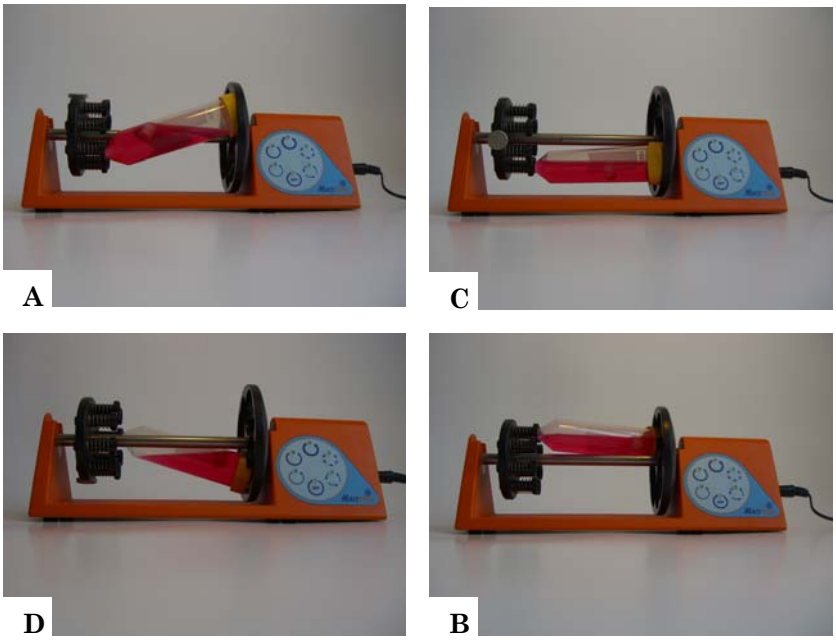

Figure 40 The tilted rotating cultivation system. (A)-(D) show the various positions of the aerated vessel during the dynamic cultivation. The cell scaffold construct is continuously exposed to a tilting and rotating motion with the medium flushing nutrients into and around the construct.

3.2.5.3. The Fixed Bed Perfusion Bioreactor System

The bioreactor system consists of individual bioreactors, connected in a group of three, to a control unit (mcU 2000, Medorex, Bovenden), which is further connected to a computer with LINUX based control-software (mfs, Medorex), enabling network connection and exchange (Figure 41).

Figure 41 The fixed bed perfusion bioreactor assembled in the laboratory. (A) Two control and gas mixing units, each connected to a computer and a group of three bioreactors supplying each bioreactor with a constant gas mixture. Each bioreactor in turn is connected to three pumps a fresh medium supply bottle, a waste bottle and kept at 37°C through a water jacket. **(B)** A close up of one bioreactor showing the various ports, gas supply and sampling port in front.

A schematic diagram of a bioreactor system is shown in Figure 42 (adapted from Barthold, 2003). Each bioreactor consists of a cylindrical glass vessel with connectors to a temperated water bath, maintaining the bioreactor at 37°C throughout the cultivation period. Inside the outer glass vessel, an inner conical glass vessel contains the cultivation medium and the scaffold perfusion chamber. The cultivation medium is continuously mixed through a magnetic stirrer at 120 rpm. Both vessels are screwed to and sealed with the reactor lid, which contains ports for temperature, dissolved oxygen and filling level sensors. The port in the middle connects the perfusion chamber to a peristaltic pump (1), which draws medium out of the cultivation reservoir through the scaffold chamber and back into the cultivation reservoir (inner vessel) at 0.2 ml/min. The perfusion chamber was designed to have a conical shape with minimized dead space in the upper part, directing the flow perfusion path through the scaffold and not confined to running down only at the edges surrounding the cell-scaffold construct (Barthold, 2003).

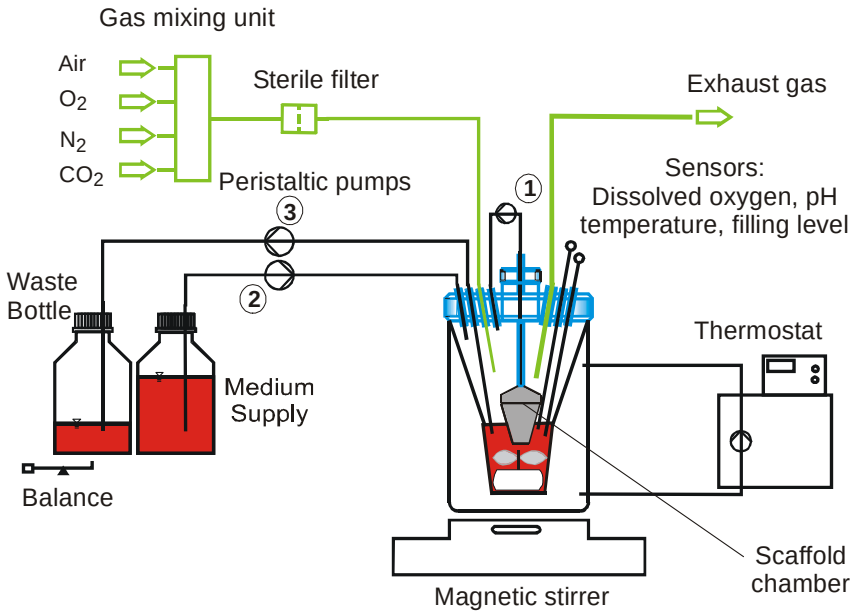

Figure 42 Schematic Illustration of the fixed bed perfusion bioreactor adapted from Barthold (2003).

Further, two more pumps were connected to the ports on the lid as well. The medium input pump (2) connected to the fresh medium reservoir set at a continuous rate of 7 µl/min and a peristaltic pump connected to the waste bottle (3), which is set to pump upon receiving a signal from the filling level

sensor. The pumps are connected to the control computer via RS-232 serial ports. The sensors were linked to the digitally controlled measurement and control unit via connecting cables. Therefore, the control unit is able to measure and monitor the temperature and dissolved oxygen. The station allows the mixing of air, oxygen, carbon dioxide and nitrogen in preset proportions. For all experiments in this study, a constant mixture of gas containing 20% dissolved oxygen was supplied through one of the ports on the bioreactor lid. Sampling can be performed continuously through a sampling port without stopping the cultivation (Figure 41B).

The scaffold-chamber was manufactured from PEEK™ (polyarylether-ether-ketone) as well as the ports and the lid. PEEK™ can withstand heat sterilization and offers the advantage of being molded easily into different sizes and shapes, allowing the cultivation of different shapes of biomaterials (Figure 43). Figure 43B shows the medium outlet boring at the bottom of the scaffold perfusion chamber through which medium flows out after being pumped in through the medium inlet connected to the lid of the cultivation vessel.

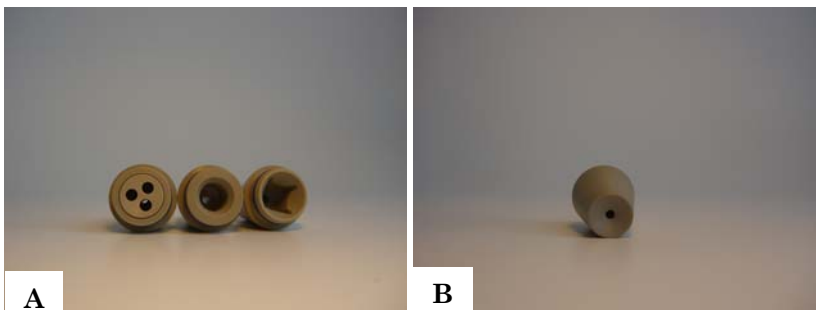

Figure 43 Photomicrographs showing the PEEK™ scaffold chamber. (A) custom built for three different biomaterial shapes and **(B)** the outlet boring at the bottom of the chamber through which medium flows out into the medium reservoir of the bioreactor.

Prior to a cultivation experiment, the bioreactor was assembled and heat sterilized at 115°C for 20 minutes. The freshly seeded cell scaffold construct was first cultured statically for 24 hours for complete cell adherence to occur in an aerated 50 ml tube with 30 ml osteogenic medium. Subsequently the bioreactor system was placed in a laminar flow hood to unscrew the perfusion chamber and carefully load it with the cell-scaffold construct. For all experiments, the following parameters were chosen: perfusion rate 0.2 ml/min,

medium input rate (7 µl/min**)** and partial oxygen pressure of 20% (Barthold, 2003).

3.2.6. Alkaline Phosphatase Determination in Cell-Scaffold Constructs

For alkaline phosphatase analysis, cell-scaffold constructs were harvested at predetermined time points, washed with 1x PBS and stored at -70ºC. The supernatant was sampled over the 35-day cultivation period as well and stored at -20ºC until assayed. For the analysis, the constructs were crushed using a disperser (Ultra Turrax® T 25) in 1 ml 0.1% (v/v) Triton X-100 solution (Meinel, 2004b) for cell lysis. The resulting lysate was then clarified by centrifugation (10 minutes at 800rpm) and the supernatant was assayed for ALP by using the biochemical assay from Sigma, based on the conversion of p-nitrophenyl phosphate to p-nitrophenol in the presence of alkaline phosphatase as described in chapter 2 (section 2.2.10.). Briefly, 50 µl of the supernatant were mixed with 50 µl of the reagent and incubated for 30 minutes at 37ºC. The production of
p-nitrophenol was measured at 405 nm. Alkaline phosphatase specific activity was expressed as milli-units per milligram of protein (mU/mg). Samples were measured in at least doublets.

3.2.7. Total Protein Determination in Cell-Scaffold Constructs

For the determination of total protein, the cell lysate (prepared as described in the above section) was assayed with the Micro BCA™ protein assay kit (section 2.2.4, chapter 2.). Briefly, 100 µl of the cell lysate supernatant was mixed with the protein assay reagent and incubated for 2 hours at 37ºC. Samples were measured in at least doublets.

3.2.8. WST-1 Assay for Cell-Scaffold Constructs

For the assessment of cell viability and proliferation of human osteogenic cells in conjunction with a PLGA/CaP scaffold, WST-1 was measured by adapting

the colorimetric assay described earlier in chapter 2 (section 2.2.3.) for the two dimensional culture. The cell-scaffold constructs were removed from the culture system at predetermined time points, cut in half with a surgical blade, and washed twice with 1x PBS. They were then placed in 15 ml tubes and immersed with 2 ml WST-1 working solution (1:10) and incubated at 37°C for 2 hours. A naked scaffold without cells was incubated as well for a negative control. 75 µl of the supernatant were pipetted into 96-well plates and the absorbance of the supernatant was measured at 450nm in at least doublets, subtracting the control value of the non-seeded scaffold.

3.2.9. Histological Analysis

For histological processing, the constructs were washed with 1x PBS and divided in the centre with a surgical blade into two halves where necessary. The constructs were fixed in 4% buffered paraformaldehyde solution (PFA, see Appendix II) overnight at 4ºC. If not processed immediately, they were immersed in 1x PBS and stored at 4ºC.

For paraffin embedding, the tissue samples were put into appropriate plastic cassettes and placed into an automatic paraffin infiltration instrument (Shandon Citadel™ TissueProcessor 1000) for the ease of handling several samples simultaneously and to ensure complete and thorough infiltration of the porous biomaterial. The program chosen included the following steps: the tissue samples were first washed in water for 2 hours, dehydrated in successive ethanol washes (70%, 80%, two changes of 96%), each wash for one hour. Then transferred to 100% ethanol (2 washes) before they were immersed in a xylene substitute (Histoclear™) for two washes, each lasting one hour. Then the fixed cell-scaffold constructs were finally immersed into liquidized paraffin at 56ºC for two subsequent immersions, each for two hours. The paraffin infiltrated cell-scaffold constructs were then taken out of the embedding machine to be molded into readily sliceable paraffin blocks using an embedding instrument (Histocentre 2, Tissue Embedding System, Shandon) by carefully casting warm liquid paraffin onto the tissue samples,

placed in stainless steel moulds. The resulting paraffin blocks were left to congeal on a cooling plate (CP-4, Kunze Instruments) and released from the moulds for sectioning. 4, 10 and 20 µm thick tissue sections were cut with a rotary microtome (Shandon 0325), horizontal to the front face of the disc. The transverse sections were stretched in a pre-warmed (45ºC) flotation bath (Histotherm water bath Hir-3, Kunz Instruments), filled with distilled water to remove wrinkles and distortions created during the sectioning.
The sections were mounted on poly-L-lysine coated slides to improve adhesion (see Appendix II). The sections were then left on a thermo hot plate (Shandon) at 50°C to avoid wrinkles. Finally, sections were left to dry in an oven at 60°C for 30-40 minutes The tissue section mounted slides were dried at room temperature, first by standing them up vertically and allowing them to drain to be then transferred to an oven for 30-40 minutes at 60ºC.

3.2.10. Scanning Electron Microscopy

For topographical morphological analysis and to analyze cell attachment and detect collagen fibril formation, cultivated cell-scaffold constructs were washed with 1x PBS and then fixed in a mixture of 2% glutaraldehyde and 5% formaldehyde in cacodylate buffer (see Appendix II) for one hour at 4ºC. Samples were washed with 1x PBS and stored in 1x PBS at 4ºC until further processing by the department of Microbiology, Helmholtz Centre for Infection Research (Braunschweig). The fixed samples were dehydrated through the following series of acetone concentrations: 10%, 30%, 50%, 70%, 90%, and 100%, each for 15 minutes at 4ºC with the final dehydration step in 100% acetone at room temperature (repeated 2-3 times). Samples were then critically dried and sputtered with gold to be then analyzed with the electron microscope DSM 982 Gemin (Zeiss, Jena).

3.2.11. Haematoxylin & Eosin, van Gieson and Toluidine Blue

Prior to staining, sections were de-paraffinized and re-hydrated to enable dye uptake. De-paraffinization was performed by dipping the sections in two

consecutive washes, each for 10 minutes in a xylene substitute (Histoclear™), followed by 100% ethanol, 90% ethanol, 80% ethanol, 70% ethanol, each step for 5 minutes. Sections were then rinsed in distilled water (1-5 minutes) for re-hydration and stained with either van Gieson, toluidine blue or with haematoxylin (see Appendix II for detailed staining procedure). Sections were viewed under a BX51 System Microscope (Olympus, Tokyo, Japan) and photomicrographs were taken with ColorView IIIu digital camera, U-CMAD3 (Soft Imaging System, Olympus, Muenster).

3.2.12. Immunohistochemical Staining and Confocal Laser Scanning Microscopy of Paraffin Sections

To perform immunohistochemical staining on paraffin sections, a heat induced epitope retrieval step was performed using an antigen retrieval solution (DakoCytomation, S1700) according to the instructions of the manufacturer. Briefly, sections were de-paraffinized (section 3.2.11.) and after the re-hydration step in distilled water, the sections were immersed into a glass trough filled with the pre-heated target retrieval solution (95-99ºC) and incubated for 40 minutes in a water-bath at 95-99ºC. The solution was allowed to cool and the sections were then rinsed in 0.02% Triton X for 10 minutes at room temperature for permeabilization. Confocal imaging was performed on the sections with an LSM META510 confocal scanning laser system (Zeiss, Jena) on an Axiovert 200M microscope (Zeiss, Jena). Images were viewed and edited using LSM 5 Image Browser (Zeiss, Jena).

3.2.12.1. Collagen Type I

Permeabilized sections were incubated with 2% blocking goat serum (in 1x PBS), which decreases subsequent non-specific binding. The primary monoclonal mouse IgG1 anti-human collagen I antibody was applied at 1:200 in 1x PBS for one hour and then washed with 0.02% Triton X three times for one minute, then 3 minutes and after that for 10 minutes. The antibody recognizes the native (helical) form of human collagen type I and shows no

cross reactivity with other collagen types (e.g. II or III). The secondary antibody goat-anti-mouse conjugated to Alexa 488 was applied for 30 minutes in a humid chamber to visualize the collagen-I fibrils green upon excitation. Sections were washed with 1x PBS three times (1 min, 3 min and 10 minutes). For actin staining, the sections were incubated with Alexa 546 labeled phalloidin at 1:400 in 1x PBS, visualizing the cytoskeletal actin component in red. Nuclei were counterstained with DRAQ5™ at 1:100 in PBS for 15 minutes, staining the DNA blue and then the section was washed again three times in 1x PBS. Slides were mounted in glycerol gelatin. As a negative control, a section was treated as above, without administration of the primary antibody and replacing it with 1x PBS.

3.2.12.2. Connexin 43

Triton X-100-permeabilised samples were blocked with 2% goat serum and then incubated with the primary monoclonal rabbit antibody against human connexin 43 at 1:2000 in 1x PBS followed by the secondary antibody Alexa 488-conjugated goat-anti-rabbit IgG, to later visualize connexin 43 positive sites in green after excitation. Sections were thereafter treated as mentioned in the section above.

3.3. Results and Discussion

3.3.1. Characterization of the Biomaterial: the PLGA/CaP Scaffold

The surface morphology of the scaffold alone was analyzed by scanning electron microscopy, which revealed micropores (< 100 µm) as small as 50 µm in size to macropores of up to 2000 µm large (Figure 44). A highly porous scaffold was chosen as the cells were meant to migrate into the whole material and cover the scaffold.

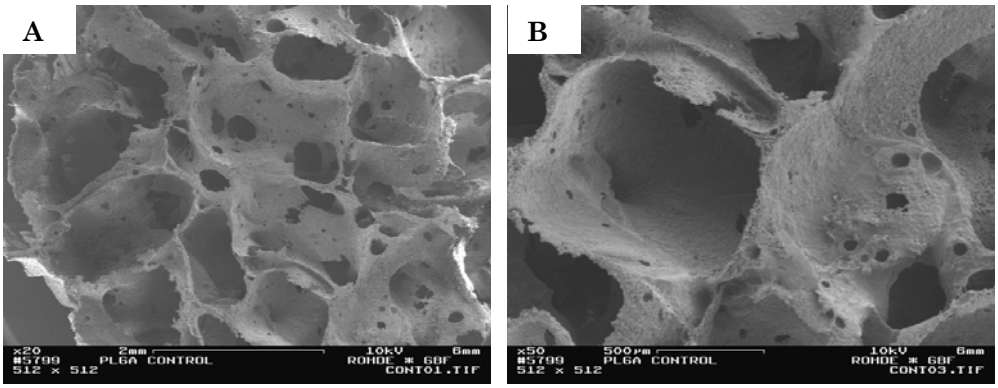

Figure 44 SEM micrographs of the naked surface (without cells) of the PLGA/CaP scaffold. (A) Micropores as well as macropores in an interconnected network mimicking trabecular bone in structure ranging in size from 50 to 2000 µm. Scale bar = 2mm. (B) Pores at a larger magnification. Scale bar= 500 µm.

3.3.2. Cell Growth and Differentiation on Surface Modified PLGA/CaP Scaffolds: Determination of the Optimal Surface Coating

Trabecular bone derived cells were cultured on PLGA/CaP scaffolds ($5x10^6$ cells/scaffold) coated with either collagen Type I, fibronectin, medium or human serum for 7 days in expansion medium (ZKT-1 basal medium+15% human serum). Best proliferation, as was indicated by the highest protein content and highest metabolic activity, was achieved with human serum coating (Figure 45A and B).

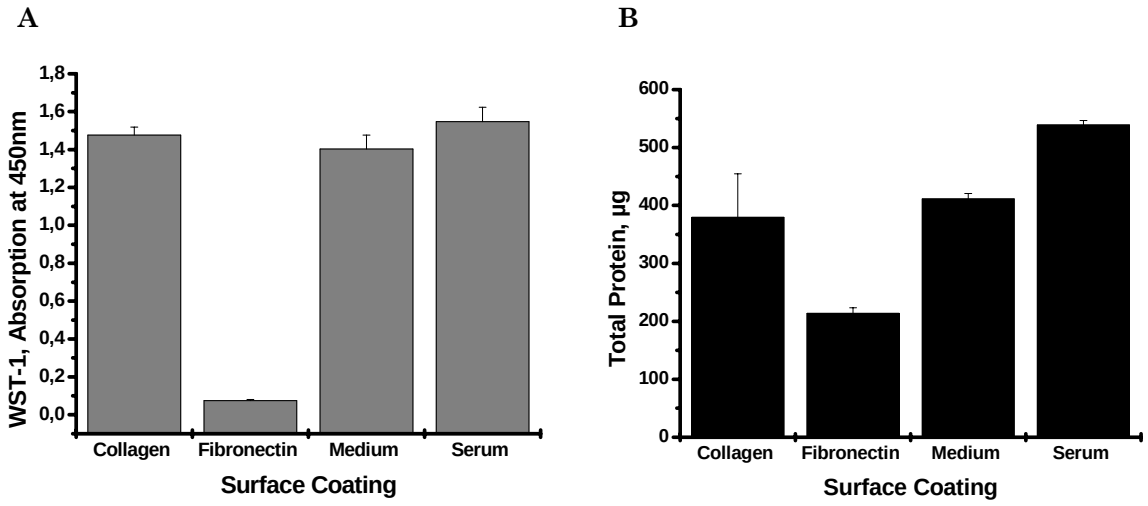

Figure 45 Total protein content and cell viability of human trabecular bone derived cells in conjunction with PLGA/CaP scaffolds coated with either collagen, fibronectin, medium or human serum. Cell-scaffold constructs were cultivated statically for 7 days in expansion medium (ZKT-1 basal medium supplemented with 15% human serum and 1% Pen/Strep). **(A**) Total protein content was highest for human serum coated scaffolds compared to the other surface coatings. The highest vitality was as well measured for PLGA/CaP scaffolds coated with human serum **(B)**. Error bars, means ± standard deviation for n=2 scaffolds, each measured in at least triplets.

The effect of the surface coating was further tested on differentiation of the osteogenic cells by measuring the levels of newly produced collagen type I after 6 and 10 days of culturing the cell-scaffold construct in osteogenic medium. The quantitative determination of CICP levels in the supernatant revealed higher collagen I production rate by cells cultured on a human serum treated surface (Figure 46).

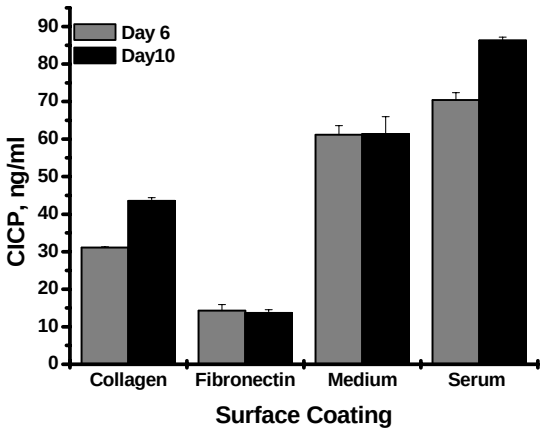

Figure 46 The effect of surface coating on differentiation of human trabecular bone derived cells measured by collagen Type I levels (CICP). The bars in grey represent CICP levels after 6 days of treatment in osteogenic medium and the black bars after 10 days. Osteoprogenitors cultured on human serum coated scaffolds yielded highest collagen I levels. Error bars, means ± standard deviation for n=2.

Note : PLGA/CaP scaffolds were also coated with fetal bovine serum, displaying very similar results to human serum coating, leading to improved attachment and proliferation of cells compared to the other surface coatings (data not shown).

3.3.3. The Tilted Rotating Bioreactor

In the tilted rotating bioreactor, the cell-scaffold construct was kept in continuous motion at 12 rpm. The tilted rotating movement generated fluctuations in the medium flow around the free falling cell-scaffold construct, exposing the cells to improved mass transfer and low levels of shear stress.

3.3.3.1. Three Dimensional Osteogenic Differentiation in the Tilted Rotating Bioreactor System: Alkaline Phosphatase Activity

Alkaline phosphatase activity of the cell-scaffold construct was determined throughout the 35 day cultivation period in osteogenic medium (Figure 47). Cells cultured in the tilted rotating bioreactor appeared to have lower initial alkaline phosphatase activity on day 7 and 14 compared to the static culture, followed by a steep increase peaking on day 27 (12.89 ± 0.25 mU/mg). The static culture reached a maximum value as well but at an earlier time point (5.29 ± 0.03 mU/mg) on day 14. Cells in both culture modes displayed higher ALP activity than the control cultures cultivated statically in expansion medium (ZKT-1 basal medium + 15 % human serum) without the addition of osteogenic factors. The control culture is represented as hatched bars in Figure 47.

The reciprocal relationship between the decline in proliferative activity and the subsequent matrix maturation and eventual mineralization, with an enhanced expression of alkaline phosphatase following the down regulation of collagen I production, was elaborated in Chapter 2 on two dimensional cultures. Translating this to the three dimensional cultivation, the later peak in ALP activity for cells cultivated dynamically in the tilted rotating system could be explained by still ongoing proliferation (matrix formation, i.e. ongoing

collagen I production) until some time point between day 14 and day 27, where matrix maturation took place.

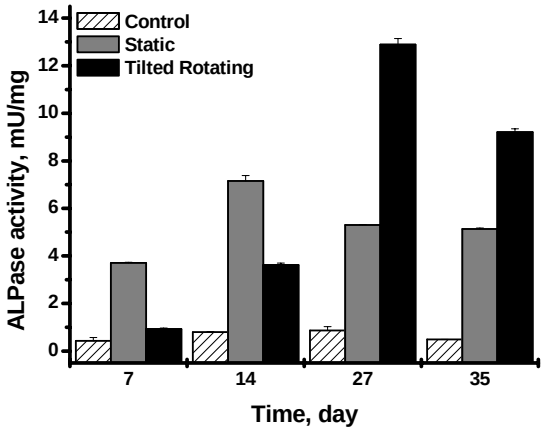

Figure 47 Alkaline phosphatase activity of human trabecular bone derived cells over 35 days of culture on PLGA/CaP scaffolds in osteogenic medium. The ALP activity of cells after 7, 14, 27 and 35 days cultured in the tilted rotating system under dynamic conditions (dark black bars) was significantly higher than cells cultured under static conditions (grey shaded bars) over time. The hatched bars represent human trabecular bone derived cells cultured on PLGA/CaP scaffolds in expansion medium without the addition of osteogenic factors. Error bars, means ± standard deviation for n=3.

3.3.3.2. Viability of the Cell-Scaffold Construct: WST-1 an Indicator for Proliferation and Metabolic Activity of the Cells

Absorption was determined on both day 7 and day 14. Human trabecular bone derived cells cultured dynamically in the tilted rotating system demonstrated higher WST-1 values corresponding to higher metabolic activity and thus viability than those cultivated under static conditions (Figure 48). Further, the WST-1 absorption for cells cultivated statically showed a lower value on day 14 (1.04 ± 0.04) compared to day 7 (1.23 ± 0.03), coinciding with a peak in specific alkaline phosphatase activity on day 14 (Figure 47), while the dynamically cultivated cells in the tilted rotating bioreactor system showed an increase from day 7 (1.34 0.06) to day 14 (1.62 ± 0.052). This being in accordance with the later peak in alkaline phosphatase activity noted above (on day 27 or at a time point between day 14 and day 27), indicating a later onset of differentiation probably due to still ongoing proliferation.

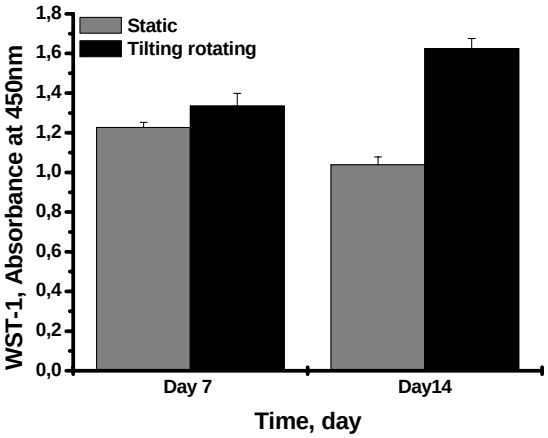

Figure 48 WST-1 of human trabecular bone derived cells cultured in conjunction with a PLGA/CaP scaffold after 7 and 14 days of culture in osteogenic medium as a function of culture conditions. The cell-scaffold construct cultivated in the tube rotor under dynamic conditions (dark black bars) demonstrated higher absorption values than those in the static system (grey shaded bars). Error bars, means ± standard deviation, n=2-3 scaffolds each measured in at least triplets.

3.3.3.3. Histological Analysis: Cell Growth Pattern and Distribution as a Function of the Cultivation System

To reveal the growth pattern and distribution of the human trabecular bone derived cells in and througout the PLGA/CaP scaffold, paraffin transverse sections at similar depths (approx. 200 µm deep) were stained with haematoxillin and eosin for a general histological overview. Section from constructs cultivated in the tilted rotating bioreactor system under dynamic conditions were compared to statically cultivated constructs after 35 days of cultivation in osteogenic medium. From the representative section in Figure 49, an even cell distribution towards the interior of the PLGA/CaP scaffold was achieved by culturing the cell-scaffold construct dynamically with cells migrating and proliferating as deep as 5 mm from the outer scaffold surface deep into the pores (Figure 49A). While the static cultivation led only to cell acculumation at the rim of the scaffold, leaving the interior empty (Figure 49B).

To further elaborate the intensive and uniform cell ingrowth of the human trabecular bone derived cells, cultured in the tilted rotating system, a cut out of a transverse section, representing the central part of the scaffold was investigated closer (Figure 50). An overview staining with haematoxylin and eosin shows completely filled pores throughout the cross section, revealing

migratory and proliferative abilities of the human trabecular bone derived cells throughout the whole PLGA/CaP scaffold.

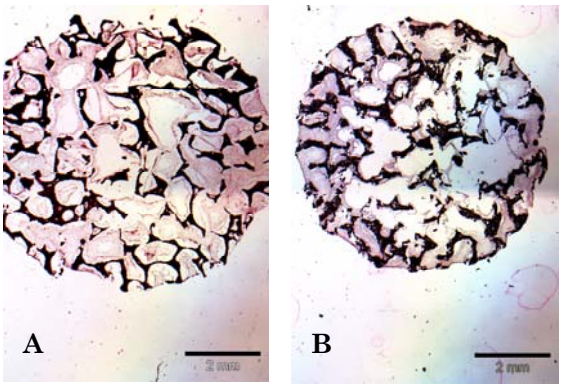

Figure 49 Micrographs of paraffin transverse cross sections for human trabecular bone derived cells cultured in conjunction with a PLGA/CaP scaffold for 35 days in the tilted rotating bioreactor versus static culture. Haematoxylin and eosin staining (10µm thick section) showing cell distribution (pink areas) in the PLGA/CaP scaffold (dark areas) after cultivation (A) in the tilting rotating bioreactor under dynamic conditions and (B) under static conditions. (Original magnification: x 12.5; scale bar 2 mm).

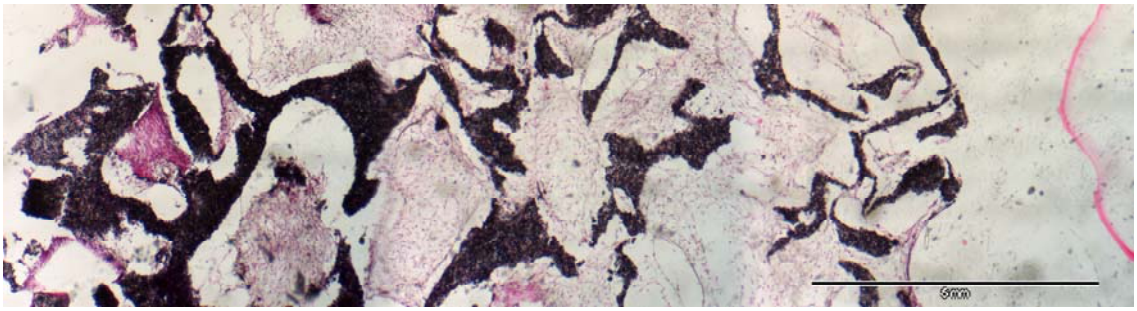

Figure 15 Micrograph showing a cut out of the central part of a transverse section for human trabecular bone derived cells cultured in conjunction with a PLGA/CaP scaffold for 35 days in the tilted rotating bioreactor. A close-up of a Haematoxylin and Eosin stained cross section showing ubiquitous cell and tissue distribution (pink areas) in the PLGA/CaP scaffold (dark grey flecks). (Original magnification: x 4; scale bar 5mm).

3.3.3.4. Connective Tissue Staining: Identifying *de novo* Formed Tissue with van Gieson; Tilted Rotating *vs.* Static Culture.

To further examine the trabecular bone derived cells cultured on the PLGA/CaP scaffold in the tilted rotating system and the newly laid down tissue, paraffin cross sections were stained with van Gieson. A connective

tissue stain known to react with collagen and osteoid, staining these violet or reddish (Bancroft and Gamble, 2001). Cells were observed to completely fill the pores, laying down a fibrous extracellular matrix in an organized manner, with cells embedded within this matrix, aligned to the flow direction (Figure 51A and B). In Figure 51C, the cells can be seen to connect to each other through filapodia (long cellular processes) forming a network through which the cells can communicate, adhering apparently very strongly to the PLGA/CaP surface, as cells are seen to almost invade the biomaterial (indicated by the arrow). Examining the cells closer at higher magnification (x40) in Figure 51D, the typical osteocytic cell shape (van der Plas and Nijweide, 2005) could be identified at several locations.

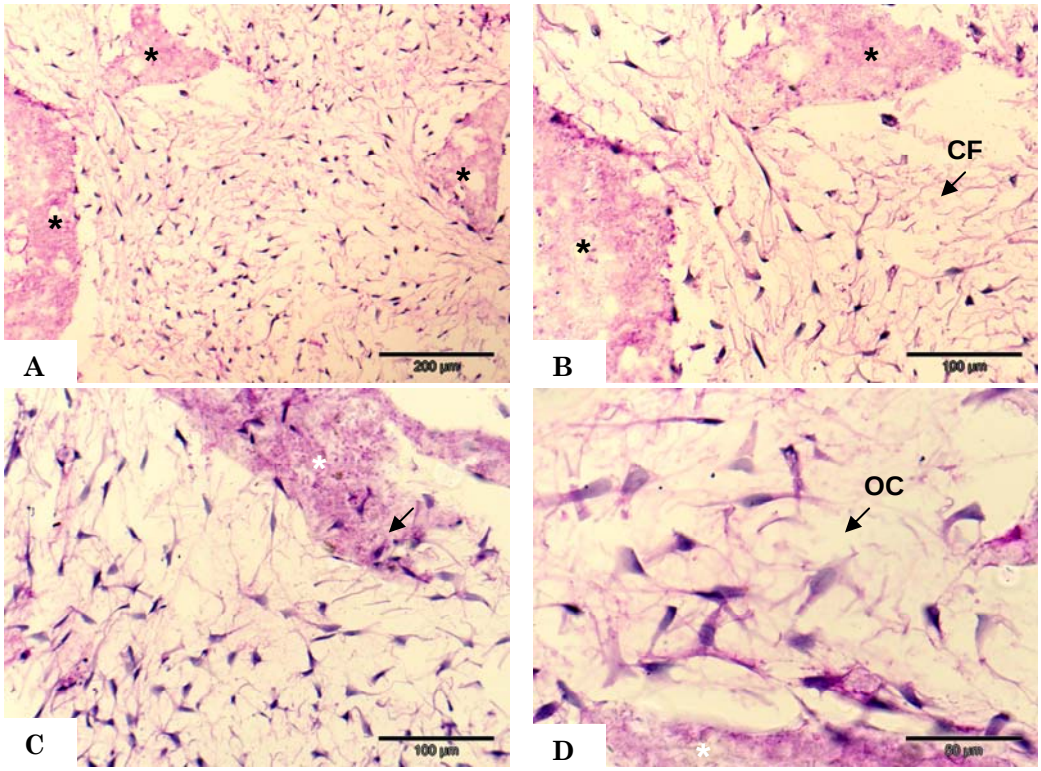

Figure 51 Van Gieson staining of human trabecular bone derived cells seeded on PLGA/CaP scaffolds after 35 day cultivation in the tilt-rotating bioreactor system. (A) A representative cross section shows completely filled pores with positive van Gieson staining the intercellular spaces, indicating *de novo* laid down tissue matrix. Cell nuclei stained dark violet and the PLGA/CaP biomaterial stained pink is indicated by the asterisk*. Original magnification: x100; scale bar 200µm. **(B)** Higher magnification of the rectangular area in A, cells organising themselves in the collagenous rich matrix, squeezing through a pore alongside the medium flow. Original magnification: x200, scale bar 100µm. **(C)** A network of cells, in contact with each other through short processes and attaching very strongly to the PLGA/CaP surface as indicated by the arrow. Original magnification: x200, scale bar 100 µm. **(D)** Osteocyte like cells with their branching filapodia could be identified at several locations. Original magnification: x400, scale bar 50 µm. OC= Osteocyte-like cell. CF= Collagen-like fibres.

Van Gieson staining of cells cultured under static conditions on the other hand, revealed a less organized appearance (Figure 52). Cells were only observed at the rim of the PLGA/CaP scaffold with several layers of cells concentrated on the edges of the scaffold, forming a tissue-like capsule around the biomaterial ~200µm thick (Figure 52A). The connective tissue staining confirmed, that cell ingrowth only took place at the peripheries filling the first row of pores faced by the cells, without able to invade deeper towards the interior.

Morphologically, the cells appeared to acquire a weak and brittle appearance the further away the cell was from the edge of the scaffold. The edges of the section in Figure 52A are shown at a higher magnification in Figure 52B and C. Pink stained intercellular space indicating newly laid down collagenous matrix was also observed to a lesser extent than in the tilted rotating system.

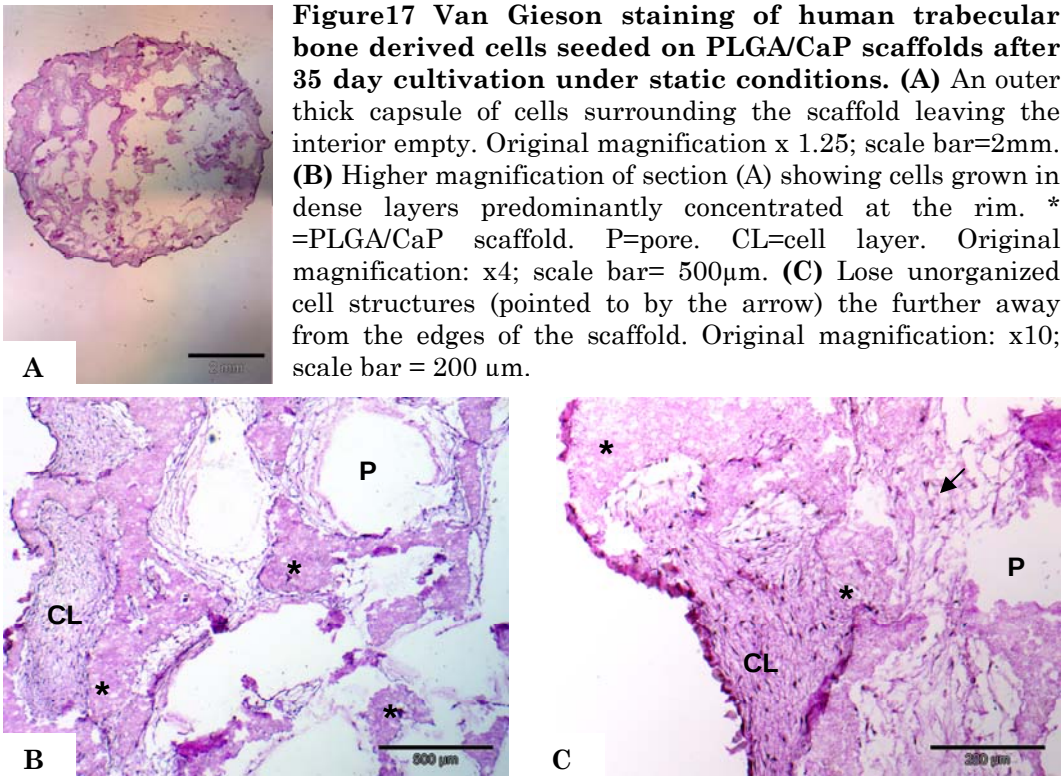

Figure17 Van Gieson staining of human trabecular bone derived cells seeded on PLGA/CaP scaffolds after 35 day cultivation under static conditions. (A) An outer thick capsule of cells surrounding the scaffold leaving the interior empty. Original magnification x 1.25; scale bar=2mm. **(B)** Higher magnification of section (A) showing cells grown in dense layers predominantly concentrated at the rim. * =PLGA/CaP scaffold. P=pore. CL=cell layer. Original magnification: x4; scale bar= 500µm. **(C)** Lose unorganized cell structures (pointed to by the arrow) the further away from the edges of the scaffold. Original magnification: x10; scale bar = 200 um.

In Figure 53, the results of the two three-dimensional cultivation models are summarized. Representative transverse cross sections of the upper, central and lower part of the cylindrical PLGA/CaP scaffold after 35 days cultivation in the tilted rotating bioreactor system are compared to static cultivation. In case of the tilted rotating system, cells reached almost 5000 µm below the

surface with ostecyte-like cells entrapped within the collagenous rich laid down extracellular matrix, while the cells in the case of the static system are mostly concentrated at the peripheries of the scaffolds near the edges, leaving the interior empty at all depths.

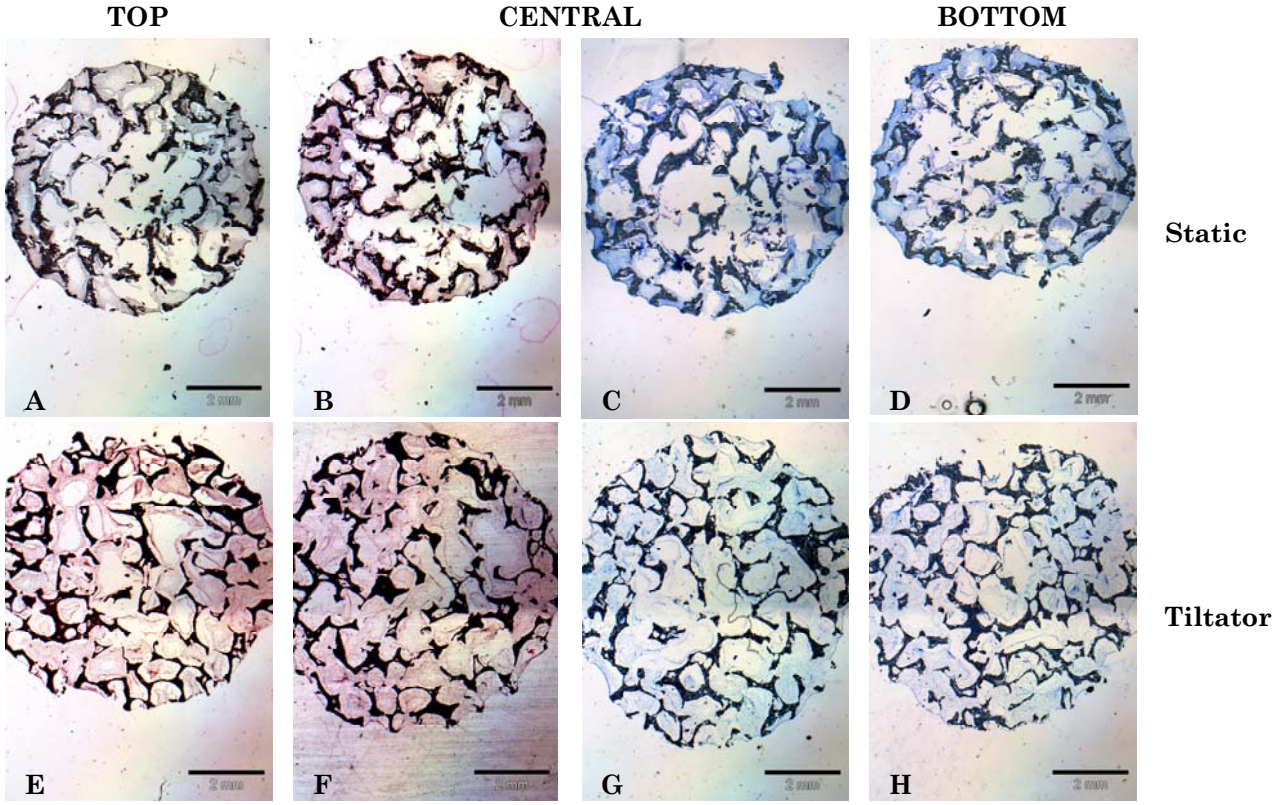

Figure 53 Representative transverse sections of paraffin embedded human trabecular bone derived cells cultured in conjunction with a PLGA/CaP scaffold for 35 days in osteogenic medium either under static or dynamic conditions (tilting rotating) at different depths within the scaffold. (A-D) Representing static culture. **(E-H)** Tilting rotating culture. A and E represent the upper part of the cylindrical PLGA/CaP scaffold. **(B,C)** and **(F,G)** the central part and **(D)** and **(H)** the bottom part of the scaffold. Very high cell densities were found near the edges in all cross sections cultivated under static conditions. While the dynamic cultivation model led to ubiquitous cell distribution throughout the scaffold. Original magnification: x 12.5. Scale bar= 2 mm. H&E staining: A,B,E,F. Toluidine blue staining: C,D,G,H.

3.3.3.5. Connexin 43 Immunohistochemistry; Gap Junctions in Dynamically Cultivated Cell-Scaffold Constructs

To confirm the osteogenic character of the *in vitro* connective tissue that was identified histologically to contain networks of cells communicating through long slender processes, paraffin embedded sections were stained with an antibody specific for human connexin 43.

Observations under the confocal microscope revealed differentiated osteocyte-like cells organized in a network demonstrating strong positive staining with anti- connexin 43 (Figure 54). Stained green dots indicate two adjacent cells communicating through gap junctional channels made up mainly of connexin 43. The cell nuclei were stained with DRAQ5™ (appearing blue) and the cytoskeleton stained red with Phalloidin 546.

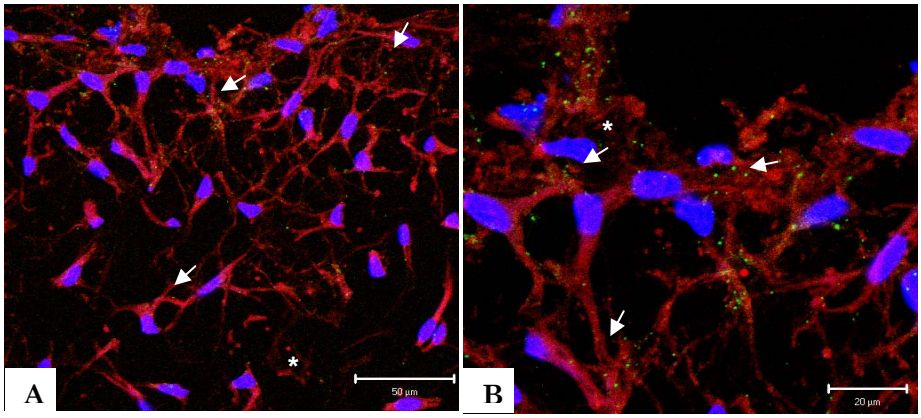

Figure 54 Connexin-43 immunohistochemical staining of human trabecular bone derived cells cultured in conjunction with a PLGA/CaP scaffold for 35 days in the tilting rotating bioreactor system. (A) At cell-cell contact, positive staining of the gap junctional protein Connexin-43 was identified and visualised as green fluorescent dots with Alexa 488 as a secondary antibody. Some points of contact are pointed to by the arrows. Nuclei stained blue with DRAQ5™ and cell bodies were stained red with Phalloidin 546. The red autofluorescence of the PLGA/CaP biomaterial can be seen at several spots indicated by the asterisk.**(B)** represents a cropped region of the upper left corner in **(A)**.(Original magnification : x400).

3.3.3.6. Scanning Electron Microscopy of the Cell-PLGA/CaP Constructs after Dynamic Cultivation in the Tilted Rotating Bioreactor (tiltator) *vs.* Static Cultivation

Scanning electron microscopy of the cell-scaffold constructs after 35 days cultivation in osteogenic medium (Figure 55) strengthened the observations of the paraffin histology described earlier. A thin layer of extracellular matrix

and of cells as well as collagen fibrils appeared under static conditions (Figure 55A). In contrast, in the tilted rotating system, a continuous thick fibrous matrix layer was detected with clusters of crystal-like structures bulging out and aligning the collagen fibrils (Figure 55B). The bulges were also detected in the statically cultivated scaffolds but occurring less frequently and smaller in size. Similar structures were observed in two dimensional cultivation of osteogenic cells where these accumulations stained positive with alizarin red, calcein and von Kossa, indicating mineralization, the final stage of the osteoblastic phenotype (chapter 2 section 2.3.6.4.).

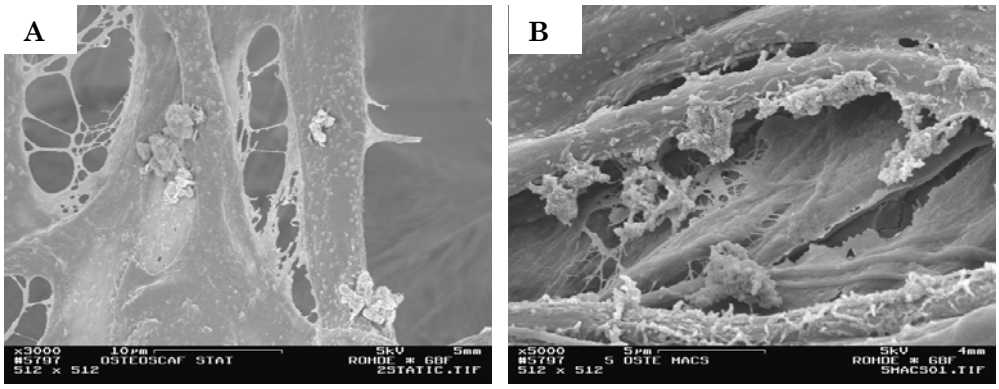

Figure 55 Scanning electron micrographs of human trabecular bone derived cells cultured in conjunction with a PLGA/CaP scaffold for 35 days in osteogenic medium. (A) In static culture, cells formed a thin layer of extracellular matrix with lose collagen fibrils while **(B)** in the dynamic tilting rotor cultivation, a thick fibrous organised layer of collagen fibrils was detected. Crystal-like accumulations were detected in both culture models, however, with them being smaller and less frequent in the static cultivation model.

3.3.3.7. Discussion of the Novel Tilted Rotating Bioreactor System

The choice of using the tilted rotating bioreactor system was inspired by the Wave Bioreactor® design (GE Healthcare Bioscience Bioprocess Corp., New Jersey, USA), which is simply made up of a sterile plastic bag on a rocking base developed by Vijay Singh in 1996. Waves are generated inside a bag by rocking it back and forth at a resonant frequency with the direction of flow being reversed, each rock leading to a turbulent wave motion providing uniform mixing, with oxygen being transferred from the headspace into the liquid phase. This motion appeared to be optimal for production of

recombinant proteins for instance, replacing steel bioreactors and enabling the use of a disposable system for cultivation of cell volumes up to 500 liters.

In translating this idea for use in tissue engineering, and in trying to simulate the wave-like turbulent motion to provide a scaffold with gentle uniform mixing, enabling cells to migrate deep into the pores, the simple set-up of the tube rotating system seemed to be ideal for investigating, whether a gentle tilting combined with rotation improved spatial and uniform cell distribution and extracellular matrix formation, especially as the use of rotating bioreactors has been shown to improve the formation of bone and cartilage-like tissue *in vitro*.

Not only was the spatial distribution of cells and their produced extracellular matrix improved by the combined tilting and rotating movement, but cells cultivated in this system also showed significantly higher alkaline phosphatase activities than cells in stationary culture, indicating improved osteogenesis. As exposing the cell-scaffold construct to the tilted rotating was the only variable introduced into the three dimensional cultivation mode, it was clearly demonstrated how the right mechanical stimulation improves *in vitro* bone formation.

Moreover, cells cultivated in the tilted rotating system were shown to actively communicate with each other through gap junctional proteins, the same gap junctions expressed by osteocytes and osteoblasts *in vivo* (connexin 43). These results are very promising, as the integration of a tissue engineered construct with an already "social" network of cells (or biosynthetically active cells), similar to the site of repair, is very probable to actually lead to defect regeneration.

Static cultivation on the other hand, only leads to formation of a thick layer of cells at the peripheries of the scaffold, leaving the interior empty the limiting factor being nutrient diffusion and this being in agreement with other studies (Goldstein et al., 2001).

3.3.4. The Fixed Bed Perfusion Bioreactor System

The suitability of the fixed bed perfusion bioreactor for cultivating human trabecular bone derived cells in conjunction with a PLGA/CaP scaffold is demonstrated in the following sections.

3.3.4.1. Early Osteogenic Differentiation Markers in the Perfusion Bioreactor: Soluble Alkaline Phosphatase and Collagen I Formation

Advantages of the fixed bed perfusion bioreactor include the possibility of online sampling throughout the cultivation period without terminating the culture. Samples were drawn through the sampling port and concentrations of the C-terminal propeptide of collagen Type I, CICP, as well as soluble alkaline phosphatase were determined. The classic rise and fall pattern in alkaline phosphatase was observed in the perfusion culture to occur, peaking at around day 14 and coinciding with the fall in collagen type I production rate as indicated by Figure 56. CICP production was initially measured to be very high and was observed to decrease with time, indicating the initial active phase of osteogenic cells laying down new extracellular matrix until the cells transit into the mineralization phase.

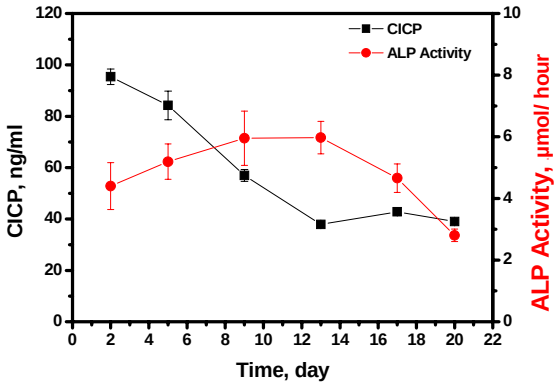

Figure 56 Early osteogenic differentiation markers in human trabecular bone derived cells cultivated in conjunction with a PLGA/CaP scaffold in the fixed bed perfusion bioreactor. Alkaline phosphatase activity reached a maximum after 13 days (red line) coincident with the decline in C-terminal propeptide of collagen type I, (black line) indicating the transition into the mineralisation phase. Error bars, means ± standard deviation. n=3.

3.3.4.2. Cell Proliferation of the Cell-Scaffold Construct Cultured in the Perfusion Bioreactor; WST-1 and Protein Content.

The viability of the cell scaffold-construct was assessed with the WST-1 test throughout the cultivation period (Figure 57). The increase in absorption values from day 5 to day 10 potentially indicates cells actively producing extracellular matrix proteins, typical of the first phase in osteogenic differentiation, the matrix formation phase. The absorption levels reached a maximum and leveled out thereafter. This coinciding with the peak in alkaline phosphatase activity, indicating transition of the cells into the differentiation phase with high viability maintained.

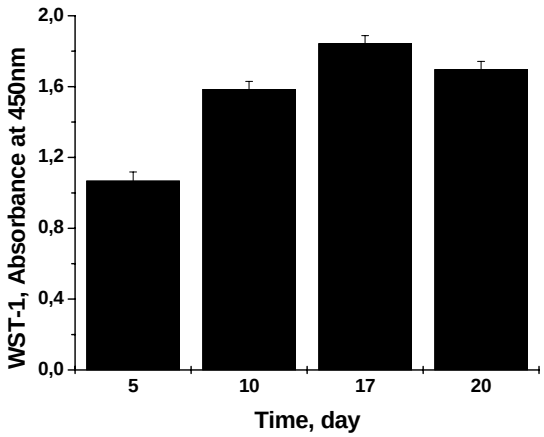

Figure 57 Viability of human trabecular bone derived cells in conjunction with a PLGA/CaP construct throughout 20 days of culture in osteogenic medium in the fixed bed perfusion bioreactor. Viability of the cells on the scaffold was determined with the WST-1 test with an increase in absorption from day 5 until day 10, indicating ongoing proliferation and reaching a plateau thereafter. Error bars, means ± standard deviation. n= 2 scaffolds with each measured in at least triplets.

Total protein determination of the cell-scaffold constructs cultivated in the fixed bed perfusion bioreactor augmented this further (Figure 58). The clear increase in protein content in the initial cultivation phase (form day 7 to day 14) indicates actively proliferating cells laying down extracellular matrix and reaching constant levels thereafter.

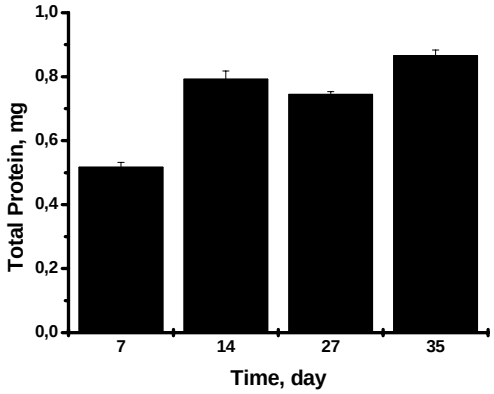

Figure 58 Total protein content in the cell-scaffold construct cultivated in the fixed bed perfusion bioreactor over 35 days cultivation in osteogenic medium. Total protein (mg) was observed to increase in the initial cultivation phase up until day 14, reaching a plateau thereafter. Error bars, means ± standard deviation. n=2 scaffolds with each measured in at least triplets.

3.3.4.3. Cell and Tissue Distribution Pattern throughout the PLGA/CaP Scaffold in the Fixed Bed Perfusion Bioreactor

Paraffin transverse cross sections at a depth ranging between 100 to 5000 µm were analysed to investigate cell and tissue distribution within the PLGA/CaP scaffold after 35 days cultivation in the fixed bed perfusion bioreactor. A representative section at approximately 1000 µm below the surface of the biomaterial was stained with Toluidine Blue and is shown in Figure 59. Surprisingly, only scattered patches of cells and their matrix distributed non uniformly at the periphery and in the centre of the scaffold could be detected.

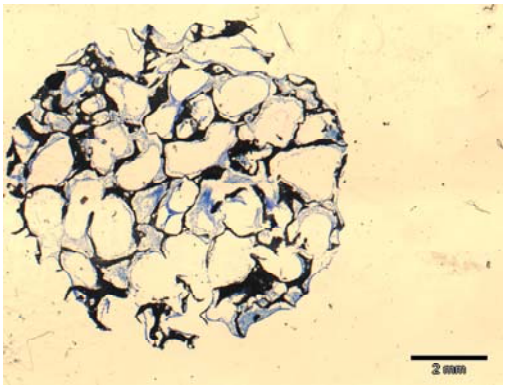

Figure 59 Representative transverse section of human trabecular bone derived cells cultured in conjunction with a PLGA/CaP scaffold in the fixed bed perfusion bioreactor for 35 days in osteogenic medium. Toluidine blue stained patches of cell and matrix were detected scattered throughout the PLGA/CaP porous network. Original magnification: 12.5; scale bar=2mm.

Although, cultivation in the perfusion bioreactor only led to the formation of patches of tissue scattered throughout the scaffold, cells did manage to migrate as deep as 5 mm towards the center, away from the surface, indicating that

continuous perfusion must have provided the cells with opimal nutrient and oxygen supply, keeping these cells vital for as long as 35 days.

Stationary culture ,on the other hand, only led to cell distribution at the rim of the biomaterial, leaving the central core empty due to limted nutrient diffusion (Figure 60). Despite the thick and dense cell layer that was detected surrounding the biomaterial, cells did not leave the periphery and those that were detected below the surface only managed to migrate 200-400 µm with a rather necrotic appearance.

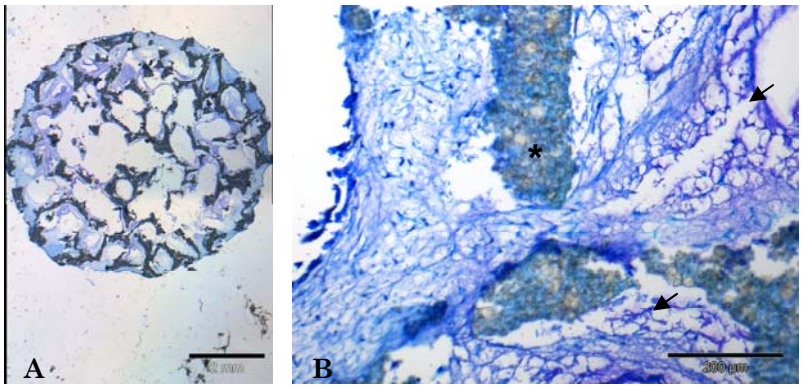

Figure 60 Micrographs showing an overview of a toluidine blue stained transverse section for human trabecular bone derived cells cultivated statically in conjunction with a PLGA/CaP scaffold for 35 days. (A) A transverse section showing extensive cell growth around the scaffold and metachromatic areas once these cells try to migrate deeper into the scaffold. Original magnification: x12.5; scale bar =2mm. **(B)** Higher magnification from the edge of the section in **(A)**, showing a thick layer of cells around the scaffold intensely blue stained and metachromatic purplish areas indicating changes in the cells and potentially in their viability once trying to surpass the first pore wall of the biomaterial. Original magnification: x100. Scale bar= 200µm. Asterisk *=PLGA/CaP scaffold, dark grey flecks.

A closer microscopical examination of the patches formed in the perfusion bioreactor, especially in comparison to cell-scaffold constructs cultivated under static conditions, revealed a remarkably organized and vital osteoblastic phenotype as opposed to the thin, necrotic appearance of cells cultured statically (Figure 61). The positive effect of the perfusion strain was clearly seen on cellular organization and morphology.

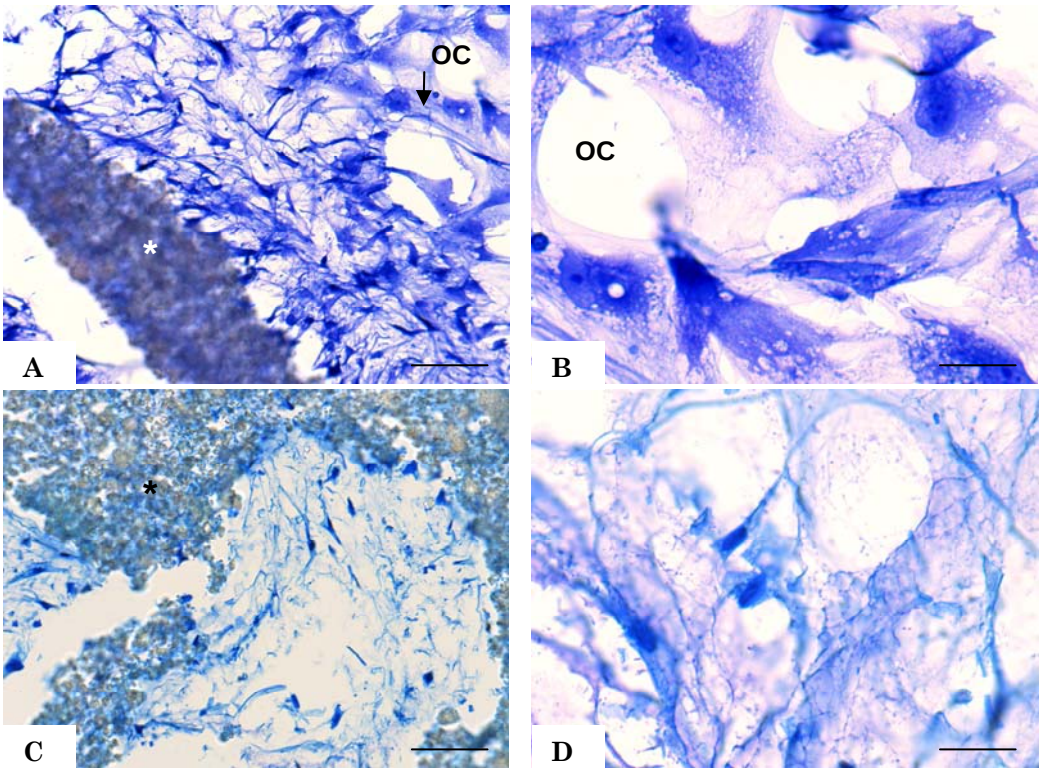

Figure 61 Toluidine blue staining of human trabecular bone derived cells cultured in conjunction with a PLGA/CaP scaffold in the fixed bed perfusion bioreactor versus static cultivation. (A) Transverse section at ~2000µm depth revealing osteocyte-like cells communicating with each other and strongly adhering to the PLGA/CaP surface (*) at adhesion points. Original magnification: x200; scale bar=100µm. **(B)** Larger magnification of an area in (A) showing the typical osteocyte-like stellate shape of one cell communicating through its processes with neighbouring cells. Original magnification: x600; scale bar=20µm. **(C)** Statically cultivated cells at ~2000µm below the scaffold surface. Random cells with a rather necrotic cell morphology. Original magnification: x200; scale bar=100µm. **(D)** A magnified close up of an area of the section (C) showing a flattened cell shape. Original magnification: x600; scale bar=20µm.

3.3.4.4. Connective Tissue Formation in the Fixed Bed Perfusion Bioreactor; van Gieson Staining

The bone-like matrix deposited by the osteogenic cells after 35 days cultivation in the perfusion bioreactor was characterized with van Gieson staining. Sections at depths between 1000-2000 µm from the top surface of the scaffold, revealed that cells were organized in a dense extracellular matrix made up of bundles of collagen fibrils filling the pores (Figure 62A). Furthermore, in the organized cell layers, at least two different cell types could be identified: osteoblast-like cells with a cuboidal morphology were observed at several locations organizing themselves in the matrix as well as more stellate-like shaped (Thi et al., 2003) cells with numerous long processes resembling

osteocytes (Figure 62D). These osteocyte-like cells were observed lining the scaffold surface and attaching strongly through focal contacts, offering strong adsorption points of the cellular plasma membrane to the biomaterial surface pointed to in Figure 62C. The focal adhesion contacts, can also be seen among the cells within the extracellular matrix in Figure 62D at a higher magnification.

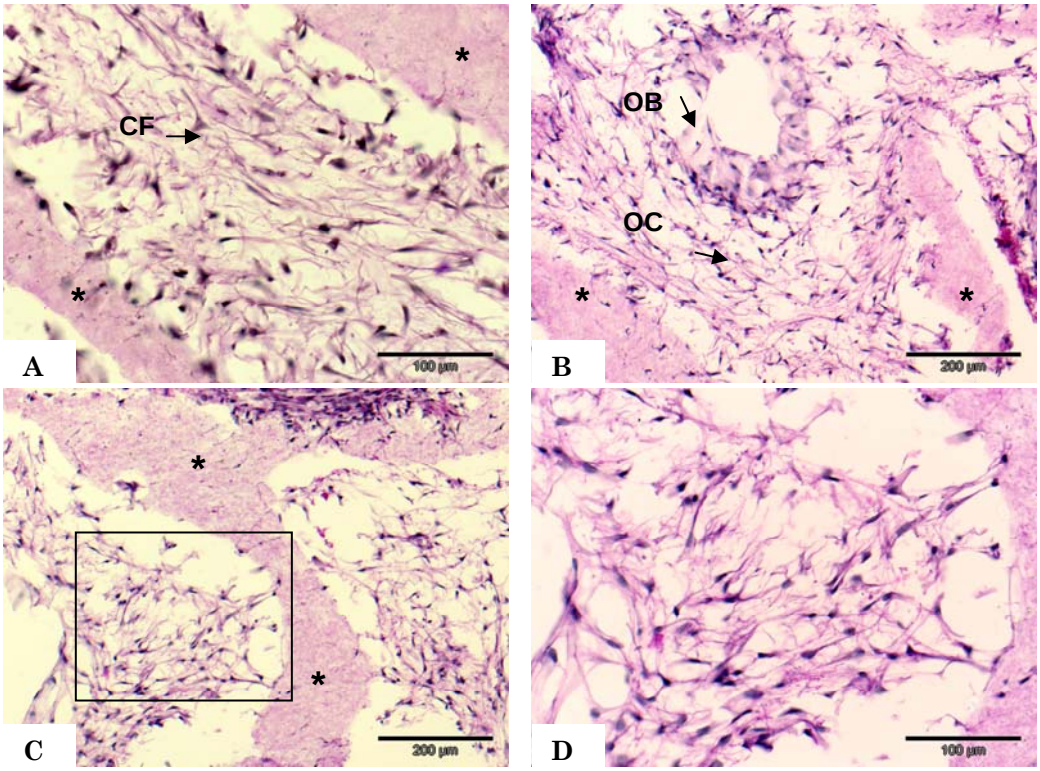

Figure 62 Van Gieson staining of human trabecular bone derived cells cultured in conjunction with a PLGA/CaP scaffold in the process of bone tissue formation in the fixed bed perfusion bioreactor. (A) Cells filling a pore laying down extracellular matrix in ordered collagen bundles following the flow direction. CF=Collagen fibrils. Original magnification: x200; scale bar=100 µm. **(B)** Osteocyte-like (OC) cells as well osteoblast-like cells (OB) could be identified organizing themselves within the dense extracellular matrix. Original magnification: x100; scale bar= 200 µm. **(C)** Osteocyte-like cells strongly adhere to the surface of the PLGA/CaP biomaterial through local adhesion points. Original magnification: x100; scale bar= 200 µm.**(D)** Enlargement of the boxed area in (C) showing numerous osteocyte-like cells communicating with each other through their long extended slender processes. Original magnification: x200; scale bar=100 µm. The PLGA/CaP scaffold is designated by an asterisk*.

The cell-biomaterial interaction demonstrated above by the organized cell layers and strong adhesion points through cultivation in the perfusion bioreactor is in line with what was reported by Pavalko et al. (1998), who have studied the effect of fluid shear stress on focal adhesion points. They have shown that fluid shear induced changes in actin organization (increased stress

fibers and focal adhesion development) and that cells respond to fluid flow by increasing their formation, so that the perfusion produced in the fixed bed bioreactor actually leads to cytoskeletal reorganization.

3.3.4.5. Immunohistochemical Staining of Collagen I and Connexin 43: *de novo* Bone-like Tissue Formation in the Fixed Bed Perfusion Bioreactor

The mature osteoblastic phenotype of the cells cultured in conjunction with the PLGA/CaP scaffold was confirmed by detecting the bone specific markers: type I collagen and connexin 43 in paraffin embedded cell-scaffold constructs cultivated for 35 days in osteogenic medium in the perfusion bioreactor.
Collagen fibrils of type I were detected within the matrix with an anti-human collagen antibody (Figure 63).

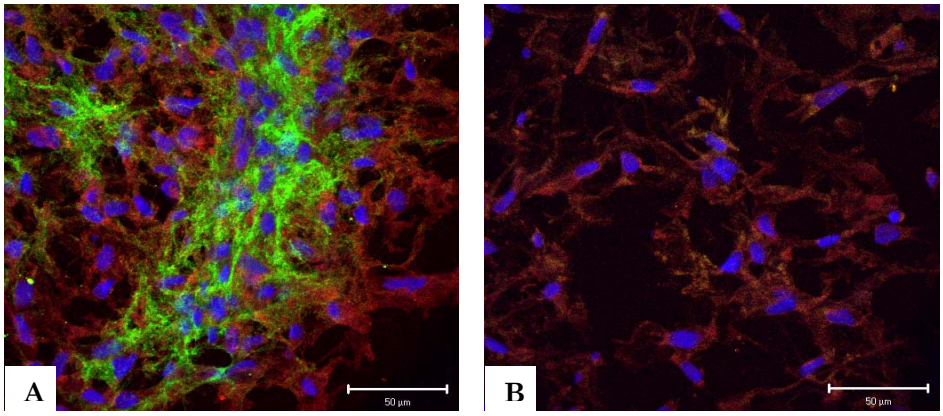

Figure 63 Type I collagen immunohistochemistry in paraffin sections of human trabecular bone derived cells cultivated in conjunction with a PLGA/CaP scaffold in the fixed bed perfusion bioreactor for 35 days in osteogenic medium. (A) The matrix laid down by the cells stained positive with anti Collagen type I visualised in green fluorescence by the secondary antibody conjugated to Alexa 488, cell nuclei stained blue with DRAQ5™ and the cytoskeleton is stained red with Phalloidin Alexa 546. **(B)** Negative control by omitting the primary antibody on a parallel paraffin section. Original magnification: x400; scale bar=50µm.

Further, gap junction-mediated cell-cell communication between the bone forming cells within the PLGA/CaP scaffold was detected through connexin 43 immunohistochemistry. Representative transverse sections from the cell-PLGA/CaP construct were immunostained with antihuman connexin 43 and

visualized with a secondary antibody conjugated to Alexa 488 as green dots, concentrated at the tips of the cell processes at points of contact with neighboring cells throughout the matrix (Figure 64).

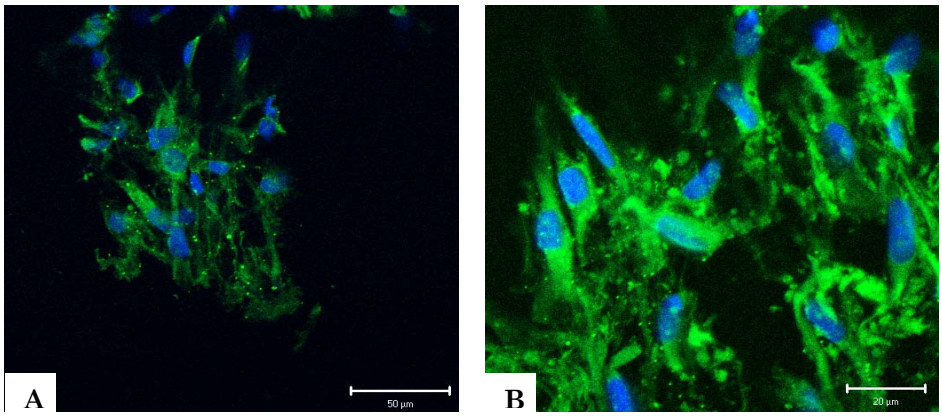

Figure 64 Connexin-43 immunohistochemistry showing gap junctional communication between bone forming cells within the PLGA/CaP scaffold cultivated in the fixed bed perfusion bioreactor for 35 days in osteogenic medium. (A) Connexin-43 is visualised by Alexa 488 conjugated to the secondary antibody against anti-connexin-43 as green dots at cell-cell contact. Cell nuclei are stained blue with DRAQ5™. Original magnification: x 400; scale bar=50µm. **(B)** Cropped region of A (a) showing a close up of the intracellular communication. Scale bar=50µm.

Thi et al. (2003) have shown that fluid shear stress modifies the expression and distribution of connexin 43 as well as its *de novo* formation, depending on the magnitude of the shear stress experienced by osteocytic and osteoblastic cells. The group has reported on the change in the cell processes, which became smaller in diameter and increased in numbers by changing the applied shear stress. The morphological changes that were observed in the cell-network formed in the perfusion bioreactor (Figure 64) compared to that formed in the tube rotor (Figure 54) might be explained by this hypothesis that different shear forces led to different rearrangement of bone cells within the matrix, leading to a different pattern of communication between cells in the perfusion bioreactor.

3.3.4.6. Scanning Electron Microscopy of Cell-Scaffold Constructs in Fixed Bed Perfusion Bioreactor Cultivation

Corroborating with what was observed in the light and confocal microscopical analysis, scanning electron microscopy revealed that cells attached strongly to the surface of the PLGA/CaP scaffold, however, only at selected sites (Figure 65A). These cells formed organized collagen fibrils (Figure 65B) and along these fibrils, accumulations of crystal-like structures could be detected (Figure 65C and D), aligning themselves parallel to the collagen axis- these acting as a nucleation site for the formation and growth of mineralized structures as described by Boskey (2005).

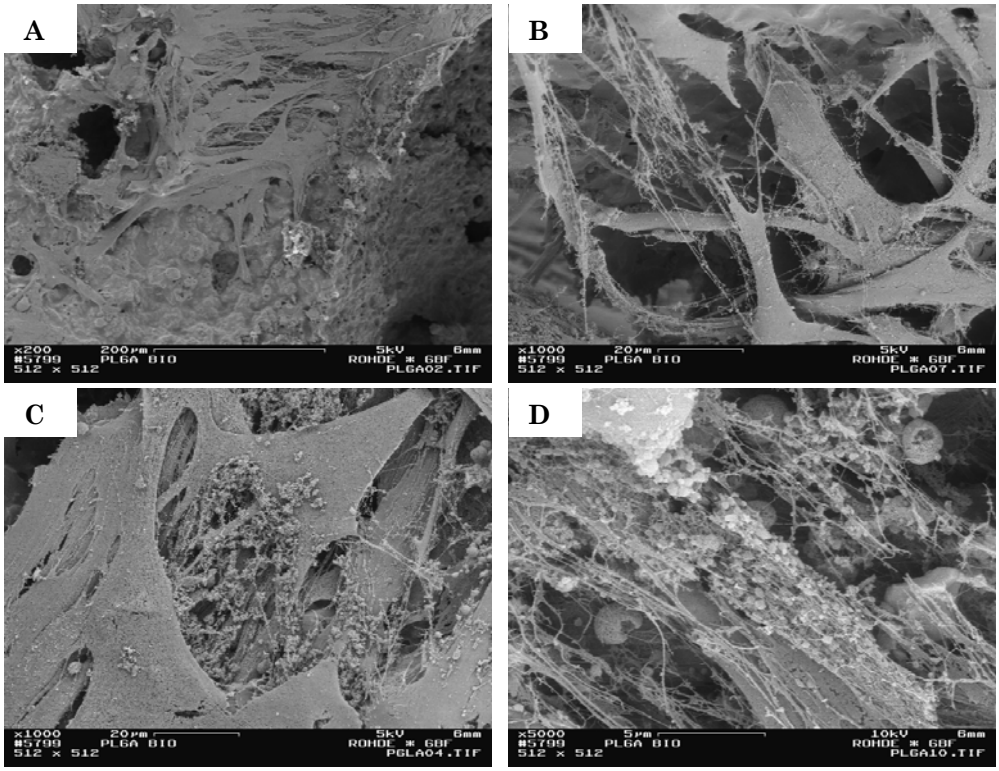

Figure 65 Scanning electron micrographs of human trabecular bone derived cells cultured in conjunction with a PLGA/CaP scaffold in the fixed bed perfusion bioreactor for 20 days in osteogenic medium. (A) A cell layer strongly attaching to the PLGA/CaP scaffold covering parts of the pore surface, while patches of 'naked' biomaterial could also be detected. **(B)** Cross-banded collagen fibrils forming the extracellular matrix. **(C)** Crystal-like structures alongside the collagen fibrils indicating mineralization. **(D)** Collagen fibrils decorated with the mineral-like structures at a higher magnification.

3.3.4.7. Discussion of the Fixed Bed Perfusion Bioreactor Cultivation

The results revealed by the detailed histological analysis, showing that cells cultivated in the perfusion bioreactor only formed patches of tissue scattered throughout the porous structure of the PLGA/CaP scaffold, came against all expectations. Especially when compared to the simple tilted rotating model, which led to completely uniform cellular distribution.

Several studies have shown that perfusion induces osteogenesis and improves cellular distribution in a three dimensional environment (Wendt et al., 2003; Wendt et al., 2006), however, histological analysis of sections as deep as 5000 µm was never demonstrated in detail in these studies. Further, Barthold in his doctoral thesis (2003) developed and evaluated the fixed bed perfusion bioreactor system using rat derived cells. Rat cells are known to proliferate and differentiate faster with more intense mineralization *in vitro* than human derived cells (Rickard et al., 1994), producing a stronger extracellular matrix which might withstand the continuous perfusion in the bioreactor.

Despite the fact that not the whole scaffold was uniformly filled with tissue, those parts that were filled with patches, contained organized cell layers spatially distributed in a newly laid down matrix and strongly attaching to the surface of the scaffold via focal adhesion points. The cells did demonstrate *de novo* bone formation shown by positive collagen type I staining and connexin 43 staining, revealing actively communicating osteocyte-like cells within the extracellular matrix. Moreover, the mechanical stimulation by the flow perfusion was demonstrated to affect cellular morphology, leading to cytoskeletal reorganization when compared to static cultivation, which showed a rather flattened cell morphology. Actual osteogenesis was also augmented by the biochemical analysis undertaken, revealing the typical osteogenic differentiation pattern. Moreover, the organized structure of collagen fibrils revealed by scanning electron microscopy confirmed the potential for *de novo* bone formation with the collagenous matrix acting as a nucleation site for the formation and growth of mineral crystals. Finally, cells were shown to migrate towards the interior central part of the scaffold, as far as 5 mm away from the

surface. There was no cell concentration in a certain area due to diffusion nutrient limitation as in static culture, where cells only stay at the peripheries. Therefore, the goal of delivering nourishing medium and dissolved oxygen reaching the core of a three dimensional scaffold was achieved in the fixed bed perfusion bioreactor. Although, no spatial and uniform cell and tissue distribution was achieved throughout the whole PLGA/CaP scaffold, those cellular patches that filled parts of the porous network did reach terminal osteogenic differentiation.

The scattered patch formation in the bioreactor indicated that through the types of mechanical stimulation produced in continuous perfusion through a fixed bed holding the scaffold, medium flow was successfully directed to reach the central part of the scaffold. However, the shear stress produced by the flow was not enough to spatially distribute the cells uniformly throughout the porous network of the PLGA/CaP scaffold, taking into consideration that the dimensions of 10x10 mm are relatively high compared to what has been mostly studied (Vunjak-Novakovic, 2003; Meinel et al., 2004a; Marolt et al., 2006). So that probably a supportive motion for optimizing seeding efficiency prior to the fixed bed perfusion process might be needed to distribute the cells throughout the whole porous structure of the scaffold or exchanging the initial static seeding of cells with a dynamic one.

Alternatively, another explanation for the patch formation might be due to the fact that not enough cells were there to start with. The experimental design of this bioreactor perfusion culture included seeding the cells on the scaffold for 24 hours statically and then placing the cell-scaffold construct in the fixed matrix holder, starting pump-generated perfusion directly at a rate of 0.2 ml/min in a continuous mode. The initial shear stress produced by the perfusion could have been too high, affecting cell attachment negatively, in that some cells might have been flushed away once placed in the bioreactor and only those cells that attached heartedly to the surface of the material actually could withstand the continuous perfusion thereafter. Osteogenic differentiation is known to be accelerated by mechanical stimulation especially perfusion (Bancroft et al., 2002; Goldstein et al., 2001). They showed that at a 0.3 ml/min perfusion rate, osteoblastic differentiation was increased by

increased levels of alkaline phosphatase activity as well as increased expression of osteopontin. Having initiated differentiation in the PLGA/CaP at an earlier time point in the bioreactor perfusion model, is evident from the ALP/CICP graph (Figure 56), where the rise and fall in alkaline phosphatase activity happened at a relatively early time point.

It can be postulated that perfusion leads to redistribution of cells within a porous network, inducing cells to produce an extracellular matrix around them, rather than promoting cell doubling. From the WST-1 values and the protein content, cells did undergo an initial cell proliferation or matrix formation phase before transiting into differentiation but only in those areas to which cells have migrated.

Overall, this study has shown that perfusion does induce osteogenesis and with directed medium flow, nutrients can be delivered towards the central interior of the scaffold. The postulations to why only patches of tissue have formed and the scaffold was not uniformly filled will have to be examined further by either increasing initial cell seeding density or to start at a lower perfusion rate progressing gradually to 0.2 ml/min at a later stage, or by introducing intermittent perfusion. All these factors are worth considering in future studies and would need further elaboration.

3.4. Conclusion

In summary, both dynamic systems improved cell distribution and osteogenesis, when compared to stationary culture, overcoming a major limitation in current bone tissue engineering protocols involving the homogenous delivery and diffusion of nutrients in large porous scaffolds. However, uniform and spatial cell and tissue distribution was observed to occur consistently throughout the PLGA/CaP scaffold, when cultivated in the tilted rotating system. The tilting and rotating motion generated and the free fall of the scaffold was shown to be superior compared to holding the scaffold fixed in place with directed medium perfusion.

This type of motion generated in the simple tube rotator could serve as a prototype bioreactor version for bone tissue engineering. Supplying the system with features like automated medium supply and exchange, monitoring and control of O_2, CO_2 as well as the pH can lead to the development of a closed system for the automated and controlled production of bone tissue *in vitro*.

The clinical relevance of the *in vitro* generated bone-tissue was qualitatively high, considering the fact that the constructs were histologically shown to be quite similar to *in vivo* bone. The cells embedded within the *de novo* generated extracellular matrix were shown to communicate trough connexin 43 gap junctions which are known to be the major gap junctional protein that mediates cell-cell communication within osteoblasts and osteocytes *in vivo* (Donahue et al., 1995; You et al., 2000). Furthermore, this approaches functional restoration of bone *in vivo* to an extent that, to our knowledge, has not been shown before. Sikavitsas et al. (2001) have elaborated the role of communication in osteocytes, via gap junctions in that the transfer of signals through the gap junctions of the osteocytic network might lead to osteoblast recruitment and in turn result in bone growth. This is exactly the role that an *in vitro* engineered bone construct is to play if implanted in the body to help the body regenerate a defect that otherwise would have been too large for spontaneous intrinsic healing.

Moreover, the tissue-engineered constructs may be used for further *in vitro* studies of osteogenesis, drug efficacy, bone metabolism as well as an alternative to animal models to study orthopedic diseases.

Concluding, this study has successfully demonstrated the reconstruction of a three dimensional bone-like construct with a very high chance of being integrated *in vivo*, representing a highly promising tool for bone regeneration therapy options.

Ultimately, to elucidate the positive effects of suitable dynamic culture conditions on osteogenesis, bone forming capability will have to be confirmed by *in vivo* implantation of the cell-scaffold construct, primarily in an adequate animal model.

4. Outlook

This study has demonstrated the conversion of osteoprogenitor cells derived from human adult tissue to a viable bone-like tissue construct generated *in vitro*. The tissue engineered construct showed high resemblance to native bone tissue in terms of osteocyte-like cell shape and gap junctional communication. Despite of the promising results obtained, the true clinical potential of using the right cells in the right medium with the right scaffold in the right cultivation model (microenvironment) can only be highlighted by complimenting this study with *in vivo* bone regeneration studies. Bone forming capability is to be confirmed by *in vivo* implantation of the cell-scaffold construct hoping that the *in vitro* generated bone-like construct will give early support at site of repair or defect of the host bone tissue facilitating intrinsic regeneration. This inevitability will have to be applied in preclinical relevant animal models.

However, before a tissue engineered construct is ready for clinical transplantation, there are still scientific and technical obstacles that need to be overcome including the following (Nerem 2006):

- The optimal cell source: whether the cells are to be autologous or allogenic, whether differentiated or still in the progenitor stage (stem cells).
- Off the shelf availability of the cells in case implantation is to be carried out on short notice not leaving enough time for cell expansion.
- The suitable microenvironment for the generation of a tissue constructs in vitro (regulatory approved bioreactor).
- Storage and delivery of the constructs (fresh or cryopreserved) as well as maintaining sterility contamination control.
- At what point should the *in vitro* generated scaffold be implanted and moved from the laboratory bioreactor to the body; the *in vivo* bioreactor.
- Regulating the immune response of the body after implantation.

- GMP conformity and regulatory approval of the methods and appliancations essential for the generation of clinically relevant tissue engineered constructs.

Moreover, for optimal *in vivo* remodelling to occur two main issues that still need attention are: vascularisation and innervation of the tissue engineered construct requiring co-culture of vascular cells along with osteoprogenitor cells and eventually the incorporation of neuronal cell (Nerem 2006).

5. References

1. Anderson, H.C., 1969. Vesicles associated with calcification in the matrix of epiphyseal cartilage. J Cell Biol 41, 59-72.
2. Anderson, H.C., 1995. Molecular biology of matrix vesicles. Clin Orthop Relat Res, 266-280.
3. Anderson, H.C., 2003. Matrix vesicles and calcification. Curr Rheumatol Rep 5, 222-226.
4. Arsenault, A.L., Frankland, B.W., Ottensmeyer, F.P., 1991. Vectorial sequence of mineralization in the turkey leg tendon determined by electron microscopic imaging. Calcif Tissue Int 48, 46-55.
5. Aubin, J.E., 2001. Regulation of osteoblast formation and function. Rev Endocr Metab Disord 2, 81-94.
6. Bancroft, G.N., Sikavitsas, V.I., Mikos, A.G., 2003. Design of a flow perfusion bioreactor system for bone tissue-engineering applications. Tissue Eng 9, 549-554.
7. Bancroft, G.N., Sikavitsas, V.I., van den Dolder, J., Sheffield, T.L., Ambrose, C.G., Jansen, J.A., Mikos, A.G., 2002. Fluid flow increases mineralized matrix deposition in 3D perfusion culture of marrow stromal osteoblasts in a dose-dependent manner. Proc Natl Acad Sci U S A 99, 12600-12605.
8. Bancroft, J.D. and Gamble, M., 2001. Theory and Practice of Histological Techniques. Fifth Edition, Churchill Livingstone, 96.
9. Barthold M., 2003. Züchtung primärer osteogener Zellen auf neuartigen Gerüststrukturen in Kleinfermentern zur Herstellung von Knochenimplantaten in vitro. Dissertation Technische Universitaet Braunschweig.
10. Beresford, J.N., 1989. Osteogenic stem cells and the stromal system of bone and marrow. Clin Orthop Relat Res, 270-280.
11. Beresford, J.N., Gallagher, J.A., Poser, J.W., Russell, R.G., 1984. Production of osteocalcin by human bone cells in vitro. Effects of 1,25(OH)2D3, 24,25(OH)2D3, parathyroid hormone, and glucocorticoids. Metab Bone Dis Relat Res 5, 229-234.
12. Berger, T.G., Feuerstein, B., Strasser, E., Hirsch, U., Schreiner, D., Schuler, G., Schuler-Thurner, B., 2002. Large-scale generation of mature monocyte-derived dendritic cells for clinical application in cell factories. J Immunol Methods 268, 131-140.
13. Bianco, P., Robey, P.G., 2001. Stem cells in tissue engineering. Nature 414, 118-121.
14. Blanck, T.J., Peterkofsky, B., 1975. The stimulation of collagen secretion by ascorbate as a result of increased proline hydroxylation in chick embryo fibroblasts. Arch Biochem Biophys 171, 259-267.
15. Boskey, AL, 2005. The organic and inorganic matrices. In: Hollinger, J.O., Einhorn, T.A., Doll, B.A., Sfeir C. (Eds.). Fundamentals of Bone Tissue Engineering, C.R.C. Press, Boca Raton, 91-123.
16. Bradley, R., 1999. BSE transmission studies with particular reference to blood. Dev Biol Stand 99, 35-40.
17. Brown, K.L., Cruess, R.L., 1982. Bone and cartilage transplantation in orthopaedic surgery. A review. J Bone Joint Surg Am 64, 270-279.
18. Bruder, S.P., Caplan, A.I., 1990. Osteogenic cell lineage analysis is facilitated by organ cultures of embryonic chick periosteum. Dev Biol 141, 319-329.
19. Bruder, S.P., Fox, B.S., 1999. Tissue engineering of bone. Cell based strategies. Clin Orthop Relat Res, S68-83.
20. Bruder, S.P., Jaiswal, N., Haynesworth, S.E., 1997. Growth kinetics, self-renewal, and the osteogenic potential of purified human mesenchymal stem cells during extensive subcultivation and following cryopreservation. J Cell Biochem 64, 278-294.
21. Buckwalter, J.A., Glimcher, M.J., Cooper, R.R., Recker, R., 1996a. Bone biology. I: Structure, blood supply, cells, matrix, and mineralization. Instr Course Lect 45, 371-386.

22. Buckwalter, J.A., Glimcher, M.J., Cooper, R.R., Recker, R., 1996b. Bone biology. II: Formation, form, modeling, remodeling, and regulation of cell function. Instr Course Lect 45, 387-399.
23. Buttery, L.D., Bourne, S., Xynos, J.D., Wood, H., Hughes, F.J., Hughes, S.P., Episkopou, V., Polak, J.M., 2001. Differentiation of osteoblasts and in vitro bone formation from murine embryonic stem cells. Tissue Eng 7, 89-99.
24. Cancedda, R., Castagnola, P., Cancedda, F.D., Dozin, B., Quarto, R., 2000. Developmental control of chondrogenesis and osteogenesis. Int J Dev Biol 44, 707-714.
25. Caplan, A.I., 1991. Mesenchymal stem cells. J Orthop Res 9, 641-650.
26. Caplan, A.I., 2003. Embryonic development and the principles of tissue engineering. Novartis Found Symp 249, 17-25; discussion 25-33, 170-174, 239-141.
27. Caplan, A.I., 2005. Review: mesenchymal stem cells: cell-based reconstructive therapy in orthopedics. Tissue Eng 11, 1198-1211.
28. Cheng, B., Zhao, S., Luo, J., Sprague, E., Bonewald, L.F., Jiang, J.X., 2001. Expression of functional gap junctions and regulation by fluid flow in osteocyte-like MLO-Y4 cells. J Bone Miner Res 16, 249-259.
29. Cheng, S.L., Yang, J.W., Rifas, L., Zhang, S.F., Avioli, L.V., 1994. Differentiation of human bone marrow osteogenic stromal cells in vitro: induction of the osteoblast phenotype by dexamethasone. Endocrinology 134, 277-286.
30. Chung, C.H., Golub, E.E., Forbes, E., Tokuoka, T., Shapiro, I.M., 1992. Mechanism of action of beta-glycerophosphate on bone cell mineralization. Calcif Tissue Int 51, 305-311.
31. Civitelli, R., Beyer, E.C., Warlow, P.M., Robertson, A.J., Geist, S.T., Steinberg, T.H., 1993. Connexin43 mediates direct intercellular communication in human osteoblastic cell networks. J Clin Invest 91, 1888-1896.
32. Cooper, M.S., Hewison, M., Stewart, P.M., 1999. Glucocorticoid activity, inactivity and the osteoblast. J Endocrinol 163, 159-164.
33. Cooper, R.R., Milgram, J.W., Robinson, R.A., 1966. Morphology of the osteon. An electron microscopic study. J Bone Joint Surg Am 48, 1239-1271.
34. De Bari C, D.A.F., Tylzanowski P, Luyten FP., 2001. Multipotent mesenchymal stem cells from adult human synovial membrane. Arthritis Rheum. 44, 1928-1942.
35. Diaz-Flores, L., Gutierrez, R., Lopez-Alonso, A., Gonzalez, R., Varela, H., 1992. Pericytes as a supplementary source of osteoblasts in periosteal osteogenesis. Clin Orthop Relat Res, 280-286.
36. Doll Bruce, 2005. Developmental Biology of the Skeletal System; in Bone Tissue Engineering: J. O. Hollinger, T. A. Einhorn, B. Doll and C. Sfeir Eds., Boca Raton, Fla. CRC Press, 3-26.
37. Donahue, H.J., McLeod, K.J., Rubin, C.T., Andersen, J., Grine, E.A., Hertzberg, E.L., Brink, P.R., 1995. Cell-to-cell communication in osteoblastic networks: cell line-dependent hormonal regulation of gap junction function. J Bone Miner Res 10, 881-889.
38. Donahue Henry J., Siedlecki Christoph A., Vogler Erwin, 2005. Cell Biology of the Skeletal System, in Bone Tissue Engineering: J. O. Hollinger, T. A. Einhorn, B. Doll and C. Sfeir Eds., Boca Raton, Fla. CRC Press, 44-54.
39. Doty, S.B., 1981. Morphological evidence of gap junctions between bone cells. Calcif Tissue Int 33, 509-512.
40. Dragoo, J.L., Choi, J.Y., Lieberman, J.R., Huang, J., Zuk, P.A., Zhang, J., Hedrick, M.H., Benhaim, P., 2003. Bone induction by BMP-2 transduced stem cells derived from human fat. J Orthop Res 21, 622-629.
41. Dreinhoefer, 2000. Dt Ärztebl 2000; 97: [Heft 51–52]. A 3478–3481.
42. Duray, P.H., Hatfill, S.J., Pellis, N.R., 1997. Tissue culture in microgravity. Sci Med (Phila) 4, 46-55.
43. Erices, A., Conget, P., Minguell, J.J., 2000. Mesenchymal progenitor cells in human umbilical cord blood. Br J Haematol 109, 235-242.
44. Fargali S., 2006. *In vitro* Etablierung eines Kaninchenmodells zur Herstellung von hochvitalen Knochenimplantaten auf Basis osteogener Zellen und bioresorbierbarer Trägergerüste. Dissertation Technische Universitaet Braunschweig.

45. Ferretti, M., Palumbo, C., Bertoni, L., Cavani, F., Marotti, G., 2006. Does static precede dynamic osteogenesis in endochondral ossification as occurs in intramembranous ossification? Anat Rec A Discov Mol Cell Evol Biol 288, 1158-1162.
46. Fibbe, W.E., 2002. Mesenchymal stem cells. A potential source for skeletal repair. Ann Rheum Dis 61 Suppl 2, ii29-31.
47. Friedenstein, A.J., Gorskaja, J.F., Kulagina, N.N., 1976. Fibroblast precursors in normal and irradiated mouse hematopoietic organs. Exp Hematol 4, 267-274.
48. Gay V. Carol, 2005. The Osteoclast; in Bone Tissue Engineering: J. O. Hollinger, T. A. Einhorn, B. Doll and C. Sfeir Eds., Boca Raton, Fla. CRC Press, 55-87.
49. Genge, B.R., Sauer, G.R., Wu, L.N., McLean, F.M., Wuthier, R.E., 1988. Correlation between loss of alkaline phosphatase activity and accumulation of calcium during matrix vesicle-mediated mineralization. J Biol Chem 263, 18513-18519.
50. Gerhart, T.N., Kirker-Head, C.A., Kriz, M.J., Holtrop, M.E., Hennig, G.E., Hipp, J., Schelling, S.H., Wang, E., 1993. Healing segmental femoral defects in sheep using recombinant human bone morphogenetic protein. Clin Orthop Relat Res, 317-326.
51. Goldstein, A.S., Juarez, T.M., Helmke, C.D., Gustin, M.C., Mikos, A.G., 2001. Effect of convection on osteoblastic cell growth and function in biodegradable polymer foam scaffolds. Biomaterials 22, 1279-1288.
52. Goulet, J.A., Senunas, L.E., DeSilva, G.L., Greenfield, M.L., 1997. Autogenous iliac crest bone graft. Complications and functional assessment. Clin Orthop Relat Res, 76-81.
53. Granet, C., Laroche, N., Vico, L., Alexandre, C., Lafage-Proust, M.H., 1998. Rotating-wall vessels, promising bioreactors for osteoblastic cell culture: comparison with other 3D conditions. Med Biol Eng Comput 36, 513-519.
54. Gratzl, M. (Herausgeber), 2002. Junqueira, Carneiro, Kelley: Lehrbuch Histologie, Springer, 5.Auflage.
55. Greenspan, P., Mayer, E.P., Fowler, S.D., 1985. Nile red: a selective fluorescent stain for intracellular lipid droplets. J Cell Biol 100, 965-973.
56. Gregory, C.A., Gunn, W.G., Peister, A., Prockop, D.J., 2004. An Alizarin red-based assay of mineralization by adherent cells in culture: comparison with cetylpyridinium chloride extraction. Anal Biochem 329, 77-84.
57. Gregory, C.A., Prockop, D.J., Spees, J.L., 2005. Non-hematopoietic bone marrow stem cells: molecular control of expansion and differentiation. Exp Cell Res 306, 330-335.
58. Gronthos, S., Stewart, K., Graves, S.E., Hay, S., Simmons, P.J., 1997. Integrin expression and function on human osteoblast-like cells. J Bone Miner Res 12, 1189-1197.
59. Guan, L., Davies, J.E., 2004. Preparation and characterization of a highly macroporous biodegradable composite tissue engineering scaffold. J Biomed Mater Res A 71, 480-487.
60. Hale, L.V., Ma, Y.F., Santerre, R.F., 2000. Semi-quantitative fluorescence analysis of calcein binding as a measurement of in vitro mineralization. Calcif Tissue Int 67, 80-84.
61. Hall, G.E., Kenny, A.D., 1985. Role of carbonic anhydrase in bone resorption induced by 1,25 dihydroxyvitamin D3 in vitro. Calcif Tissue Int 37, 134-142.
62. Hankemeier, S., Keus, M., Zeichen, J., Jagodzinski, M., Barkhausen, T., Bosch, U., Krettek, C., Van Griensven, M., 2005. Modulation of proliferation and differentiation of human bone marrow stromal cells by fibroblast growth factor 2: potential implications for tissue engineering of tendons and ligaments. Tissue Eng 11, 41-49.
63. Heinegard, D., Oldberg, A., 1989. Structure and biology of cartilage and bone matrix noncollagenous macromolecules. Faseb J 3, 2042-2051.
64. Hollister Scott J., Taboas Juan M., Schek Rachel M., Lin Chen-Yu, Chun Tien Min, 2005. Design and Fabrication of Bone Tissue Engineering Scaffolds; in Bone Tissue Engineering: J. O. Hollinger, T. A. Einhorn, B. Doll and C. Sfeir Eds., Boca Raton, Fla. CRC Press, 167-192.
65. Holtorf, H.L., Jansen, J.A., Mikos, A.G., 2005. Flow perfusion culture induces the osteoblastic differentiation of marrow stroma cell-scaffold constructs in the absence of dexamethasone. J Biomed Mater Res A 72, 326-334.

66. Hutmacher, D.W., 2000. Scaffolds in tissue engineering bone and cartilage. Biomaterials 21, 2529-2543.
67. Hutmacher, D.W., Goh, J.C., Teoh, S.H., 2001. An introduction to biodegradable materials for tissue engineering applications. Ann Acad Med Singapore 30, 183-191.
68. Hutmacher, D.W., Sittinger, M., 2003. Periosteal cells in bone tissue engineering. Tissue Eng 9 Suppl 1, S45-64.
69. In 't Anker, P.S., Scherjon, S.A., Kleijburg-van der Keur, C., de Groot-Swings, G.M., Claas, F.H., Fibbe, W.E., Kanhai, H.H., 2004. Isolation of mesenchymal stem cells of fetal or maternal origin from human placenta. Stem Cells 22, 1338-1345.
70. Jaeger, V., Barthold, M., 2004. United States patent application publication. Pub. No.: US 2004/0253716 A1.
71. Jaeger, V., Lehmann, J., Friedl, P., 1988. Serum-free growth medium for the cultivation of a wide spectrum of mammalian cells in stirred bioreactors. Cytotechnology. 1, 319-329.
72. Jaiswal, N., Haynesworth, S.E., Caplan, A.I., Bruder, S.P., 1997. Osteogenic differentiation of purified, culture-expanded human mesenchymal stem cells in vitro. J Cell Biochem 64, 295-312.
73. Jeffrey, J.J., Martin, G.R., 1966. The role of ascorbic acid in the biosynthesis of collagen. I. Ascorbic acid requirement by embryonic chick tibia in tissue culture. Biochim Biophys Acta 121, 269-280.
74. Jones, L.J., Gray, M., Yue, S.T., Haugland, R.P., Singer, V.L., 2001. Sensitive determination of cell number using the CyQUANT cell proliferation assay. J Immunol Methods 254, 85-98.
75. Kakar Sanjeev, Einhorn Thomas A., 2005. Tissue Engineering of Bone; in Bone Tissue Engineering: J. O. Hollinger, T. A. Einhorn, B. Doll and C. Sfeir Eds., Boca Raton, Fla. CRC Press, 277-302.
76. Karageorgiou, V., Kaplan, D., 2005. Porosity of 3D biomaterial scaffolds and osteogenesis. Biomaterials 26, 5474-5491.
77. Kasper C., Suck K., Anton F., Scheper T., Kall S., van Griensven M., 2007. A newly developed rotating bed bioreactor for bone tissue engineering. In: Topics in Tissue Engineering, Vol. 3. Ashammakhi N., Reis R. L., Chiellini (eds.).
78. Kassem, M., Stenderup K., Justesen J., Kveiborg M., 2003. In vitro senescence of human osteoblasts. In S.C.Kul and R.Wadhwa (eds.) Aging of cells in and outside the body, Kluwer Academic Publisher, UK.67-84.
79. Kato, Y., Windle, J.J., Koop, B.A., Mundy, G.R., Bonewald, L.F., 1997. Establishment of an osteocyte-like cell line, MLO-Y4. J Bone Miner Res 12, 2014-2023.
80. Kim, H.J., Kim, U.J., Leisk, G.G., Bayan, C., Georgakoudi, I., Kaplan, D.L., 2007. Bone Regeneration on Macroporous Aqueous-Derived Silk 3-D Scaffolds. Macromol Biosci 7, 643-655.
81. Kuehnel, Wolfgang, 2002. Taschenatlas der Zytologie, Histologie und mikroskopischen Anatomie 11., Thieme, Stuttgart , 146-157.
82. Kveiborg, M., Flyvbjerg, A., Rattan, S.I., Kassem, M., 2000. Changes in the insulin-like growth factor-system may contribute to in vitro age-related impaired osteoblast functions. Exp Gerontol 35, 1061-1074.
83. Langer, R., Vacanti, J.P., 1993. Tissue engineering. Science 260, 920-926.
84. Lecanda, F., Towler, D.A., Ziambaras, K., Cheng, S.L., Koval, M., Steinberg, T.H., Civitelli, R., 1998. Gap junctional communication modulates gene expression in osteoblastic cells. Mol Biol Cell 9, 2249-2258.
85. Lian, J.B., Stein, G.S., Stein, J.L., van Wijnen, A.J., 1998. Transcriptional control of osteoblast differentiation. Biochem Soc Trans 26, 14-21.
86. Lidgren, L., 2000. The Bone and Joint Decade 2000-2010: an update. Acta Orthop Scand 71, 3-6.
87. Lidgren, L., 2003. The bone and joint decade 2000-2010. Bull World Health Organ 81, 629.
88. Makowski, L., Caspar, D.L., Phillips, W.C., Goodenough, D.A., 1977. Gap junction structures. II. Analysis of the x-ray diffraction data. J Cell Biol 74, 629-645.
89. Malda, J., van den Brink, P., Meeuwse, P., Grojec, M., Martens, D.E., Tramper, J., Riesle, J., van Blitterswijk, C.A., 2004. Effect of oxygen tension on adult articular chondrocytes in microcarrier bioreactor culture. Tissue Eng 10, 987-994.

90. Marolt, D., Augst, A., Freed, L.E., Vepari, C., Fajardo, R., Patel, N., Gray, M., Farley, M., Kaplan, D., Vunjak-Novakovic, G., 2006. Bone and cartilage tissue constructs grown using human bone marrow stromal cells, silk scaffolds and rotating bioreactors. Biomaterials 27, 6138-6149.
91. Maroudas, N.G., 1977. Sulphonated polystyrene as an optimal substratum for the adhesion and spreading of mesenchymal cells in monovalent and divalent saline solutions. J Cell Physiol 90, 511-519.
92. Marra Kacey G., 2005. Biodegradable Polymers and Microspheres in Tissue Engineering; in Bone Tissue Engineering: J. O. Hollinger, T. A. Einhorn, B. Doll and C. Sfeir Eds., Boca Raton, Fla. CRC Press, 149-165.
93. Martin, I., Muraglia, A., Campanile, G., Cancedda, R., Quarto, R., 1997. Fibroblast growth factor-2 supports ex vivo expansion and maintenance of osteogenic precursors from human bone marrow. Endocrinology 138, 4456-4462.
94. Martin, I., Wendt, D., Heberer, M., 2004. The role of bioreactors in tissue engineering. Trends Biotechnol 22, 80-86.
95. Martinez, M.E., del Campo, M.T., Medina, S., Sanchez, M., Sanchez-Cabezudo, M.J., Esbrit, P., Martinez, P., Moreno, I., Rodrigo, A., Garces, M.V., Munuera, L., 1999a. Influence of skeletal site of origin and donor age on osteoblastic cell growth and differentiation. Calcif Tissue Int 64, 280-286.
96. Martinez, M.E., Medina, S., Sanchez, M., Del Campo, M.T., Esbrit, P., Rodrigo, A., Martinez, P., Sanchez-Cabezudo, M.J., Moreno, I., Garces, M.V., Munuera, L., 1999b. Influence of skeletal site of origin and donor age on 1,25(OH)2D3-induced response of various osteoblastic markers in human osteoblastic cells. Bone 24, 203-209.
97. Mason, D.J., Hillam, R.A., Skerry, T.M., 1996. Constitutive in vivo mRNA expression by osteocytes of beta-actin, osteocalcin, connexin-43, IGF-I, c-fos and c-jun, but not TNF-alpha nor tartrate-resistant acid phosphatase. J Bone Miner Res 11, 350-357.
98. Meinel, L., Karageorgiou, V., Fajardo, R., Snyder, B., Shinde-Patil, V., Zichner, L., Kaplan, D., Langer, R., Vunjak-Novakovic, G., 2004a. Bone tissue engineering using human mesenchymal stem cells: effects of scaffold material and medium flow. Ann Biomed Eng 32, 112-122.
99. Meinel, L., Karageorgiou, V., Hofmann, S., Fajardo, R., Snyder, B., Li, C., Zichner, L., Langer, R., Vunjak-Novakovic, G., Kaplan, D.L., 2004b. Engineering bone-like tissue in vitro using human bone marrow stem cells and silk scaffolds. J Biomed Mater Res A 71, 25-34.
100. Miura, M., Gronthos, S., Zhao, M., Lu, B., Fisher, L.W., Robey, P.G., Shi, S., 2003. SHED: stem cells from human exfoliated deciduous teeth. Proc Natl Acad Sci U S A 100, 5807-5812.
101. Nakahara, H., Bruder, S.P., Goldberg, V.M., Caplan, A.I., 1990. In vivo osteochondrogenic potential of cultured cells derived from the periosteum. Clin Orthop Relat Res, 223-232.
102. Nerem, R.M., 2006. Tissue engineering: the hope, the hype, and the future. Tissue Eng 12, 1143-1150.
103. Noth, U., Osyczka, A.M., Tuli, R., Hickok, N.J., Danielson, K.G., Tuan, R.S., 2002. Multilineage mesenchymal differentiation potential of human trabecular bone-derived cells. J Orthop Res 20, 1060-1069.
104. Nuttall, M.E., Patton, A.J., Olivera, D.L., Nadeau, D.P., Gowen, M., 1998. Human trabecular bone cells are able to express both osteoblastic and adipocytic phenotype: implications for osteopenic disorders. J Bone Miner Res 13, 371-382.
105. Ogawa, R., Mizuno, H., Watanabe, A., Migita, M., Shimada, T., Hyakusoku, H., 2004. Osteogenic and chondrogenic differentiation by adipose-derived stem cells harvested from GFP transgenic mice. Biochem Biophys Res Commun 313, 871-877.
106. Owen, M., 1988. Marrow stromal stem cells. J Cell Sci Suppl 10, 63-76.
107. Owen, T.A., Aronow, M., Shalhoub, V., Barone, L.M., Wilming, L., Tassinari, M.S., Kennedy, M.B., Pockwinse, S., Lian, J.B., Stein, G.S., 1990. Progressive development of the rat osteoblast phenotype in vitro: reciprocal relationships in expression of genes associated with osteoblast proliferation and differentiation during formation of the bone extracellular matrix. J Cell Physiol 143, 420-430.
108. Palumbo, C., Palazzini, S., Marotti, G., 1990. Morphological study of intercellular junctions during osteocyte differentiation. Bone 11, 401-406.

109. Pavalko, F.M., Chen, N.X., Turner, C.H., Burr, D.B., Atkinson, S., Hsieh, Y.F., Qiu, J., Duncan, R.L., 1998. Fluid shear-induced mechanical signaling in MC3T3-E1 osteoblasts requires cytoskeleton-integrin interactions. Am J Physiol 275, C1591-1601.
110. Pittenger, M.F., Mackay, A.M., Beck, S.C., Jaiswal, R.K., Douglas, R., Mosca, J.D., Moorman, M.A., Simonetti, D.W., Craig, S., Marshak, D.R., 1999. Multilineage potential of adult human mesenchymal stem cells. Science 284, 143-147.
111. Pri-Chen, S., Pitaru, S., Lokiec, F., Savion, N., 1998. Basic fibroblast growth factor enhances the growth and expression of the osteogenic phenotype of dexamethasone-treated human bone marrow-derived bone-like cells in culture. Bone 23, 111-117.
112. Pschyrembel Klinisches Wörterbuch, 2002. 259. Auflage. Berlin, de Gruyter.
113. Puchtler, H., Meloan, S.N., 1978. Demonstration of phosphates in calcium deposits: a modification of von Kossa's reaction. Histochemistry 56, 177-185.
114. Rickard, D.J., Kassem, M., Hefferan, T.E., Sarkar, G., Spelsberg, T.C., Riggs, B.L., 1996. Isolation and characterization of osteoblast precursor cells from human bone marrow. J Bone Miner Res 11, 312-324.
115. Rickard, D.J., Sullivan, T.A., Shenker, B.J., Leboy, P.S., Kazhdan, I., 1994. Induction of rapid osteoblast differentiation in rat bone marrow stromal cell cultures by dexamethasone and BMP-2. Dev Biol 161, 218-228.
116. Rodan, G.A., Martin, T.J., 2000. Therapeutic approaches to bone diseases. Science 289, 1508-1514.
117. Romeis, B., Boeck P., 1989. Mikroskopische Technik, 17. Auflage, Urban&Schwarzenberg Verlag, München.
118. Rosada, C., Justesen, J., Melsvik, D., Ebbesen, P., Kassem, M., 2003. The human umbilical cord blood: a potential source for osteoblast progenitor cells. Calcif Tissue Int 72, 135-142.
119. Rosenberg A., Roth S., 2007. Bone. In: Mills S., ed. Histology for Pathologists. Lippincott Williams & Wilkins (LWW), third edition, 75-95.
120. Salgado, A.J., Coutinho, O.P., Reis, R.L., 2004. Bone tissue engineering: state of the art and future trends. Macromol Biosci 4, 743-765.
121. Sautier, J.M., Nefussi, J.R., Forest, N., 1992. Mineralization and bone formation on microcarrier beads with isolated rat calvaria cell population. Calcif Tissue Int 50, 527-532.
122. Scott, B.L., Pease, D.C., 1956. Electron microscopy of the epiphyseal apparatus. Anat Rec 126, 465-495.
123. Scott, C.K., Hightower, J.A., 1991. The matrix of endochondral bone differs from the matrix of intramembranous bone. Calcif Tissue Int 49, 349-354.
124. Sekiya, I., Larson, B.L., Smith, J.R., Pochampally, R., Cui, J.G., Prockop, D.J., 2002. Expansion of human adult stem cells from bone marrow stroma: conditions that maximize the yields of early progenitors and evaluate their quality. Stem Cells 20, 530-541.
125. Siggelkow, H., Rebenstorff, K., Kurre, W., Niedhart, C., Engel, I., Schulz, H., Atkinson, M.J., Hufner, M., 1999. Development of the osteoblast phenotype in primary human osteoblasts in culture: comparison with rat calvarial cells in osteoblast differentiation. J Cell Biochem 75, 22-35.
126. Sikavitsas, V.I., Bancroft, G.N., Holtorf, H.L., Jansen, J.A., Mikos, A.G., 2003. Mineralized matrix deposition by marrow stromal osteoblasts in 3D perfusion culture increases with increasing fluid shear forces. Proc Natl Acad Sci U S A 100, 14683-14688.
127. Sikavitsas, V.I., Bancroft, G.N., Mikos, A.G., 2002. Formation of three-dimensional cell/polymer constructs for bone tissue engineering in a spinner flask and a rotating wall vessel bioreactor. J Biomed Mater Res 62, 136-148.
128. Sikavitsas, V.I., Temenoff, J.S., Mikos, A.G., 2001. Biomaterials and bone mechanotransduction. Biomaterials 22, 2581-2593.
129. Sobotta/Welsch 2005. Lehrbuch Histologie, Urban & Fischer, 2.Auflage.
130. Sottile, V., Halleux, C., Bassilana, F., Keller, H., Seuwen, K., 2002. Stem cell characteristics of human trabecular bone-derived cells. Bone 30, 699-704.
131. Sottile, V., Thomson, A., McWhir, J., 2003. In vitro osteogenic differentiation of human ES cells. Cloning Stem Cells 5, 149-155.

132. Spees, J.L., Gregory, C.A., Singh, H., Tucker, H.A., Peister, A., Lynch, P.J., Hsu, S.C., Smith, J., Prockop, D.J., 2004. Internalized antigens must be removed to prepare hypoimmunogenic mesenchymal stem cells for cell and gene therapy. Mol Ther 9, 747-756.
133. Stein, G.S., Lian, J.B., 1993. Molecular mechanisms mediating proliferation/differentiation interrelationships during progressive development of the osteoblast phenotype. Endocr Rev 14, 424-442.
134. Stenderup, K., Justesen, J., Clausen, C., Kassem, M., 2003. Aging is associated with decreased maximal life span and accelerated senescence of bone marrow stromal cells. Bone 33, 919-926.
135. Stute, N., Holtz, K., Bubenheim, M., Lange, C., Blake, F., Zander, A.R., 2004. Autologous serum for isolation and expansion of human mesenchymal stem cells for clinical use. Exp Hematol 32, 1212-1225.
136. Suck, K., Behr, L., Fischer, M., Hoffmeister, H., van Griensven, M., Stahl, F., Scheper, T., Kasper, C., 2007. Cultivation of MC3T3-E1 cells on a newly developed material (Sponceram) using a rotating bed system bioreactor. J Biomed Mater Res A 80, 268-275.
137. Suda, T., Takahashi, N., Martin, T.J., 1992. Modulation of osteoclast differentiation. Endocr Rev 13, 66-80.
138. Syftestad, G.T., Weitzhandler, M., Caplan, A.I., 1985. Isolation and characterization of osteogenic cells derived from first bone of the embryonic tibia. Dev Biol 110, 275-283.
139. Thi, M.M., Kojima, T., Cowin, S.C., Weinbaum, S., Spray, D.C., 2003. Fluid shear stress remodels expression and function of junctional proteins in cultured bone cells. Am J Physiol Cell Physiol 284, C389-403.
140. Thompson, Z., Miclau, T., Hu, D., Helms, J.A., 2002. A model for intramembranous ossification during fracture healing. J Orthop Res 20, 1091-1098.
141. Tuan, R.S., Boland, G., Tuli, R., 2003. Adult mesenchymal stem cells and cell-based tissue engineering. Arthritis Res Ther 5, 32-45.
142. Tuyaerts, S., Noppe, S.M., Corthals, J., Breckpot, K., Heirman, C., De Greef, C., Van Riet, I., Thielemans, K., 2002. Generation of large numbers of dendritic cells in a closed system using Cell Factories. J Immunol Methods 264, 135-151.
143. Uchimura, E., Machida, H., Kotobuki, N., Kihara, T., Kitamura, S., Ikeuchi, M., Hirose, M., Miyake, J., Ohgushi, H., 2003. In-situ visualization and quantification of mineralization of cultured osteogenetic cells. Calcif Tissue Int 73, 575-583.
144. Unsworth, B.R., Lelkes, P.I., 1998. Growing tissues in microgravity. Nat Med 4, 901-907.
145. Vacanti, C.A., 2006. History of tissue engineering and a glimpse into its future. Tissue Eng 12, 1137-1142.
146. van der Plas, A., Nijweide, P.J., 2005. JBMR anniversary classic. Isolation and purification of osteocytes. A van der Plas A, PJ Nijweide. Originally published in Volume 7, Number 4, pp 389-96 (1992). J Bone Miner Res 20, 706-714.
147. Verfaillie, M., 2006. "Adult" Stem Cells : Tissue Specific or Not ?. In: Lanza R, ed. Essentials of. Stem Cell Biology. Oxford: Elsevier Academic Press, 11-22.
148. Vunjak-Novakovic, G., 2003. The fundamentals of tissue engineering: scaffolds and bioreactors. Novartis Found Symp 249, 34-46; discussion 46-51, 170-174, 239-141.
149. Vunjak-Novakovic, G., Altman, G., Horan, R., Kaplan, D.L., 2004. Tissue engineering of ligaments. Annu Rev Biomed Eng 6, 131-156.
150. Walsh, S., Jefferiss, C., Stewart, K., Jordan, G.R., Screen, J., Beresford, J.N., 2000. Expression of the developmental markers STRO-1 and alkaline phosphatase in cultures of human marrow stromal cells: regulation by fibroblast growth factor (FGF)-2 and relationship to the expression of FGF receptors 1-4. Bone 27, 185-195.
151. Weissman, I.L., 2000. Stem cells: units of development, units of regeneration, and units in evolution. Cell 100, 157-168.
152. Wendt, D., Marsano, A., Jakob, M., Heberer, M., Martin, I., 2003. Oscillating perfusion of cell suspensions through three-dimensional scaffolds enhances cell seeding efficiency and uniformity. Biotechnol Bioeng 84, 205-214.

153. Wendt, D., Stroebel, S., Jakob, M., John, G.T., Martin, I., 2006. Uniform tissues engineered by seeding and culturing cells in 3D scaffolds under perfusion at defined oxygen tensions. Biorheology 43, 481-488.
154. Wickham, M.Q., Erickson, G.R., Gimble, J.M., Vail, T.P., Guilak, F., 2003. Multipotent stromal cells derived from the infrapatellar fat pad of the knee. Clin Orthop Relat Res, 196-212.
155. Woolf, A.D., Pfleger, B., 2003. Burden of major musculoskeletal conditions. Bull World Health Organ 81, 646-656.
156. Yaszemski, M.J., Payne, R.G., Hayes, W.C., Langer, R., Mikos, A.G., 1996. Evolution of bone transplantation: molecular, cellular and tissue strategies to engineer human bone. Biomaterials 17, 175-185.
157. Yellowley, C.E., Li, Z., Zhou, Z., Jacobs, C.R., Donahue, H.J., 2000. Functional gap junctions between osteocytic and osteoblastic cells. J Bone Miner Res 15, 209-217.
158. You, J., Yellowley, C.E., Donahue, H.J., Zhang, Y., Chen, Q., Jacobs, C.R., 2000. Substrate deformation levels associated with routine physical activity are less stimulatory to bone cells relative to loading-induced oscillatory fluid flow. J Biomech Eng 122, 387-393.
159. Zheng, M.H., Wood, D.J., Papadimitriou, J.M., 1992. What's new in the role of cytokines on osteoblast proliferation and differentiation? Pathol Res Pract 188, 1104-1121.
160. Zuk, P.A., Zhu, M., Mizuno, H., Huang, J., Futrell, J.W., Katz, A.J., Benhaim, P., Lorenz, H.P., Hedrick, M.H., 2001. Multilineage cells from human adipose tissue: implications for cell-based therapies. Tissue Eng 7, 211-228.

6. Appendix I

6.1. Chemicals and Reagents

Name	Manufacturer
Acetic acid, glacial 100%	Merck, Darmstadt
AdipoRed™ Assay reagent	Cambrex Bio Science Inc., Walkersville, USA
Albumax I 10% Solution	Invitrogen Corporation, Paisley, UK
Alcian Blue	Sigma Aldrich Chemie GmbH, Steinheim
Alexa Fluor®488 goat anti-mouse IgG	Molecular Probes/Invitrogen, Karlsruhe
Alexa Fluor®488 goat anti-rabbit IgG	Molecular Probes/Invitrogen, Karlsruhe
Alexa Fluor®594 goat anti-mouse IgG	Molecular Probes/Invitrogen, Karlsruhe
Alizarin Red Sodium Sulfonate	ICN biomedicals Inc., Aurora, USA
Calcein, Anhydrous	Sigma Aldrich Chemie GmbH, Steinheim
Calcium chloride	Sigma Aldrich Chemie GmbH, Steinheim
Collagen I antibody mouse anti-human	Abcam Limited, Cambridge, UK
Collagen Solution, Type1, 0.1%	Sigma Aldrich Chemie GmbH, Steinheim
Collagenase, lyophillized	Invitrogen Corporation, Paisley, UK
Connexin 43 antibody rabbit anti-human	Sigma Aldrich Chemie GmbH, Steinheim
CyQUANT® Cell Proliferation Assay Kit	Invitrogen Corporation, Paisley, UK
Dexamethasone	Sigma Aldrich Chemie GmbH, Steinheim
Dimethyl sulfoxide	Sigma Aldrich Chemie GmbH, Steinheim
DRAQ5™	Biostatus Limited, Shepshed, UK
Eosin Y solution 0.5%	Carl Roth GmbH, Karlsruhe
Epidermal growth factor, recombinant human	RELIATech GmbH, Braunschweig
Ethanol, 100% p.A.	J.T.Baker, Phillipsburg, USA
Fetal bovine serum, lot 40G5311K	Invitrogen Corporation, Paisley, UK
Fibroblast growth factor, recombinant human	RELIATech GmbH, Braunschweig
Fibronectin	Sigma Aldrich Chemie GmbH, Steinheim
Formaldehyde 37%	Carl Roth GmbH, Karlsruhe
Glutaraldehyde solution, 25%	Sigma Aldrich Chemie GmbH, Steinheim
Glycerol-Gelatine, Kaiser's	Merck, Darmstadt
Goat serum	Invitrogen Corporation, Paisley, UK
Hematoxylin, Hem alum solution acid acc. to Mayer	Carl Roth GmbH, Karlsruhe
HEPES buffer	Sigma Aldrich Chemie GmbH, Steinheim
Histoclear™	Thermo electron corporation, Dreieich
Human Serum	Medical School Hannover, Hannover
Human Serum , PAA Lot CO 2104-0167	PAA, Paschingen, Austria
Human Serum, Pan Biotech Lot P50208, P520221	Pan Biotech, Aidenbach
HybridoMed Dif 1000 with L-Glutamin, w/o bovine serum albumin, w/o bovine transferrin, w/o bovine insulin, w/o oleic acid (ZKT-1)	Biochrom AG, Berlin
Hydrochloric acid, 37%	Carl Roth GmbH, Karlsruhe
Hydrocortisone, 98%	Sigma Aldrich Chemie GmbH, Steinheim
Indomethacin	Sigma Aldrich Chemie GmbH, Steinheim
Insulin	Invitrogen corporation, UK
Insulin like growth factor, recombinant human	Peprotech, Rocky Hill, USA
Isobutylmethylxanthin 99%	Sigma Aldrich Chemie GmbH, Steinheim
Isopropanol	J.T.Baker, Phillipsburg, USA
ITS+3 Liquid Media Supplement	Sigma Aldrich Chemie GmbH, Steinheim
L-Ascorbic acid 2-phosphate Sesquimagnesium salt	Sigma Aldrich Chemie GmbH, Steinheim
L-Proline	Sigma Aldrich Chemie GmbH, Steinheim
Magnesium chloride	Sigma Aldrich Chemie GmbH, Steinheim
Methanol	J.T.Baker, Phillipsburg, USA
Metra CICP EIA kit	OSTEOmedical Group, Buende

▪ Micro BCA™ Protein Assay Reagent Kit	Pierce, Rockford, USA
▪ Nitrophenyl phosphate disodium salt hexahydrate	Fluka, Seelze
▪ Paraformaldehyde	Sigma Aldrich Chemie GmbH, Steinheim
▪ Penicillin-Streptomycin solution	Invitrogen Corporation, Paisley, UK
▪ Picric acid	Merck, Darmstadt
▪ Platelet derived growth factor, recombinant human	RELIATech GmbH, Braunschweig
▪ p-Nitrophenol Standard Solution, 10mM	Sigma Aldrich Chemie GmbH, Steinheim
▪ Poly-L-Lysine solution	Sigma Aldrich Chemie GmbH, Steinheim
▪ Potassium chloride salt	Fluka, Seelze
▪ Potassium phosphate monobasic	Fluka, Seelze
▪ Proline	Sigma Aldrich Chemie GmbH, Steinheim
▪ Pyronin-G	Fluka, Seelze
▪ Resorcin-Fuchsin-solution according to Weigert	Carl Roth GmbH, Karlruhe
▪ Saccharose	Sigma Aldrich Chemie GmbH, Steinheim
▪ Shandon Histoclear –Xylolersatz	Thermo electron corporation, Dreieich
▪ Shandon Histoplast, paraffin pellets 56-57°C	Thermo electron corporation, Dreieich
▪ Shandon Xylene substitute mountant	Thermo Electron Corporation, Dreieich
▪ SigmaFast ™,pNPP Alkaline phosphatase substrate tablet set	Sigma Aldrich Chemie GmbH, Steinheim
▪ Sigma Fast™, BCIP/NBT Alkaline phosphatase substrate tablet set	Sigma Aldrich Chemie GmbH, Steinheim
▪ Sigmacote®, Sl-2	Sigma Aldrich Chemie GmbH, Steinheim
▪ Silver nitrate	Sigma Aldrich Chemie GmbH, Steinheim
▪ Sodium bicarbonate	Biochrom AG, Berlin
▪ Sodium cacodylate trihydrate	Sigma Aldrich Chemie GmbH, Steinheim
▪ Sodium carbonate anhydrous	Carl Roth GmbH, Karlsruhe
▪ Sodium chloride	Merck, Darmstadt
▪ Sodium hydroxide pellets	Sigma Aldrich Chemie GmbH, Steinheim
▪ Sodium Pyruvate, 100mM solution	Sigma Aldrich Chemie GmbH, Steinheim
▪ Sodium tetraborate decahydrate	Sigma Aldrich Chemie GmbH, Steinheim
▪ Tareget Retrieval solution	DakoCytomation, Hamburg
▪ Toluidine Blue O	Sigma Aldrich Chemie GmbH, Steinheim
▪ Transferrin	Biotest, Dreieich
▪ Transforming growth factor-beta 1, recombinant human	R&Dsystems, Minneapolis, USA
▪ Triton X-100	Sigma Aldrich Chemie GmbH, Steinheim
▪ Trypan blue	Merck, Darmstadt
▪ Trypsin/EDTA (1x)	Invitrogen Corporation, Paisley, UK
▪ Weigert's Hematoxylin solution A	Carl Roth GmbH, Karlsruhe
▪ Weigert's Hematoxylin solutionB	Carl Roth GmbH, Karlsruhe
▪ WST-1, Cell Proliferation Reagent	Roche, Mannheim
▪ ß-Glycerophosphate disodium salt	Sigma Aldrich Chemie GmbH, Steinheim

6.2. Consumables

Consumable	Manufacturer
▪ Cell culture well plates, 12, 24,48,96	Becton Dickinson, Heidelberg
▪ Cell strainer, 70µm Nylon	Becton Dickinson, Heidelberg
▪ Cryo-vials	Nalgene, Rochester, USA
▪ Embedding cassettes (double) with lids	bio Optica, Milan, Italy
▪ Filter AcroCap™ 0.1 µm, for liquid filtration	Pall Life Sciences Ann Arbor, USA
▪ Filter, 0.2µm, 25 mm disposable syringe filter	Nalgene, Rochester, USA
▪ Filter, Millex®-FG,0.2µm,for sterile venting of autoclaved vessels	Millipore Corporation, Bedford, USA
▪ Pall, Acrodisc Syringe Filter, 0.1µm	Pall Life Sciences, Ann Arbor, USA
▪ Pharmed tubing, ID:1.02mm, Wall:0.85mm (pumps)	Ismatec, Zuerich, Switzerland
▪ Pharmed tubing, ID:1.52mm, Wall:0.85mm, (sampling port)	Ismatec, Zuerich, Switzerland
▪ Polysine™, Microscope slides	Menzel-Gläser, Braunschweig
▪ Safe-lock tubes (1.5ml, 2 ml)	Eppendorf, Hamburg
▪ Scalpel	B.Braun, Melsungen
▪ Shandon MB35 Premier blades	Thermo electron corporation, Dreieich
▪ Silicon tubing (perfusion bioreactor)	TIP, Braunschweig
▪ Syringes 2, 20,50 ml	B.Braun, Melsungen
▪ Tissue culture flasks, 25, 75,175 cm^2	Becton Dickinson, Heidelberg
▪ TPP, tissue culture tubes	TPP AG, Trasadingen, Switzerland
▪ Universals, polystyrene conical tubes (15ml,50ml)	Becton Dickinson, Heidelberg

6.3. Instruments

Instrument	Manufacturer
▪ ELISA-Reader, Spectrophotometer, SLT 340, ATTC	ATTC Labinstruments, Crailsheim
▪ Fluorescence microplate reader, CytoFlourII	Applied Biosystems, Foster City, USA
▪ IKA-Ultra-Turrax® T25 basic	IKA-Werke, Staufen
▪ Incubator Biocentre 2001	Integra, Fernwald, Switzerland
▪ Incubator Cytoperm2	Heraeus/Kendro, Hanau
▪ MACSmix™ tube rotator	Miltenyi Biotec GmbH, Bergisch Gladbach
▪ Neubauer chamber	Omnilab, Braunschweig
▪ Plateshaker, Thermomixer comfort	Eppendorf, Hamburg
▪ Scalpel , knife to prepare bone samples	Aesculap, Tuttlingen
▪ Scanning electron microscope DSM 982 Gemin	Zeiss, Jena
▪ Shandon Citadel™ Tissue Processor (Citadel 1000)	Thermo electron corporation, Dreieich
▪ Shandon Histocentre 2, Tissue Embedding System	Thermo electron corporation, Dreieich
▪ Shandon Microtome 0325	Thermo electron corporation, Dreieich
▪ Stainless steel embedding moulds, BIO-MOLD 33x24x12mm	bio Optica, Milan Italy
▪ Variomag®,Magnetic stirrer base	H+P Labortechnik GmbH, Oberschleissheim
▪ YSI 2700 Biochemistry Analyzer	Yellow Springs, USA

7. Appendix II

7.1. General Cell Culture Methodology

7.1.1. Cryopreservation and Resuscitation of Cryopreserved Cells

To enable stocks of cells to be stored cells were cryopreserved. Sub-confluent cell monolayers were trypsinised as described above and centrifuged. The pellet was thereafter re-suspended, counted and centrifuged again to re-suspend 3-5 x10^6 cells in 1ml freezing medium (10% DMSO as a cryoprotectant, 10% ZKT-1 medium and 80% human serum), transferred to a cryo-vial and slowly frozen over night at -70ºC inside a passive freezer (Mr Frosty, Nalgene) filled with 70% isopropanol) to be then transferred to a liquid nitrogen cryotank for long term storage.

For thawing, the vials were collected from the cryotank, and dipped for 1 minute in a 37°C water bath to thaw. The contents of the vial were then re-suspended by drawing them up carefully using a 1 ml sterile pipette and transferred to a universal containing fresh supplemented culture medium, centrifuged as above and the pellet re-suspended in fresh medium to dilute out the DMSO and start a new stock culture swirling the cell suspension upon seeding for uniform distribution in the culture vessel.

7.1.2. Subculture of Adherent Human cells

At sub-confluence (80-90% confluence) the cell monolayer was trypsinised by carefully removing the spent medium and washing the cell layer with 1xPBS (ca.300 µl/cm^2) by gently swirling the culture flask for about 30 seconds to wash away any medium or serum residuals. PBS was completely removed and the cell layer was covered with 0.25% Trypsin/EDTA solution (ca.300 µl/cm^2) *, completely covering the monolayer and then incubated for 5 minutes at 37°C. Cell detachment was confirmed microscopically (Axiovert 120, Zeiss, Jena) as adherent cells float becoming round once dislodged. To loosen any attached cell remainders, the culture container was gently tapped at the side to ensure

complete separation from the culture surface. The enzyme reaction was neutralized after maximum 5 minutes using an equal volume of serum supplemented medium**. The cell suspension was then transferred with a sterile pipette to a 15 ml (or 50 ml) conical tube and centrifuged at 800 rpm for three minutes at room temperature. The clear supernatant was removed and the pellet carefully re-suspended in a determined volume of fresh medium to determine the cell number in a haemocytometer (Trypan blue exclusion). Cells were then either cryopreserved or further sub-cultured at $5x10^3$ or $1x10^4$ cells/cm^2.

*The amount of trypsin varied according to the cell culture area from 1.5 ml for a T25 flask, 3 ml for a T75 flask and 5 ml for a T175 flask and 20 ml per layer in a cell factory.

**For cell detachment solutions (PBS, Trypsin/EDTA and medium were all pre-warmed in a 37°C water bath

7.1.3. Determination of Cell Number (Trypan Blue Exclusion)

Adherent cells were brought into suspension as described above using Trypsin/EDTA and re-suspened in a volume of fresh medium, gently pipetting up and down to break up any clumps. 100-200 µl of cell suspension were aseptically removed and diluted with an equal volume of Trypan Blue solution (dilution factor=2)*. Cells were counted using an improved Neubauer chamber, filling both sides of the chamber (ca.10 µl) with cell suspension and then viewed under a phase contrast light microscope (Axiovert 120, Zeiss, Jena) using x10 magnification. Viable cells, appearing as round bright cells in the 4 squares of the Neubauer chamber were counted and non-viable cells stained blue** were counted as well. The concentration of cells (cells/ml) was calculated using the following equation:

(Cell number x dilution factor) / Number of squares counted.

Total number of cells= concentration of viable cells (cells/ml) x volume of cell suspension (ml).

*The cell suspension was diluted depending on cell density (i.e. a higher dilution factor in case of a high cell density).

**Trypan blue is a dye that would penetrate only dead cells because of the ruptured cell membrane.

7.2. Cell Culture Media

All solutions and buffers were prepared using deionized water (Milli-Q-Water filtration system, Millipore) and either autoclaved at 121ºC for heat sterilisation or if heat labile, solutions filtered through 0.1µm AcroCap™ filters or through 0.2µm syringe filters.

7.2.1. ZKT-1 Basal Medium

ZKT-1 refers to the following medium composition:

Hybridomed Dif 1000	12.1 g
$NaHCO_3$	3.6 g
Deionized water	ad 1000 ml

The medium was filtered through a 0.1 µm filter and stored at 4ºC.

Hybridomed Dif 1000 is based on a 1:1 mixture of lscove's Modified Dulbecco's Medium and Ham's Medium F12 medium and was developed in the cell culture technology department of the Helmholtz Centre for Infection Research (Jaeger 1988).

7.2.2. Osteogenic Differentiation Medium

ZKT-1 basal medium was supplemented with the following at a final concentration in the cultivation medium:

Human Serum or Fetal bovine serum	10% (v/v)
β-Glycerophosphat	10 mM
L-Ascorbat	0.20 mM
Dexamethasone	10 nM

7.2.3. Adipogenic Differentiation Medium

ZKT-1 basal medium was supplemented with the following at a final concentration in the cultivation medium:

FBS	10% (v/v)
Isobutylmethylxanthine	0.5 mM
Indomethacin	200 µM
Insulin	5 µg/ml
Hydrocortisone	0.5 mM

7.2.4. Chondrogenic Differentiation Medium

ZKT-1 basal medium was supplemented with the following at the final concentration in the cultivation medium:

Albumin	1 mg/ml
Sodium Pyruvate	100 µg/ml
Proline	40 µg/ml
L-Ascorbate	50 µg/ml
Dexamethasone	100 nM
TGF-β	10 ng/ml
1x ITS (Insulin+Transferrin+ Seleneous acid)	6.25 µg/ml

7.3. Buffers, Supplements and Working Solutions

7.3.1. Cacodylate Buffer, 0.1M

To prepare one liter of 0.1M cacodylate buffer, the following protocol was applied:

Sodium cacodylate	21.41 g
Saccahrose	38.80 g
$MgCl_2$	2.04 g
$CaCl_2$	1.48 g
Deionized water	ad 1000 ml

The pH was adjusted with to 6.9 and the solution stored at 4°C.

7.3.2. Human Serum Inactivation

To remove complement from serum, inactivate potentially available viruses and reduce the cytotoxic action of immunoglobulins, human serum was pooled

and heat inactivated at 56°C for 30 minutes (Hankey et al., 2001). Aliquots were stored at -20°C.

7.3.3. Paraformaldehyde Fixative Solution, 4%

To prepare 4% paraformaldehyde solution the following protocol (Bancroft and Gamble, 2001) was applied:

Solution A	Solution B
NaH_2PO_4 2.26 g	NaOH 2.52 g
Deionized water ad 100 ml	Deionized water ad 100 ml

Paraformaldehyde	4 g
Solution A	83 ml
Solution B	ad 100 ml

The solution was stirred under a fume hood and warmed up to 60°C, filtered and cooled (pH 7.2-7.4). Aliquots were stored at –20°C.

7.3.4. Penicillin-streptomycin

Refers to a ready made solution ordered from Invitrogen Corporation prepared with 10,000 units/ml penicillin G sodium and 10,000µg/ml streptomycin sulphate in 0.85% saline. Medium was supplemented with the antibiotic mixture at a final concentration of 1% (v/v) (antibiotic mixture/complete medium).

7.3.5. Phosphate Buffered Saline (PBS)

PBS was prepared according to the following protocol:

NaCl	150 mM
Na_2HPO_4	8 mM
KCl	3 mM
KH_2PO_4	1.5 mM

The solution (pH 7.4) was heat sterilized at 121ºC and stored at 4ºC.

7.3.6. Triton-X Solution

A 2% Triton-X solution was prepared in deionized water according to the following protocol:

Triton X-100	2% (v/v)
HEPES	50 mM
NaCl	100 mM

7.3.7. Trypan Blue Solution, 0.25%

Trypan blue	0.2 g
NaCl	0.9 g
Deionized water	ad 100 ml

7.4. Histological Methods and Staining Solutions

7.4.1. Calcein Solution

Calcein solution for the calcium quantification assay as well as for histological staining was prepared after the following protocol:

Calcein	5 µg
Deionized water	ad 100ml

The solution was stored at 4°C in the dark.

7.4.2. Haematoxylin-Eosin Staining

After sections were deparaffinized and rehydrated, haematoxylin and eosin staining was performed according to the following protocol:

Haematoxylin solution (according to Mayer)	5 min
Tap water rinsing	15 min
1% acetic acid solution	1 min
Deionized water	1 min
70% ethanol	2 min
90% ethanol	2 min

Eosin Y solution 0.5%	5 min
90% ethanol	a quick dip
100% ethanol	3x 2min
Xylene substitute	2x 10min
Xylene substitute mountant	

7.4.3. von Kossa staining

5% silver nitrate solution (stored dark)

$AgNO_3$	5 g
Deionized water	ad 100 ml

5 % sodium carbonate solution (containing 0.2% Formaldehyde)

Na_2CO_3	5 g
Formaldehyde 37%	0.55 ml
Deionized water	ad 100 ml

7.4.4. Toluidine Blue Staining

After sections were deparaffinized and rehydrated, Toluidine Blue staining was performed according to the following protocol:

Toluidine Blue solution*	15 min
Deionized water	1 min
96% ethanol	2x a quick dip
100% ethanol	2x 1 min
Xylene substitute	2x 10 min
Xylene substitute mountant	

***Toluidine Blue Solution:**

Solution A	**Solution B**
Sodium tetraborate 8 g Toluidine blue 8 g Deionized water ad 800 ml	Pyronin G 2 g Deionized water ad 200 ml

Toluidine Blue solution was prepared by mixing solution A with solution B for 15 minutes on a magnetic stirrer.

7.4.5. Van Gieson Staining

After sections were deparaffinized and rehydrated, van Gieson staining was performed according to the following protocol:

Resorcin Fuchsin solution (Weigert)	30 min
Rinse under tap water	5-10 min
95% ethanol	quick dip
100% ethanol.	quick dip
Deionized water	1 min
Weigert's iron haematoxylin *	5 min
Rinse under tap water	5-10 min
Deionized water	1 min
van Gieson solution**	5 min
96% ethanol	1 min
100% ethanol	1 min
Xylene substitute	2x 10 min
Xylene substitute mountant	

***Weigert's iron hematoxylin :**

40 ml of Weigert's solution A (5 g Hematoxylin in 500 ml Ethanol p.A.) were added to 30 ml of Weigert's solution B (475 ml deionized water and 5 ml 25% HCl and 20 ml liquoferrisesquinchlorati).

****van Gieson solution:**

A 3% picric acid solution was prepared:

30 g picric acid ad 1000 ml deionized water, dissolved on a hot plate under a fume hood, cooled and filtered.

50 ml 2% Acid Fuchsin solution and 5 ml 2% acetic acid solution were added.

7.4.6. Poly-L-Lysine Slide Coating

To minimize the loss of the tissue section from the slide during the histological staining procedure, the glass slides were coated with a tissue adhesive. Briefly,

the poly-l-lysine solution (0.1% w/v) was diluted 1:10 with deionized water (Bancroft and Gamble, 2001) the slides were placed in a trough filled with the solution and left for 5 minutes at room temperature. Slides were then drained and dried at 60ºC in an oven for 1 hour.

7.5. Osteogenic Differentiation of Human Mesenchymal Cells using Fetal Bovine Serum

Since the concept of inducing osteogenesis with a mineralisation pattern involving the formation of vesicular like structure in medium containing human serum has been proven (chapter 2, section 2.3.6.), it was investigated whether cells show a similar mineralisation pattern in fetal bovine serum (FBS) supplemented medium (Figure 66). Cryopreserved human bone marrow cells (male, age: 19 years) were cultivated and expanded in ZKT-1 basal medium containing 15% FBS instead of 15% human serum until passage three (section 2.2.1.). Osteogenic differentiation was investigated by seeding the cells in 48-well plates at a plating density of $5x10^3$ cells/cm² in osteogenic medium containing 10% FBS instead of 10% human serum The osteogenic differentiation was assessed over a 35 day time course study. Cells were seeded at $5x10^3$ cells/cm² in 48-well-plates kept in expansion medium for 5 days until confluence and then changed to osteogenic medium (section 7.2.2.).
Mineralisation of the extracellular matrix is demonstrated in Figure 66 by Alizarin red, von Kossa and calcein staining showing an almost identical eventual pattern of mineralization observed with human serum. However, it was noted that the onset of mineralisation was noted to be earlier in case of the cells cultivated in FBS. In all three histological staining methods, mineralized nodules were observed as early as day 14, this could be explained by either the presence of mitogenic factors in FBS not found in human serum or due to the fact that human bone marrow derived cells used for the assessing experiment were obtained from a young donor (age 19 years).
It can be concluded that both sera can be used interchangeably for osteogenic differentiation studies and essentially proof of concept was demonstrated with human serum.

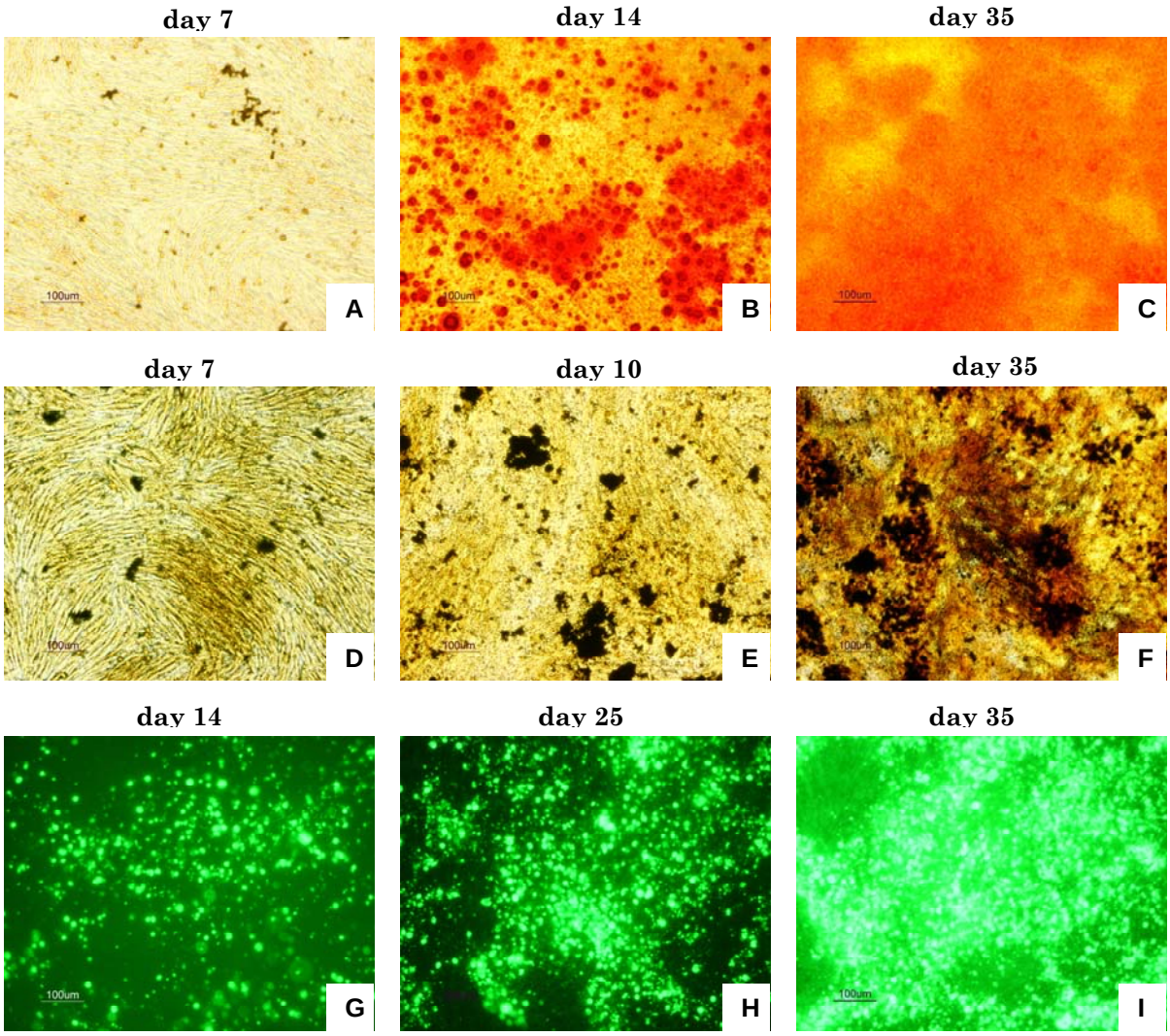

Figure 66 Phase contrast micrographs showing terminal and complete mineralization of the extracellular matrix in human bone marrow derived cells cultivated in foetal bovine serum in the process of bone formation. Cells were seeded at $5x10^3$cells/cm^2 and induced with osteogenic medium at confluence Cell layers were fixed at days 7,10,14,25 and 35. **(A), (B) and (C)** show a strong Alizarin red staining pattern from day 7 with progressed intensity on days 14 and 35 with mineralised nodules appearing in red. **(D), (E) and (F)** Von Kossa staining after 7, 10 and 35 days in osteogenic medium showing black mineral depositions increasing in number and size with time. **(G), (H) and (I)** Fluorescence microscopy of the mineralised extracellular matrix revealed the calcein binding pattern showing intense calcification (green fluorescence) of the bone marrow derived cells. Original magnification: x100; scale bar=100 µm.

8. Abbreviations

ALP	Alkaline Phosphatase
BCA	Bicinchoninic Acid
BCIP	5-Bromo-4-Chloro-3-Indolyl Phosphate
BSE	Bovine Spongiform Encephalopathy
CaP	Calcium Phosphate
CF	Collagen Fibers
CICP	Collagen type I COOH terminal Propeptide
DMSO	Dimethyl Sulfoxide
DNA	Deoxyribonucleic Acid
ECM	Extracellular Matrix
EDTA	Ethylenediaminetetraacetic acid Disodium salt Dihydrat
EGF	Epidermal Growth Factor
FBS	Fetal Bovine Serum
FCS	Fetal Calf Serum
FGF	Fibroblast Growth Factor
H&E	Haematoxylin and Eosin
HEPES	4-(2-Hydroxyethyl)piperazine-1-ethanesulfonic acid
HS	Human Serum
IGF	Insulin like Growth Factor
IgG	Immunoglobulin G
IRB	Institutional Review Board
ITA	Insulin, Transferrin, Albumin
ITS	Insulin, Transferrin, Seleneous acid
MSC	Mesenchymal Stem Cell
NASA	National Aeronautics and Space Administration
NBT	Nitro Blue Tetrazolium
OB	Osteoblast
OC	Osteocyte
PBS	Phosphate Buffered Saline
PCL	Polycaprolactone
PDGF	Platelet Derived Growth Factor
PEEK	Polyarylether Ether Ketone
PFA	Paraformaldehyde
PGA	Polyglycolide
PLA	Polylactide
PLGA	Poly-(lactic-co-glycolic acid)
pNPP	p-Nitrophenyl Phosphate
rpm	Revolutions per minute
SEM	Scanning Electron Microscopy
TGF-β	Transforming Growth Factor beta
WHO	World Health Organization